

## Review

# A perspective on the radiopharmaceutical requirements for imaging and therapy of glioblastoma

Julie Bolcaen<sup>1</sup>, Janke Kleynhans<sup>2,3</sup>, Shankari Nair<sup>1</sup>, Jeroen Verhoeven<sup>4</sup>, Ingeborg Goethals<sup>5</sup>, Mike Sathekge<sup>2,3</sup>, Charlot Vandevoorde<sup>1</sup> and Thomas Ebenhan<sup>2,6</sup>✉

1. Radiobiology, Radiation Biophysics Division, Nuclear Medicine Department, iThemba LABS, Cape Town, South Africa.
2. Nuclear Medicine Research Infrastructure NPC, Pretoria, South Africa.
3. Nuclear Medicine Department, University of Pretoria and Steve Biko Academic Hospital, Pretoria, South Africa.
4. Laboratory of Radiopharmacy, Ghent University, Ghent, Belgium.
5. Ghent University Hospital, Department of Nuclear Medicine, Ghent, Belgium.
6. Nuclear Medicine Department, University of Pretoria, Pretoria, South Africa.

✉ Corresponding authors: E-mail: thomas.ebenhan@up.ac.za, thomas.ebenhan@gmail.com; +27 12 354 4713, +27 79 770 2531.

© The author(s). This is an open access article distributed under the terms of the Creative Commons Attribution License (<https://creativecommons.org/licenses/by/4.0/>). See <http://ivyspring.com/terms> for full terms and conditions.

Received: 2020.12.01; Accepted: 2021.03.29; Published: 2021.07.06

## Abstract

Despite numerous clinical trials and pre-clinical developments, the treatment of glioblastoma (GB) remains a challenge. The current survival rate of GB averages one year, even with an optimal standard of care. However, the future promises efficient patient-tailored treatments, including targeted radionuclide therapy (TRT). Advances in radiopharmaceutical development have unlocked the possibility to assess disease at the molecular level allowing individual diagnosis. This leads to the possibility of choosing a tailored, targeted approach for therapeutic modalities. Therapeutic modalities based on radiopharmaceuticals are an exciting development with great potential to promote a personalised approach to medicine. However, an effective targeted radionuclide therapy (TRT) for the treatment of GB entails caveats and requisites. This review provides an overview of existing nuclear imaging and TRT strategies for GB. A critical discussion of the optimal characteristics for new GB targeting therapeutic radiopharmaceuticals and clinical indications are provided. Considerations for target selection are discussed, i.e. specific presence of the target, expression level and pharmacological access to the target, with particular attention to blood-brain barrier crossing. An overview of the most promising radionuclides is given along with a validation of the relevant radiopharmaceuticals and theranostic agents (based on small molecules, peptides and monoclonal antibodies). Moreover, toxicity issues and safety pharmacology aspects will be presented, both in general and for the brain in particular.

Key words: targeted radionuclide therapy; radiochemistry; glioblastoma; theranostics; PET SPECT imaging

## 1. Introduction

Gliomas represent 80% of all primary brain tumours and are a heterogeneous group of tumours of the central nervous system (CNS). Diagnosis is often predicted by patient clinical history, but confirmation by neuroimaging is required. Before beginning treatment, histological characterisation and determination of the malignancy grade is imperative [1,2]. Previously, the classification of CNS tumours by the World Health Organization's (WHO) grading system was solely based on histology; varying from grade I, which is characterised by lesions with low proliferative potential and possibility of cure, up to grade IV. However, several studies over the past two decades illustrate the diagnostic importance of

characterising the molecular status of the individual patient's brain tumour. Hence, a new WHO classification, including both, histology and molecular genetic features, was established in 2016 [3,4]. Glioblastomas (GB) are classified as grade IV CNS tumours; neoplasms which are cytological malignant and mitotically active. They are typically associated with extensive invasion of the surrounding tissue and rapid proliferation commensurate with disease progression [5].

Individuals who are diagnosed with GB have a poor prognosis and the quest for efficient therapy is ongoing. The standard GB treatment consists of debulking surgery, temozolomide (TMZ) chemo-

therapy and concomitant external beam radiotherapy (EBRT). However, total resection is not possible in most patients. Despite optimal treatment protocols; the median survival is only 12-14 months [6-9]. Current therapies fail as the result of therapeutic resistance and heterogeneous tumour cell population effects. GB often presents with different grades of cell-differentiation within the same tumour, indicating the presence of distinct cell populations with differing sensitivity to therapy. Resistance is often caused by the presence of a small subset of highly resistant tumour cells that display stem cell-like properties [10,11].

Target-based diagnostics and therapeutics focus on several mutations and alterations in key molecular pathways that have been linked to GB pathogenesis and/or prognosis. These include, phosphatase and tensin homolog (PTEN) and 1p/19q combined deletions, mutations of the isocitrate dehydrogenase 1 or 2 (IDH) genes and telomerase reverse transcriptase (TERT) promoter region, epidermal growth factor receptor (EGFR) amplification and tumor protein (TP53) mutations [12,13]. The advantage of targeting the molecular characteristics that drive the malignant GB phenotype with theranostic radiopharmaceuticals is the possibility of selectively identifying and subsequently treating GB cells without damaging the surrounding healthy brain tissue. The identification of new GB genetic biomarkers has led to a growing interest in the development of new radiopharmaceuticals for GB imaging and therapy [14,15].

TRT is a strategy in nuclear medicine for the treatment of GB enabling the visualization of molecular biomarkers and pathways on a subcellular level using a biochemical vector coupled to a radionuclide either for diagnosis or for therapy. A major prerequisite for the administration of TRT is to confirm the presence of the GB tumour target using non-invasive nuclear imaging techniques before deciding on treatment options. This review includes an overview of current GB imaging options, a detailed perspective on TRT strategies for GB followed by a critical assessment of the TRT requirements to reach optimal treatment outcome in GB patients. Special attention is given to the selection of the optimal target and its accessibility, choice of the biochemical vector, risk for toxicity and desired validation process.

## 2. Nuclear imaging and theranostics in neuro-oncology

Historically, contrast-enhanced magnetic resonance imaging (MRI) played an important role in the diagnosis and the assessment of treatment efficacy in GB. This is still the case, however, the use of contrast enhancement is controversial since it is

non-specific and it primarily reflects the passage of contrast material (e.g. gadolinium) across a disrupted blood-brain barrier (BBB). Pseudo-progression is often incorrectly reflected as tumor progression on contrast-enhanced MRI in approximately 20-30% of glioma patients, especially within the first three months after concurrent chemoradiation. In addition, the use of antiangiogenic agents during treatment can result in a 'pseudo-response' on contrast-enhanced MRI [16,17]. To accurately assess treatment response, new response criteria for Response Assessment in Neuro-Oncology were introduced in 2010 [17]. This includes 2D-tumour size as measured on T2- and Fluid Attenuated Inversion Recovery (FLAIR)-weighted MR images, in addition to contrast-enhanced MRI.

Non-invasive, functional and molecular imaging techniques have become recognised as more relevant in the last decade, including MR spectroscopy, perfusion weighted MRI, Positron Emission Tomography/Computed Tomography (PET/CT) or Single-photon Emission Computerized Tomography (SPECT/CT). PET has a clear advantage over SPECT in terms of spatial resolution and is therefore the image modality of choice regarding GB investigations. Imaging gliomas using PET has been reviewed in depth elsewhere [18-21]. When a theranostic approach is used for GB treatment, the major role of PET or SPECT includes confirmation of the presence of the specific molecular target before TRT. Carefully interpreted Nuclear Medicine imaging facilitates the prediction and monitoring of tumour response and individualised dosimetry [22-24]. Biodistribution analysis of the imaging partner permits improved patient-based treatment and thereby prevents unnecessary therapy and associated toxicity [25]. This may be achieved by, for example, exchanging the therapeutic radionuclide (e.g.  $\beta$ -emitter Lutetium-177) with a gamma- or positron-emitting radionuclide (e.g. Gallium-68 for PET/CT) attached to the relevant biomolecule; ie. using [ $^{68}\text{Ga}$ ]Ga-DOTA-TOC-PET/CT imaging combined with [ $^{177}\text{Lu}$ ]Lu-DOTA-TATE-targeted radionuclide therapy [26]. Another approach is to use a solitary radionuclide that emits both therapeutic and imageable  $\gamma$ -rays or positrons that allows GB imaging using SPECT or PET (e.g. Iodine-131) [7].

### 2.1 Established and emerging PET/SPECT radiopharmaceuticals in neuro-oncology

The transport and cellular mechanism of routinely used PET tracers in neuro-oncology is given in **Figure 1**. GB PET radiotracers are predominantly biomimetics excessively incorporated by cancer cells in response to elevated metabolism or high

proliferation. These may include desoxy-2- $^{18}\text{F}$ fluoro-D-glucose ( $^{18}\text{F}$ FDG), L- $^{11}\text{C}$  methyl-methionine ( $^{11}\text{C}$ MET), O-2- $^{18}\text{F}$ fluoroethyl-L-tyrosine ( $^{18}\text{F}$ FET), 3,4-dihydroxy-6- $^{18}\text{F}$ fluoro-L-phenylalanine ( $^{18}\text{F}$ FDOPA) and 3'-deoxy-3'- $^{18}\text{F}$ fluoro-thymidine ( $^{18}\text{F}$ FLT) [20,27–29]. Whilst  $^{18}\text{F}$ FDG PET is widely available, the high physiological brain uptake of glucose and the non-specific uptake in cerebral inflammatory processes hampers applications of  $^{18}\text{F}$ FDG PET for brain tumor delineation and diagnosis. Amino acid radiopharmaceuticals designated for PET have improved diagnostic glioma PET imaging towards the delineation of tumor extent, treatment planning, visualization of treatment-related changes and the assessment of treatment response [21]. PET radiopharmaceutical choline analogues are considered successful as oncological PET probes because a major hallmark of cancer cells is increased lipogenesis. In the brain, discrimination between

tumor and normal tissue is feasible because of lower physiological uptake of  $^{11}\text{C}$ choline ( $^{11}\text{C}$ Cho) or  $^{18}\text{F}$ fluoroethyl-choline ( $^{18}\text{F}$ FCho) by normal brain cells [30,31]. The performance of  $^{18}\text{F}$ FCho-PET may distinguish high-grade glioma, brain metastases and benign lesions in addition to its importance for surgery management (including identifying the most malignant areas for stereotactic sampling) [32–35]. As hypoxia plays an important role in GB pathology, its detection and monitoring using PET/SPECT became clinically relevant. Radiopharmaceuticals used for these investigations include ( $^{18}\text{F}$ fluoro-misonidazole ( $^{18}\text{F}$ FMISO),  $^{18}\text{F}$ fluoro-azomycin arabinoside ( $^{18}\text{F}$ FAZA),  $^{18}\text{F}$ fluoro-erythro-nitroimidazole ( $^{18}\text{F}$ FET-NIM), 2-(2-nitro-1-H-imidazol-1-yl)-N-(2,2,3,3,3-penta- $^{18}\text{F}$ fluoropropyl)-acetamide ( $^{18}\text{F}$ EF5),  $^{18}\text{F}$ flortanidazole ( $^{18}\text{F}$ F-HX4), and Copper(II)- $^{64}\text{Cu}$ diacetyl-di(N4-methylthiosemicarbazone ( $^{64}\text{Cu}$ Cu-ATSM)) [36].

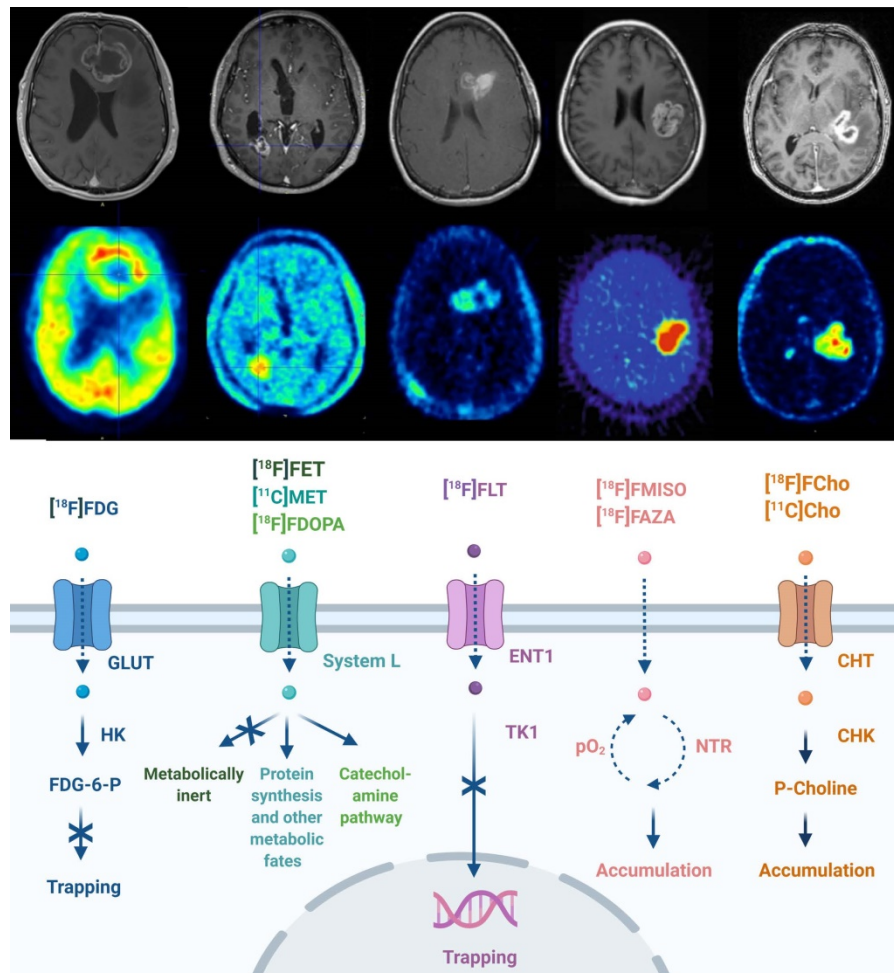


**Figure 1. Routine PET imaging in neuro-oncology.** PET/CT techniques for neuropathologic imaging are dominated by radiopharmaceuticals focussing on altered glucose metabolism (desoxy-2- $^{18}\text{F}$ fluoro-D-glucose ( $^{18}\text{F}$ FDG)), amino acid metabolism (L- $^{11}\text{C}$ -methyl-methionine ( $^{11}\text{C}$ MET), O-2- $^{18}\text{F}$ fluoroethyl-L-tyrosine ( $^{18}\text{F}$ FET), 3,4-dihydroxy-6- $^{18}\text{F}$ fluoro-L-phenylalanine ( $^{18}\text{F}$ F-DOPA)), proliferation (3'-deoxy-3'- $^{18}\text{F}$ fluoro-thymidine [ $^{18}\text{F}$ FLT]), tumoral hypoxia sensing ( $^{18}\text{F}$ fluoro-misonidazole ( $^{18}\text{F}$ FMISO),  $^{18}\text{F}$ fluoro-azomycin arabinoside ( $^{18}\text{F}$ FAZA)), and lipid metabolism ( $^{11}\text{C}$ choline ( $^{11}\text{C}$ Cho),  $^{18}\text{F}$ fluoroethyl-choline ( $^{18}\text{F}$ FCho)). Abbreviations: High affinity choline transporter (CHT), choline kinase (CHK), equilibrative nucleoside transporter (ENT), 2'-fluoro-2'-deoxy glucose-6-phosphate (FDG-6-P), glucose transporter (GLUT), hexokinase (HK), nitroreductase (NTR), partial pressure of oxygen ( $p\text{O}_2$ ), Na<sup>+</sup>-independent plasma membrane amino acid transport (System L), thymidine kinase (TK). Adapted with permission from [18], copyright 2017 Codon Publications.

An exhaustive list of the emerging PET and SPECT radiopharmaceuticals, matched with their biological targets, is summarized in **Table 1**. The rationale for the use of selected examples is described briefly as follows: The translocator protein (TSPO) is a mitochondrial membrane protein highly expressed in activated microglia, macrophages, and neoplastic cells. Imaging with the TSPO ligand [ $^{11}\text{C}$ ]-(*R*)-PK11195 demonstrated increased binding in high-grade glioma compared to low-grade gliomas and normal brain parenchyma in patients [37]. [ $^{18}\text{F}$ ]-GE-180-PET further provided a remarkably high tumour-to-background contrast in GB [38]. Radiolabeling of poly ADP ribose polymerase (PARP) inhibitors is gaining interest with numerous preclinical studies and an ongoing clinical trial in GB patients using [ $^{18}\text{F}$ ]-FluorThanatrace ([ $^{18}\text{F}$ ]-TT)-PET/CT (NCT04221061) [36,39-43]. The first clinical results of [ $^{18}\text{F}$ ]-Fluciclovine ([ $^{18}\text{F}$ ]-ACBC) for GB imaging were promising and radiolabelling of receptor tyrosine kinase inhibitors and mammalian target of rapamycin (mTOR) pathway inhibitors has also shown potential [44-51]. It is noted that PET imaging using the deoxycytidine kinase substrate [ $^{18}\text{F}$ ]-clofarabine has been shown to be a good imaging tool to localise and quantify responses in GB patients undergoing immunotherapy [52]. In addition to their application as diagnostic biomarkers, the use of theranostic (pairs of) radiopharmaceuticals that enable concomitant or subsequent imaging and therapy is gaining importance although not all have been validated in clinical trials. The  $\alpha\text{V}\beta\text{3}$  integrin receptor-targeting agent AI[ $^{18}\text{F}$ ]-NOTA-PRGD2 showed positive results in assessing sensitivity to concurrent chemoradiotherapy in GB patients. Therapeutic radionuclides coupled to arginine-glycine-aspartate (RGD) based vectors, already available, offer potential theranostic applications to target tumour angiogenesis [53]. The theranostic potential of [ $^{64}\text{Cu}/^{67}\text{Cu}$ ]Cu-cyclam-RAFT-c(RGDfK) $_4$  to treat GB *in vivo* shows promise [54-56]. Moreover, as the Food and Drug Administration (FDA) approved somatostatin receptor 2 (SSR2) targeting, gallium-68-labeled octreotide derivatives were approved ([ $^{68}\text{Ga}$ ]Ga-DOTA-TOC; alternately [ $^{68}\text{Ga}$ ]Ga-DOTA-NOC and -TATE are utilized) and subsequently studied for GB imaging. However, their specificity and selectivity towards GB have not yet been clinically determined [57,58]. Nevertheless, pilot studies in glioma patients with gallium-68- and yttrium-90-labeled SSR2-targeting ligands, have been performed [59-62]. Additionally, a fibroblast activation protein inhibitor (FAPI) labelled with gallium-68 ([ $^{68}\text{Ga}$ ]Ga-FAPI) was introduced into clinical investigations and exhibited significant uptake in IDH-wildtype GB tumours, grade III and

grade IV IDH-mutant gliomas. FAPI-targeted theranostics (pairing or gallium-68 and yttrium-90 or gallium-68 and lutetium-177) were developed. However, due to the short retention time, radionuclides with shorter half-lives (e.g. rhenium-188, samarium-153, bismuth-213 or lead-212) appeared preferable [63-65]. Furthermore, a growing number of copper-based PET tracers are being studied for use in GB investigations, with the emerging theranostic copper-64 and copper-67, characterised by a joint positron/ Auger electron and joint beta/gamma emission, respectively. In patients, PET imaging using [ $^{64}\text{Cu}$ ]CuCl $_2$  has visualized brain cancerous lesions and initial investigations using [ $^{64}\text{Cu}$ ]Cu- or [ $^{62}\text{Cu}$ ]Cu-ATSM-PET imaging may address the hypoxia status of GB, non-invasively [66-69]. Preclinically,  $^{64}\text{Cu}$ -labelled peptides and  $^{64}\text{Cu}$ -labelled cetuximab have shown promise in imaging of VEGFR and EGFR expression, respectively [70-74]. Other preliminary theranostic applications studied *in vivo* include [ $^{64}\text{Cu}$ ]Cu-ATSM, [ $^{64}\text{Cu}/^{67}\text{Cu}$ ]Cu-cyclam-RAFT-c(RGDfK) $_4$  ( $\alpha\text{V}\beta\text{3}$  integrin), [ $^{64}\text{Cu}$ ]Cu-PEP-1L (IL-13 receptor) and [ $^{64}\text{Cu}$ ]Cu-IIIa4 (ephrin type-A receptor 3) [55,56,70-77]. Interestingly, prostate-specific membrane antigen (PSMA) expression has been confirmed in the neovasculature of GB and the diagnostic role of radiolabelled PSMA PET/CT or PET/MRI in patients with gliomas and GBs has recently been reviewed [78-81]. In particular, the radiolabelled ligand [ $^{68}\text{Ga}$ ]Ga-Glu-urea-Lys(Ahx)-HBED-CC ([ $^{68}\text{Ga}$ ]Ga-PSMA-11) has shown positive results in visualizing residual or recurring GB [82,83]. A proof of concept for the theranostic potential of [ $^{68}\text{Ga}$ ]Ga-PSMA-11/[ $^{177}\text{Lu}$ ]Lu-PSMA-617 in GB has demonstrated success in 2 recent case reports [84,86]. However, large prospective studies are needed to clarify the diagnostic role of the radiolabelled PSMA ligands in GB imaging. To date, some studies are featuring imaging of cerebral cancer using novel [ $^{89}\text{Zr}$ ]Zr-/[ $^{18}\text{F}$ ]F-labelled PSMA compounds; however, the preclinical applications particularly using GB animal models are limited to one study [87-91].

## 2.2 Selection of the appropriate theranostic pair for individualised treatment

Diverse information summarised in **Table 1**, demonstrates that a broad spectrum of investigations in the field of neuro-oncology imaging are well underway. Despite the development of a variety of imaging strategies, evident in **Table 1** for example, only the most effective will be evaluated in clinical trials and, if deemed appropriate, become routinely available in Nuclear Medicine. Theranostics and nanotheranostics which include the future of theranostics and precision oncology are reviewed

[22,94,95]; for such endotherapies, visualization of GB tumour tissue is critical to predict prognosis accurately including loss in brain function. Additionally, the tracer coupled to the therapeutic radionuclide and the imaging radionuclide should not alter the drug's binding, pharmacokinetics or BBB crossing characteristics. **Table 2** lists targeted radionuclides and theranostic pairs appropriate for GB, including their advantages and disadvantages.

Examples for GB include [<sup>68</sup>Ga]Ga-DOTA-SP co-injection with [<sup>213</sup>Bi]Bi-DOTA-SP to assess the biodistribution using PET/CT and [<sup>68</sup>Ga]-pentixafor-PET/CT as a tool for *in vivo* quantification of CXCR4. This will facilitate the selection of patients who might benefit from CXCR4-directed therapy. Another example is [<sup>131</sup>I]-labeled anti-tenascin murine 81C6 mAb SPECT to assess the distribution of the radiolabeled mAb in brain parenchyma [93-96].

**Table 1.** Investigational PET/SPECT imaging in neuro-oncology

Biological target		Radiopharmaceuticals <sup>(6)</sup>	Vector <sup>(7)</sup>	References
Amino acid metabolism	C	[ <sup>18</sup> F]F-ACBC [ <sup>18</sup> F]F-tryptophan [ <sup>18</sup> F]F-Glutamine [ <sup>18</sup> F]F-FSPG [ <sup>123</sup> I]iodo-IMT [ <sup>123</sup> I]iodo-IPA	AA AA AA AA AA AA	[49,51,311-317] [318-323] [324] [325] [326] [326-328]
	P	[ <sup>18</sup> F]F-ELP [ <sup>18</sup> F]F-AMPe [ <sup>18</sup> F]F-A(M)Hep [ <sup>11</sup> C]-/ [ <sup>18</sup> F]F-tryptophan [ <sup>18</sup> F]F-Glutamine [ <sup>18</sup> F]F-IMP	AA AA AA AA AA AA	[329,333] [331] [332] [333-335] [336,337] [338]
Angiogenesis (Integrin receptor family)	C	[ <sup>18</sup> F]F-/ [ <sup>68</sup> Ga]Ga-PRGD2	Pep	[53,339-342]
	P	[ <sup>64</sup> Cu]Cu-PEG <sub>4</sub> -c(RGDyK) [ <sup>68</sup> Ga]Ga-c(GDGEAyK) [ <sup>111</sup> In]In-abegrin™ [ <sup>99m</sup> Tc]Tc-NC100692 [ <sup>18</sup> F]F-fluciclatide [ <sup>18</sup> F]F-PPRGD2 [ <sup>18</sup> F]F-RGD-K5/ [ <sup>68</sup> Ga]Ga-RGD [ <sup>64</sup> Cu]Cu-c(RGDfK) <sub>2</sub> [ <sup>64</sup> Cu]Cu-c(RGDfK) <sub>4</sub> [ <sup>64</sup> Cu]Cu-PEG <sub>4</sub> -E[PEG <sub>4</sub> -c(RGDfK)] <sub>2</sub> [ <sup>64</sup> Cu]Cu-Gly <sub>3</sub> -E[Gly <sub>3</sub> -c(RGDfK)] <sub>2</sub> [ <sup>18</sup> F]F-alfatide II	Pep Pep Ab Pep Pep Pep Pep Pep Pep Pep Pep Pep Pep	[343] [344] [345] [346] [347] [348] [349] [350] [54] [351] [351] [352]
Angiogenesis (Vascular endothelial growth factor receptor)	C	[ <sup>123</sup> I]iodo-VEGF-165	Prot	[353]
	P	[ <sup>111</sup> In]In-ZVEGFR2-Bp2 [ <sup>89</sup> Zr]Zr-bevacizumab [ <sup>64</sup> Cu]Cu-VEGF121 [ <sup>64</sup> Cu]Cu-VEGF125-136 [ <sup>111</sup> In]In-hnTf-VEGF	Abf Ab Prot Pep Pro	[354] [355] [72,74] [356] [357]
Epidermal growth factor receptor	C	[ <sup>11</sup> C]-CPD153035	SM	[358]
	P	[ <sup>124</sup> I]/ [ <sup>131</sup> I]iodo-IPQA [ <sup>11</sup> C]-/ [ <sup>18</sup> F]F-ML01/-03/-04 [ <sup>64</sup> Cu]Cu-/ [ <sup>111</sup> In]In-cetuximab [ <sup>111</sup> In]In-/ [ <sup>125</sup> I]iodo-ch806 [ <sup>18</sup> F]F-BEM-/ [ <sup>68</sup> Ga]Ga-ZEGFR.1907 [ <sup>89</sup> Zr]Zr-nimotuzumab [ <sup>188</sup> Re]Re-U2 (c) [ <sup>18</sup> F]F-B-ME07 (°) [ <sup>111</sup> In]In-hEGF	SM SM Ab Ab Abf Ab ON ON Ab	[359] [360] [361,362] [363,364] [365] [366] [367] [368] [369]
Chemokine receptor 4	C	[ <sup>68</sup> Ga]Ga-pentixafor	Pep	[94]
	P	[ <sup>11</sup> C]methyl-AMD3465	SM	[370]
Ephrin receptors	C	[ <sup>89</sup> Zr]Zr-ifabotuzumab	Ab	[371]
	P	[ <sup>64</sup> Cu]Cu-III A4 [ <sup>64</sup> Cu]Cu-TNYL-RAW [ <sup>64</sup> Cu]Cu-1C1	Ab Pep Ab	[77] [40] [362]
Hypoxia	C	[ <sup>18</sup> F]F-DiFA [ <sup>62</sup> Cu]/ [ <sup>64</sup> Cu]Cu-ATSM [ <sup>18</sup> F]F-EETNIM	SM SM SM	[372] [373-375] [376]
	P	[ <sup>18</sup> F]F-RP170 [ <sup>18</sup> F]F-HX4 [ <sup>62</sup> Cu]/ [ <sup>64</sup> Cu]Cu-ATSM	SM SM SM	[377] [378] [55,67,75,379]
Poly (ADP-ribose) polymerase	C	[ <sup>18</sup> F]F-TT	SM	[380]
	P	[ <sup>18</sup> F]F-/ [ <sup>123</sup> I]iodo-olaparib [ <sup>123</sup> I]iodo-MAPi [ <sup>123</sup> I]/ [ <sup>124</sup> I]/ [ <sup>131</sup> I]iodo-2-PARPi [ <sup>18</sup> F]F-PARPi-(FL)	SM SM SM SM	[39,381] [382] [43] [383]
Glutamate Carboxypeptidase 2	C	[ <sup>89</sup> Zr]Zr-IAB <sub>2</sub> M [ <sup>18</sup> F]F-DCFPyL	Abf Pep	[384] [385]

		[ <sup>68</sup> Ga]Ga-PSMA-617 [ <sup>68</sup> Ga]Ga-PSMA-11 [ <sup>18</sup> F]F-PSMA-1007	Pep Pep Pep	[386] [38,82,83,387-389] [90]
	P	[ <sup>18</sup> F]F-DCFPyL [ <sup>68</sup> Ga]Ga-PSMA-11	Pep Pep	[91] [91]
Translocator protein (neuronal type) ( <sup>68</sup> )	C	[ <sup>11</sup> C]-PK11195 [ <sup>18</sup> F]F-GE-180 [ <sup>123</sup> I]iodo-CLINDE	SM SM SM	[390] [38,85,391] [392]
	P	[ <sup>18</sup> F]F-14 (E) [ <sup>18</sup> F]F-VUIS1007 [ <sup>18</sup> F]DPA-714 [ <sup>18</sup> F]F-PBR06 [ <sup>18</sup> F]F-VC701 [ <sup>18</sup> F]F-AB5186	SM SM SM SM SM SM	[393] [394] [395-499] [400,401] [402] [403]
Matrix-metalloproteinases	C	[ <sup>131</sup> I]iodo-TM-601	SM	[239,404]
	P	[ <sup>89</sup> Zr]Zr-LEM2/5 [ <sup>18</sup> F]F-BR-351 [ <sup>18</sup> F]F-P-chlorotoxin [ <sup>18</sup> F]F-iCREKA [ <sup>68</sup> Ga]Ga- / [ <sup>64</sup> Cu]Cu-MMP-14	Ab SM SM Pep Pep	[405] [399] [406] [407] [408]
Fibroblast activation protein	C	[ <sup>68</sup> Ga]Ga-FAPI	SM	[63,409,410]
	P	[ <sup>18</sup> F]F-SiFa <sub>(Cl)<sub>6</sub></sub> FAPI	SM	[411]
Lipid metabolism( <sup>++</sup> )	C	[ <sup>11</sup> C]- / [ <sup>18</sup> F]F-(ethyl)choline [ <sup>11</sup> C]-Acetate	SM SM	[30-32,412,413] [414,415]
	P	[ <sup>18</sup> F]F-FPIA(*)	SM	[416]
Fibronectin (neuronal)	C	[ <sup>123</sup> I]iodo-L19( <sup>scFv</sup> ) <sub>2</sub>	Abf	[417]
	P	[ <sup>18</sup> F]F-iCREKA	Pep	[418]
Apoptosis	C	[ <sup>18</sup> F]F-ML10	SM	[419,420]
Sigma receptor	C	[ <sup>18</sup> F]F-fluspidine (*)	SM	[421-423]
Somatostatin receptor 2	C	[ <sup>68</sup> Ga]Ga- / [ <sup>111</sup> In]In-octreotide [ <sup>68</sup> Ga]Ga-octreotide	Pep Pep	[58,424] [425,426]
Deoxycytidine Kinase	C	[ <sup>18</sup> F]F-clofarabine	SM	[52,427]
Neurokinin 1 receptor	C	[ <sup>68</sup> Ga]Ga-Substance-P	Pep	[93,105]
Copper Transporter 1	P	[ <sup>64</sup> Cu]Cu-(gold)nanocluster( <sup>+</sup> )	( <sup>**</sup> )	[428]
Carbonic Anhydrase IX	P	[ <sup>18</sup> F]F-VM4-037	SM	[429]
Tenascin-C	P	[ <sup>99m</sup> Tc]Tc-TTA1 [ <sup>18</sup> F]F- / [ <sup>64</sup> Cu]Cu-GBI-10	ON ON	[430] [431]
Histone deacetylases	P	[ <sup>18</sup> F]TFAHA 2-[ <sup>18</sup> F]BzAHA	SM SM	[432] [433]
Isocitrate Dehydrogenase 1	P	[ <sup>18</sup> F]-triazine-diamine [ <sup>18</sup> F]F- / [ <sup>131</sup> I]iodo- / [ <sup>125</sup> I]iodo-AGI <sup>5198</sup> [ <sup>18</sup> F]F- / [ <sup>125</sup> I]iodo-X ( <sup>**</sup> ) [ <sup>11</sup> C]-Acetate	SM SM SM SM	[434] [435] [436] [437]
Iron transport	P	[ <sup>67</sup> Ga] / [ <sup>68</sup> Ga]Ga-citrate	SM	[438]
Glutathione transferase	P	[ <sup>18</sup> F]F-BuEA-GS	SM	[439,440]
Hepatocyte growth factor receptor	P	[ <sup>89</sup> Zr]Zr- / [ <sup>76</sup> Br]Br-onartuzumab [ <sup>89</sup> Zr]Zr-rilotumumab [ <sup>64</sup> Cu]Cu-rh-HGF	Ab Ab Pep	[441] [442] [443]
Mammalian target of rapamycin	P	[ <sup>89</sup> Zr]Zr-transferrin	Prot	[44,444]
Tyrosine kinases	P	[ <sup>18</sup> F]F-dasatinib [ <sup>64</sup> Cu]Cu-vandetanib	SM SM	[445] [445]
Myeloid cells	P	[ <sup>89</sup> Zr]Zr-anti-CD11b	Ab	[446]
Platelet-derived growth factor receptor	P	[ <sup>68</sup> Ga]Ga- / [ <sup>111</sup> In]In-ZO9591 [ <sup>131</sup> I]iodo- / [ <sup>18</sup> F]F-imatinib [ <sup>18</sup> F]F-dasatinib	Abf SM SM	[369,447] [448] [445]
Stem cells	P	[ <sup>64</sup> Cu]Cu-AC133 [ <sup>64</sup> Cu]Cu- / [ <sup>89</sup> Zr]Zr-YY146	Ab Ab	[449] [450,451]

(<sup>S</sup>) radiopharmaceutical are grouped as in preclinical (P) and clinical (C) stages of development; chelating agents for radiometal complexation were not denoted in the names to improve clarity of presentation; (++) Fatty acid synthesis (acetate) and choline metabolism for choline; pivalic acid undergoes intracellular metabolism via the fatty acid oxidation pathway (an aberrant lipid metabolite detection). (E) no trivial name available- UPAC: 7-chloro-N,N,5-trimethyl-4-oxo-3-(6-[<sup>18</sup>F]fluoropyridin-2-yl)-3,5-dihydro-4H-pyridazino[4,5-b]indole-1-acetamide, (<sup>\*\*</sup>) no names given - a small library of nonradioactive analogs were designed and synthesized based on the chemical structure of reported butyl-phenyl sulfonamide enzyme inhibitors, (\*) currently in clinical translation, (c) DNA-based oligonucleotide (aptamer), (°) RNA based oligonucleotide (aptamer), (<sup>\*\*</sup>) protein-mimic cluster, (+) dual-imaging modality - investigatory (proof-of-concept), (<sup>68</sup>) expressed on glioma-associated macrophages and microglia, (†) vectors: amino-acid (AA), antibody (Ab), antibody fragment (Abf), small biomolecule (SM), peptide (Pep), protein (Prot), oligonucleotide (ON).

### 3. Selection of the optimal target for imaging and TRT of GB

An important consideration for the selection of a GB target for TRT is the abundance of the molecular

target present in the tumour versus its negligible presence in normal cells. The target must have proven of relevance for therapy and the finally selected compound must demonstrate bioequivalence at the target site and the radiopharmaceutical must be

retained within the tumour. The pathology of most GB tumours is not based on the dysregulation of a single pathway and therefore, a strategy with a multi-targeted design should also be considered [97].

For a more detailed explanation of the principles of optimal target selection for diagnostic, therapeutic and theranostic applications in nuclear medicine, please refer to the review by Lee *et al.* [98].

**Table 2.** Physical properties and pro/cons of therapeutic radionuclides studied for glioblastoma therapy

Isotope	Range ( <i>in vivo</i> ) (mm)	T ½ (h)	Paired Isotope	Pro's for GB TRT	Cons for GB TRT	Studies in GB
<sup>225</sup> Ac 100.0% α	0.04-0.10	238.10	<sup>68</sup> Ga	<ul style="list-style-type: none"> <li>• <i>In vivo</i> range optimal for recurrent/residual GB.</li> <li>• High LET/RBE efficient towards hypoxic GB areals.</li> <li>• DOTA-complexation-simple and universal (some peptides, small molecules and mAb-fragments).</li> <li>• T ½ allows transport; RIT compatible; ideal if no leakage from the target site (upon compound internalization).</li> </ul>	<ul style="list-style-type: none"> <li>• Relatively long T ½ + multiple alpha particles generated (rapid decay chain) → substantial <sup>225</sup>Ac-based cytotoxicity [105].</li> <li>• Recoiled daughters may influence stability.</li> <li>• Not readily available worldwide.</li> </ul>	<p>C Substance P (NK-1) [93]</p> <p>P E4G10 mAb (Cadherin 5) [452]; IA-TLs (avβ3 integrin) [453]; Pep-1L (IL13RA2) [454]</p>
<sup>213</sup> Bi 2.2% α 97.8% β <sup>-</sup>	0.05-0.10	0.77	<sup>68</sup> Ga <sup>44</sup> Sc	<ul style="list-style-type: none"> <li>• <i>In vivo</i> range optimal for recurrent/residual GB.</li> <li>• High LET/RBE efficient towards hypoxic GB areals.</li> <li>• DOTA-complexation - simple and universal (some peptides, small molecules and mAb-fragments).</li> <li>• Short T ½ + gamma-energy combination efficient even upon lack of persistent internalization [105].</li> <li>• Availability: <sup>225</sup>Ac-/<sup>213</sup>Bi-generators.</li> <li>• Energy (440 keV) allows for PK/D assays.</li> <li>• Optimal formulation for intratumoral injection or CED, highly localized radioactive decay <i>versus</i> low off target effects [130].</li> </ul>	<ul style="list-style-type: none"> <li>• Short T ½ compromises the residence time required in essential (infiltrating) GB cells, i.e. ratio between cell membrane coverage (receptor affinity) and time is key (Note: irrelevant for intratumoral injection or CED).</li> </ul>	<p>C Substance P (NK-1) [105,114,241,242]</p>
<sup>211</sup> At 42.0% α 58.0% EC	0.05 [127]	7.20 [127]	<sup>125</sup> I <sup>76</sup> Br	<ul style="list-style-type: none"> <li>• <i>In vivo</i> range optimal for recurrent/residual GB.</li> <li>• High LET/RBE efficient towards hypoxic GB areals.</li> <li>• Longer T ½ allows for multistep synthetic procedures and transport.</li> <li>• Daughter (<sup>211</sup>Po): emits KX-rays useful for sample counting and <i>in vivo</i> scintigraphic imaging [244].</li> <li>• Well-suited for intratumoral injection or CED, highly localized radioactive decay <i>versus</i> low off target (systemic) effects [130].</li> </ul>	<ul style="list-style-type: none"> <li>• Limited to mAb (smaller fragments).</li> <li>• Production exclusive to a rare 25-30 MeV cyclotron (± 30 sites worldwide).</li> <li>• Often low biological/chemical stability [455].</li> </ul>	<p>C 81C6 mAb G (tenascin-C) [244]</p> <p>P L8A4 mAb (EGFRvIII) [456]</p>
<sup>131</sup> I 97.2% β <sup>-</sup> 2.8% γ	0.80 [127]	192.00 [127]	✓	<ul style="list-style-type: none"> <li>• <i>In vivo</i> range (long) efficient on the common GB type (bulky/heterogeneous/2.6-5.0 mm).</li> <li>• Good availability and relatively inexpensive.</li> <li>• Longer T ½ allows transport, compatible for RIT.</li> <li>• Well-understood radiochemistry; universally applicable (peptides, small molecules, mAb).</li> <li>• 10% gamma emission makes it a theranostic (clinical SPECT - or gamma cameras widespread application for patient dosimetry) [260].</li> </ul>	<ul style="list-style-type: none"> <li>• Limited SPECT imaging capacity (suboptimal quantitative imaging); poor spatial resolution (high energy collimators/thick crystal detectors setup).</li> <li>• Radiolabeled proteins degrade rapidly when internalized into tumors; recurrence of [<sup>131</sup>I]iodo-tyrosine and <sup>131</sup>I-activity in the blood pool → thyroid toxicity plausible.</li> </ul>	<p>C 81C6 mAb (tenascin-C) [98,208,209,446] BC-2/4 mAb (tenascin-C) [204,207] chTNT-1/B mAb (DNA-histone H1) [236-238] TM601 [239] Phenylalanine (IPA) [458]</p> <p>P L19SIP (Fibronectin) [459,460] PARPi (PARP1) [280] I2-PARPi (PARP1) [43] L8A4 mAb (EGFRvIII) [461,462] IPQA (EGFR) [359] Hyaluronectin glycoprotein [463] Phenylalanine (IPA) [464-466]</p>
<sup>90</sup> Y 100.0% β <sup>-</sup>	5.30 [127]	64.10 [127]	<sup>68</sup> Ga <sup>86</sup> Y <sup>111</sup> In	<ul style="list-style-type: none"> <li>• <i>In vivo</i> range (long) efficient on the common GB type (primary/bulky/heterogeneous/≥ 3 cm).</li> <li>• DOTA-complexation-simple and universal (some peptides, small molecules and mAb-fragments).</li> <li>• Stably retention by GB cells even after endocytosis [108].</li> <li>• Emits highly energetic β-particles [108], ideal for therapy of radioresistant GB.</li> <li>• Longer T ½ allows transport, compatible for RIT.</li> </ul>	<ul style="list-style-type: none"> <li>• Limited efficiency for minimal residual or recurrent GB: needs to be matched with GB tumor size to prevent off target (normal brain) toxicity.</li> <li>• Impractical for nuclear imaging, i.e. high activities (&gt;300 MBq) required (only succeeded for microsphere-based therapies (SIRT) for treating liver tumours [162].</li> <li>• Limited dose administration (preventing nephrotoxic and hematotoxic side effects).</li> </ul>	<p>C Octreotide (SSTR) [59-61] Lanreotide (SSTR) [62] BC-2/4 mAb (tenascin-C) [467] Biotin [149] Substance-P [241]</p> <p>P Abegrin [468]</p>
<sup>177</sup> Lu 100.0% β <sup>-</sup>	0.62-2.00 [127]	158.40 [127]	✓ or <sup>68</sup> Ga <sup>89</sup> Zr <sup>90m</sup> Tc	<ul style="list-style-type: none"> <li>• Isotope characteristics capable of affecting GB lesions typically ø &lt; 3 mm diameter [474].</li> <li>• Longer T ½ is compatible with the PK/D and radiochemistry for mAb and proteins [127].</li> <li>• Fairly straightforward conjugation chemistry [127,470].</li> </ul>	<ul style="list-style-type: none"> <li>• Moderately nephrotoxic and hematotoxic (&lt; <sup>90</sup>Y).</li> </ul>	<p>C Substance-P (NK-1) [241] PSMA-617 [84,86]</p> <p>P 6A10 Fab (CAXII) [471] CXCR4-L (CXCR4) [472] VH-DO33 (LDLR) [473] 2.5D/2.5F (Integrin) [474]</p>

				<ul style="list-style-type: none"> <li>• Good availability and low cost [469].</li> <li>• Emission of low-energy gamma - true theranostic [127].</li> <li>• [<sup>177</sup>Lu]Lu-mAb: higher specificity index (i.e. less non-specific cell killing) than analogous [<sup>90</sup>Y]Y-mAb [156].</li> </ul>			<b>L8A4 mAb</b> (EGFRvIII) [475,476] <b>III A4 mAb</b> (EphA3) [77]
<sup>188</sup> Re 100.0% β <sup>-</sup>	5.00-10.8	16.98	✓	<ul style="list-style-type: none"> <li>• <i>In vivo</i> range (long) efficient on the common GB type (primary/bulky/heterogeneous/≥ 3 cm).</li> <li>• Readily available and inexpensive via <sup>188</sup>W-/<sup>188</sup>Re-generator (carrier-free, high specific activity).</li> <li>• Gamma emission suitable for imaging (better image quality than <sup>186</sup>Re).</li> </ul>	Unfavorably-low energy characteristics [114]. Radioactive source material for generator production: Reactor-based <sup>188</sup> W production only in 2-3 reactors worldwide [482].	C P	<b>Nimotuzumab</b> (EGFR) [248,483] <b>PEG-nanoliposome</b> [440] <b>BMSC implantation</b> [479] <b>Nanocarriers</b> (CXCR4) [150] <b>Lipid nanocapsules</b> [480,481] <b>Microspheres in fibrin glue gel</b> [482] <b>U2 DNA aptamer</b> (EGFRvIII) [483,484]
<sup>64</sup> Cu 18.0% β <sup>+</sup> 39.0% β <sup>-</sup> 42.5% EC 0.5% γ	β 1.00 AE 0.13 [485]	12.70	✓	<ul style="list-style-type: none"> <li>• Readily available.</li> <li>• Radiometal complexation well understood and universally applicable (most peptides/mAb/small molecules and nanoparticles).</li> <li>• Combined β<sup>+</sup>/β<sup>-</sup> emission makes it a true theranostic.</li> <li>• Radioisotope salts ([<sup>64</sup>Cu]CuCl<sub>2</sub>): the higher intratumoral accumulation of Cu correlates with overexpression of human copper transporter 1 (hCTR1) in GB cancer cells [486].</li> <li>• AE cascade from EC are considered high LET radiation with ~ 2 keV of average energy [485].</li> </ul>	<ul style="list-style-type: none"> <li>• Radiometal complexation can be unstable <i>in vivo</i> [486,487].</li> <li>• Lack of radiometal-specific chelating agents.</li> <li>• Radiation dosimetry: complex decay scheme affects absorbed dose from high-LET AE emissions [485].</li> </ul>	P	<b>CuCl<sub>2</sub></b> [54,75,184,498,489] <b>Cyclam-RAFT-c(RGDfK)4</b> (αvβ3 integrin) [54] <b>PeP-1L</b> (IL13RA2) [454] <b>ATSM</b> (Hypoxia) [75] <b>III A4 mAb</b> (EphA3) [77] <b>TNYL-RAW</b> (EPHR) [40] <b>1C1 mAb</b> (EphA2) [362]
<sup>67</sup> Cu 100.0% β <sup>-</sup>	0.20	62.40	✓ or <sup>64</sup> Cu	<ul style="list-style-type: none"> <li>• Treats small residual or recurrent GB lesions (ø ≤5 mm) [56].</li> <li>• Combined β<sup>+</sup>/β<sup>-</sup> emission makes it a true theranostic.</li> <li>• Supports SPECT imaging of patient dosimetry [490].</li> <li>• Biochemistry of copper is well studied; radiometal complexation well understood and universally applicable (most peptides/mAb/small molecules and nanoparticles) [56,491].</li> <li>• No off-target toxicity reported (bone or organs).</li> <li>• Radioisotope salts ([<sup>67</sup>Cu]CuCl<sub>2</sub>): the higher intratumoral accumulation of copper correlates with overexpression of human copper transporter 1 (hCTR1) in GB cancer cells [486].</li> </ul>	<ul style="list-style-type: none"> <li>• Large amounts rarely available; limits research and clinical trial design [491].</li> </ul>	P	<b>RAFT-c(RGDfK)4</b> (αvβ3 integrin) [56]
<sup>125</sup> I 100.0% EC	0.002	1425.60	<sup>111</sup> In	<ul style="list-style-type: none"> <li>• Isotope applicable in brachytherapy for GB.</li> <li>• Systemic immune-therapy well tolerated [163].</li> </ul>	<ul style="list-style-type: none"> <li>• Very long T<sub>1/2</sub> may impose limitations for clinical use (radioprotection, therapeutic efficacy, slow dose rate).</li> <li>• Gamma emission energy not suitable for nuclear imaging.</li> <li>• Range and energy is not effective for heterogeneous radioresistant GB.</li> </ul>	C	<b>425 mAb</b> (EGFR) [163,166,167,227,492,495]
						P	<b>L8A4 mAb</b> (EGFRvIII) [499,500] <b>UdR</b> [165,496] <b>806 mAb</b> (EGFRvIII) [363]
<sup>125</sup> I 97.0% EC 3.0% γ	0.001-0.01	13.20	✓	<ul style="list-style-type: none"> <li>• Short T<sub>1/2</sub> and gamma emission energy suitable for scintigraphic imaging <i>in vivo</i>.</li> <li>• More suitable choice for potential use in RIT (as to <sup>125</sup>I) [156].</li> </ul>	<ul style="list-style-type: none"> <li>• Not widely available (&lt;<sup>131</sup>I).</li> <li>• T<sub>1/2</sub> is not compatible for PK/D investigation.</li> </ul>	P	<b>MAPI</b> (PARP1) [382]
<sup>111</sup> In 100.0% EC	0.04	67.20	✓	<ul style="list-style-type: none"> <li>• Characteristic suitable for <i>in vitro</i> GB studies.</li> <li>• True theranostic: gamma emission energy allows scintigraphic imaging <i>in vivo</i>.</li> </ul>	<ul style="list-style-type: none"> <li>• Complexation chemistry required; incorporation kinetics slow for radiolabeling mAb (no direct radiometal conjugation).</li> </ul>	P	<b>GA17 Ab</b> (α3 integrin) [497] <b>806 mAb</b> (EGFRvIII) [497]

(✓) Theranostic radionuclide, (\*) human case study, convection enhanced delivery (CED), pharmacokinetic/dosimetry studies (PK/D), glioblastoma (GB), radioimmunotherapy (RIT), oxygen enhancement ratio (OER), polyethylene glycol (PEG), Bone-marrow mesenchymal stem cells (BMSC), electron capture (EC), linear energy transfer (LET), Auger electron (AE), single-photon emission computed tomography (SPECT), physiological half-life (T<sub>1/2</sub>).

### 3.1 GB target abundance, stability and specificity

Large-scale genomic (Cancer Genome Atlas (TCGA)) and proteomic analysis of GB tumours have uncovered potential targets that are deemed relevant to both imaging and therapy [99,100]. Abundantly expressed targets reduce the absolute need for a

radiopharmaceutical to have high molar activity (MA). Furthermore, due to the correlation between specific activity and MA, this provides the opportunity to use radionuclides with lower specific activity for the radiosynthesis. Antigenic targets are usually tumour cell surface-expressed macromolecules, which are easily accessible by compounds present in the blood pool or extracellular

fluid. In the case of GB, this includes cell surface glycoproteins [101,102], enzymes such as PSMA [79,80], glycolipids [103], stromal components [11], components of blood vessels (e.g. VEGF) [104] and signal transduction molecules (e.g. growth factor receptors) [97]. As an example, the target of substance-P (SP), the neurokinin-1 receptor, is an appropriate target due to the high prevalence on the membrane of GB cells with strong expression on the tumour vasculature, allowing concomitant dual targeting [105]. Another example is tenascin, an extracellular matrix glycoprotein overexpressed by GB and minimally presented in normal tissue with a significant role in angiogenesis, which demonstrated encouraging results in TRT trials with GB [106]. As the tumour microenvironment (TME), hypoxia and glioma stem cells are pivotal in GB progression and resistance, their cell surface markers and specific pathways present attractive and important target options [5,10,11,107].

A homogeneous antigen expression and a very high affinity of the drug to the target are more important for  $\alpha$ -emitting and AE-emitting radiopharmaceuticals, due to the fact that there is no cross-fire effect. For radio-immunotherapy (RIT), the antigen expression should be >100000 sites per cancer cell with a uniform density on the surface of all tumour cells, no expression on normal cells, and no dispersion into the bloodstream [108]. The choice of the vector is another challenge as antibodies provide the highest total in-tumour accumulation, while smaller molecules such as peptides provide the highest tumour-to-normal organ dose ratios [109,110].

Another desirable aspect for successful imaging and effectiveness of TRT is the degree of receptor internalisation (or of other surface macromolecules) upon binding, causing continued accumulation of the radionuclide intracellularly. Phenotypic instability is a reason for caution as complex epigenetic factors exist which can upregulate or downregulate target activation. The theranostic approach is particularly useful since it allows the visualisation and quantification of the specific molecular target during planning of the adequate therapeutic approach and more importantly during therapy follow-up. The necessity for continuous validation of target expression in GB therapy is considered in the ACT IV trial on rindopepimut in patients with EGFRvIII-positive GB. This study showed a striking loss of EGFRvIII expression at recurrence in both groups of the trial, suggesting that EGFRvIII expression is unstable, which could limit its use as a target for TRT [97].

In addition, it should be noted that the interplay of receptors, compound binding and cellular uptake

pathways may cause receptor saturation upon injection of therapeutic doses. TRT approaches for GB treatment are gaining momentum and have been reviewed [14,111,112]. However, in this review, an extensive overview of prospective targets on GB is presented (**Figure 2**). Other indications for TRT in neuro-oncology, include grade I-III glioma (e.g. radiolabeled SP and anti-EGFR TRT), brain metastasis (e.g.  $^{177}\text{Lu}$ ]Lu-/[ $^{225}\text{Ac}$ ]Ac-PSMA-617), meningioma (e.g. radiolabelled DOTA-TOC and DOTA-TATE), lymphoma (e.g. [ $^{90}\text{Y}$ ]-ibritumomab tiuxetan) and neuroblastoma (e.g. [ $^{131}\text{I}$ ]iodo-MIBG) [113,114].

When the identified targets in GB are compared with recent reviews listing current targeted therapies for GB, many possible strategies, which have received little attention, exist for imaging and TRT of GB [7,15,97,115]. Such unexplored pathways include: the phosphatidylinositol 3-kinase/Akt/mTOR pathway, the cell cycle pathway, the DNA repair pathway, the notch pathway, the hypoxia pathway and immune checkpoints. Unfortunately, issues such as specificity, selectivity, sensitivity, and feasible radiochemistry (especially molecular stability) challenge the design and synthesis of radiopharmaceuticals [116].

### 3.2 Blood-brain barrier permeability

Upon successful target selection, the most important factor in managing GB is the ability of the designed radiopharmaceutical to cross the BBB and reach this target. Failure to adequately circumvent the BBB and heterogeneous perfusion to the tumour could be partially responsible for any suboptimal compound delivery to brain tumours and the lack of tangible progress in the implementation of targeted therapeutics [117]. **Figure 3** gives an overview of the different mechanisms to cross the BBB, including passive mechanisms (1-3), mediated mechanisms (4-6) and a strategy to bypass the BBB (7) [118,119]. The mechanism is significantly affected by the choice of the vector, i.e. radiolabelled small molecules, peptides or monoclonal antibodies (mAbs). Small molecules have multiple options to cross the BBB while antibodies are very limited (0.1-0.2%/ID) [12,92,119-123]. Compromised integrity of the BBB is a pathophysiological component of GB infiltration which influences the passage of radiopharmaceutical drugs, by increasing the fraction of paracellular diffusion (**Figure 3** (3)). Importantly, this increased BBB permeability is dynamic, heterogeneous and can be absent along the infiltrating edges of the GB tumour [5,117,118]. This is confirmed by contrast-enhanced MRI where often not all GB components are characterized by gadolinium uptake, which represents leakage. Affinity for efflux transporters can counteract the uptake across the BBB

(Figure 3 (2)) and it should be noted that compound assortment by any existing intact BBB transport will be performed regarding enantiomers of several PET-radiopharmaceuticals (small molecules) [118,123]. Hence, the radiopharmaceutical design needs to be well adjusted and may have to account for an enhanced BBB passage [124]. Even when the radiopharmaceutical is capable of crossing the BBB, diffusion and distribution throughout the GB tumor will be encumbered by an increased interstitial pressure, pooling in excessive (central) necrotic tissue or cystic regions, or by close proximity to ventricles [105].

### 3.3 Strategies to enhance general pharmacokinetics and BBB penetration

A very successful strategy to bypass the BBB for GB TRT is loco-regional compound injection or convection enhanced delivery (CED). This is possible because 95% of GBs manifest as a unifocal lesion that recurs within a 2 cm margin at the primary site [105]. Most clinical RIT studies for malignant gliomas were

performed via local administration [104,125,126]. Human studies using locoregional administration also showed promise in terms of tumour cell incorporation of AE-emitters [127]. In a clinical study by Krolicki *et al.*, local injection of  $[^{213}\text{Bi}]\text{Bi-DOTA-SP}$  was successfully performed 2-4 weeks after stereotactic implantation [105]. This group recommends an injection of corticosteroids and antiepileptic drugs thirty minutes before administration and up to 3 mL of injection volume. Co-injection of an imaging and therapeutic radionuclide (e.g.  $[^{68}\text{Ga}]\text{Ga-DOTA-SP}$  combined with either  $[^{213}\text{Bi}]\text{Bi-DOTA-SP}$  or  $[^{225}\text{Ac}]\text{Ac-DOTA-SP}$ ) enabled its distribution in the tumour to be monitored and subsequently the radioactivity occurrence in the whole body [105]. For CED, a catheter system, stereotactically placed intratumourally or into the post-surgical cavity, employs a pump to provide continuous positive pressure for local drug delivery (ranging from 0.1 to 10  $\mu\text{l}/\text{min}$ ) (Figure 3 and Figure 4) instead of a bolus injection [128,129]. This was proved to be a safe and effective drug delivery

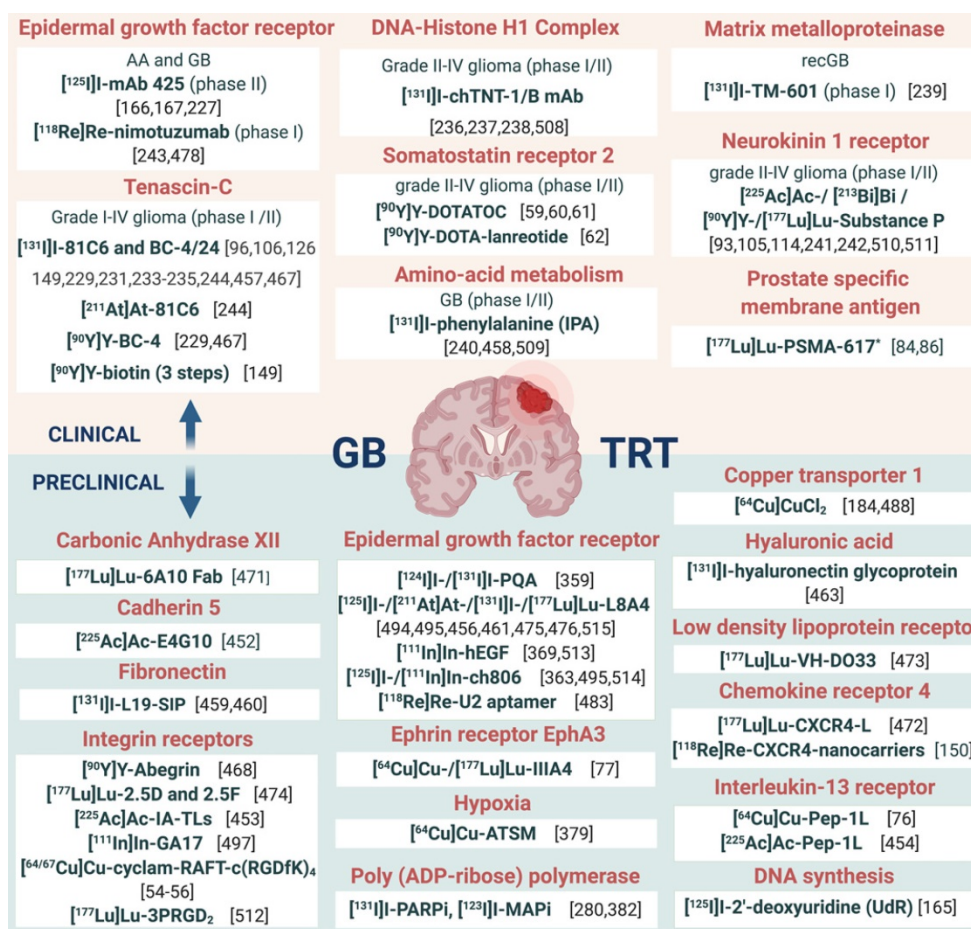


**Figure 2. Overview of current clinical and preclinical targeted radionuclide therapy studies in glioblastoma.** Abbreviations and footnoted content: Anaplastic astrocytoma (AA), convection enhanced delivery (CED), glioblastoma (GB), recurrent (rec), deoxyribonucleic acid (DNA), monoclonal antibody (mAb), targeted radionuclide therapy (TRT), (\*) human case study [46,54,55,59-62,76,77,84,86,93,96,105,106,114,126,149,150,165-167,184,227,229,231,233-244,280,359,363,369,379,382,452-454,456-461,463,467,468,471,472,473,476,478,483,488,494,495,497,508-515].

method, reaching a higher concentration of the drug within the GB tumour, and lack of systemic toxicity. This is especially favourable for  $\alpha$ -particle emitters with relatively short half-lives, such as bismuth-213 (45 min) or astatine-211 (7.2 h), as most of the radioactive decay will occur within the relevant cavity before being distributed throughout the body via the systemic and lymphatic systems [130]. Clinical trials applying CED are highlighted in recent reviews [111,131,132]. It should be noted that pre-therapy PET or SPECT imaging following traditional IV tracer injection contributes little information regarding TRT agent distribution, if CED is applied. When the position of a critical lesion makes local application of CED impossible, brain delivery of radiopharmaceuticals can still be improved by different strategies. In addition to the transcellular lipophilic pathway, the use of BBB shuttles constitute an elegant strategy to target the brain, including receptor-mediated transcytosis (RMT), carrier-mediated transcytosis (CMT) or adsorptive-mediated transcytosis (AMT) (**Figure 3**) [118,133]. RMT is another elegant strategy for the delivery of macromolecular pharmaceuticals (up to 80 nm in diameter) in the treatment of GB. However, the widespread expression of these receptors in other tissues, the small dissociation rate and potential toxicity require careful consideration [5,118]. Alternatively, relevant strategies modifying the PK of radiopharmaceuticals were recently reported [134,135]. Chimeric cell-penetrating peptides (CPP) can hereby aid the transportation of drugs (also tumour targeting peptides) unable to pass the BBB, by conjugating it to a brain drug-targeting vector. This CPP complex can cross the BBB via transcytosis; Mendes *et al.* reviewed this aspect for applications for GB therapy (**Figure 3**) [5]. Multiple prodrug strategies have been employed to facilitate transport into the CNS for brain tumour visualization and treatment, for instance carrier/ligand-drug conjugates [102]. The brain drug-targeting vector can be an endogenous peptide, a modified protein, or a peptidomimetic mAb that undergoes RMT through the BBB on endogenous receptor systems. One such example is [<sup>111</sup>In]In-EGF-SPECT-imaging, using a radiolabeled peptide conjugated to the transferrin receptor (TfR) targeting mAb OX26, which has been shown to detect brain tumours without EGF transport [136]. The diagram in **Figure 5** demonstrates other strategies to increase BBB penetration. A fractionated dose administration over time could be advantageous to

accommodate changes in blood flow and reductions in interstitial pressure caused by tumour reduction (**Figure 5 (3)**) [137]. A physical approach is the combination of low-intensity focused ultrasound (FUS) pulses with circulating microbubbles, which enhanced brain tumor delivery of trastuzumab, improving survival in a rat glioma model (**Figure 5 (4)**) [118,133,138]. The issue of a limited BBB penetration of mAbs, due their molecular size and hydrophilicity, may be overcome by using smaller antibody fragments or engineered antibodies [139]. Other noteworthy delivery platforms shuttling antibodies to the brain (tumour) may include liposomes, nanoparticle-based systems, CPPs, and whole cell-based concepts, actively studied in GB [5,140–146]. This can be combined with a pre-targeting approach, i.e. the administration of a non-radiolabeled antibody first, allowing it to localise to solid tumour sites, followed by a subsequent administration of a small molecular weight, radioactive moiety with high affinity for the tumour reactive antibody [108]. This strategy was successful using a three step yttrium-90 labelled biotin-anti-tenascin-PRIT approach in glioma. However the significant immunogenicity of streptavidin may cause negative side effects [147–149]. An active targeting approach, such as the encapsulation in polymeric nanocarriers, can be used to optimise confinement of the radioactivity near the GB cells (including daughter atoms) (**Figure 5 (6)**) [5,14,150]. The latter resulted in positive pre-clinical results [150,151]. In clinical studies of high-grade gliomas (treated with liposomal doxorubicin plus RT and TMZ) limited therapeutic efficacy was evident [118,150–152]. Finally, it should be noted that translation of nanoparticle-mediated delivery systems to the clinic is time-consuming, costly, and difficult.

#### 4. Requirements for a successful radio-nuclide therapy agent in glioblastoma

In the last decade, TRT has shown not only to be useful in a palliative context but also to prolong progression-free, overall survival and improve the quality of life of cancer patients [22]. Despite a general success of TRT implementation for numerous human investigations, such as GB therapy, and some unparalleled treatment responses, universally applicable guidelines and requirements addressing the use of such theranostic radiopharmaceuticals are yet to be established.

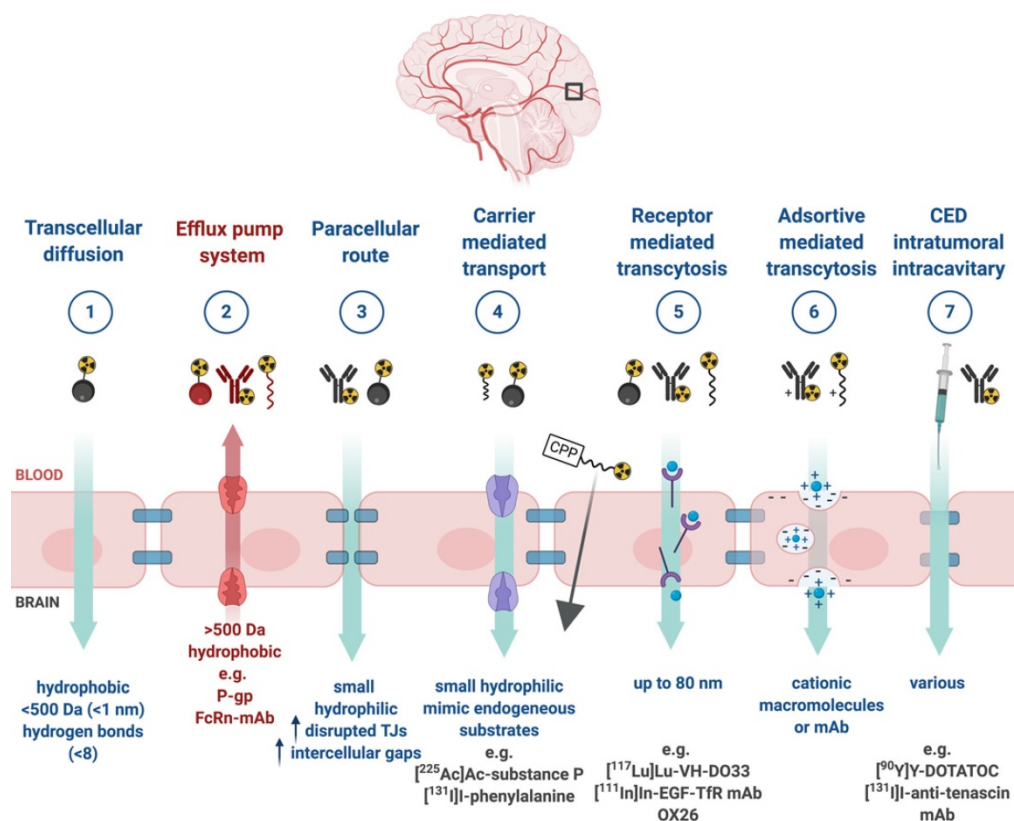


**Figure 3. Mechanisms for transport of radiopharmaceuticals across the blood-brain barrier.** Abbreviations: convection enhanced delivery (CED), cell-penetrating peptides (CPP), monoclonal antibody (mAb), P-glycoprotein (P-gp), tight-junction (TJ).

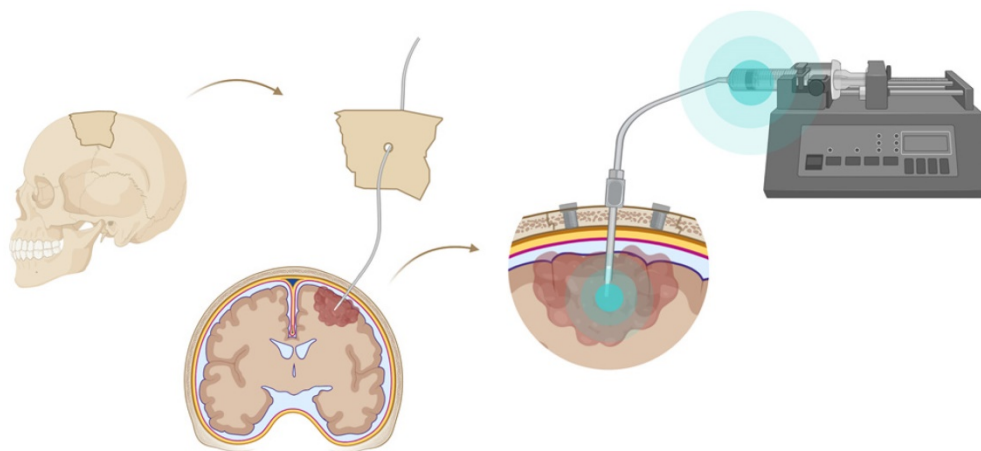


**Figure 4. Convection enhanced delivery (CED) of a radiopharmaceutical.** CED is a strategy whereby a drug is delivered directly into the tumor parenchyma via implanted catheters. Catheters are coupled with a pump to provide continuous positive-pressure microinfusion. Unlike systemic therapy, CED bypasses the blood-brain barrier (BBB) therefore making drug distribution relatively independent of its molecular charge and size [129].

### 4.1 Selection of the radionuclide, optimal LET and range

The three types of radionuclides considered for TRT of GB are  $\alpha$ -,  $\beta$ - and Auger electron-emitting radionuclides. Lutetium-177, iodine-131, rhenium-186, rhenium-188 or yttrium-90, are commonly utilized for the treatment of GB. However, targeted  $\alpha$ -particle therapy (TAT) using astatine-211, actinium-225 or bismuth-213, is gaining momentum [153]. The physical properties and the advantages

versus disadvantages of relevant therapeutic radionuclides, in particular for GB TRT, are summarised in Table 2 and Figure 6. Matching the radionuclide correctly (including decay pathway, effective tissue range, linear energy transfer (LET) and relative biological effectiveness (RBE)) to tumour characteristics (size, radiosensitivity and level of heterogeneity) is one of the primary considerations to maximise therapeutic efficacy in TRT [153–155]. The extent and location of the GB tumour in the pre-therapy state or after surgical debulking is

another major factor influencing the selection process of the appropriate radionuclide (type and/or energy), hence the importance of PET/SPECT imaging to investigate the state of therapy.

$\beta$ -emitting radionuclides, such as iodine-131 and yttrium-90, are used in approximately 90% of current clinical TRT applications [154]. Their cross-fire effect (100-300 cell diameters) and relatively long range (0.2-12 mm) make them particularly efficient for the treatment of common bulky, heterogeneous primary (not necessitating homogenous distribution) and recurrent GB with an average size of >0.5 cm. The variety of  $\beta$ -emission ranges with different energies promotes tailoring of treatment to the size of the brain tumour (Table 2) [154–156]. For example, yttrium-90 (max range 12 mm) could be used for medium-large GB masses, while lutetium-177 (range 2 mm) would be a favourable treatment for smaller GB tumours [14]. However, their lower LETs (0.2-2 keV/ $\mu$ m) and RBEs makes these  $\beta$ -emitters only efficient in case of adequate tumour oxygenation and proliferation and maybe less suitable for the treatment of radioresistant and hypoxic types of GB.

$\alpha$ -particles offer unique radiobiological characteristics, including a short tissue range (40-100  $\mu$ m) and high LET, resulting in a high tumour cell-killing efficiency and corresponding RBE [155,157]. Calculations have shown that as few as five high LET  $\alpha$ -particle traversals through the cell nucleus are enough to kill a cell, whereas 10,000-20,000 low LET

$\beta$ -particles are needed to achieve the same biological effect [130]. In addition, TAT is also suggested as a facilitator to overcome tumoral resistance to chemotherapy and the effect of radiation independently to O6-methylguanine-DNA methyltransferase promoter methylation status; the most important predictor factor in TMZ treatment [93]. Of all known  $\alpha$ -particle-emitting radionuclides, three: actinium-225, astatine-211 and bismuth-213 have received the most attention for TAT and RIT. These may be able to eradicate cerebral micro-metastases, minimally recurrent GB lesions or residual GB tumours [153,154,156].

Auger electrons (AE) emitters are characterized by an even shorter range (<100 nm) combined with a high LET and RBE. Importantly, since AE emitters are less dependent on the oxygenation state of the tumour environment, these high LET emitters could overcome the negative effects of hypoxia and necrosis [14,125,153,158-160]. AE emitters might be applicable for TRT of small GB lesions but several limitations for AE-therapy may pose major obstacles for clinical translation in GB therapy. Homogenous antigen expression within the GB tumour is necessary as target-negative GB cells will potentially escape the lethal effects of AE-mediated therapy. This is a challenge for heterogeneous types of GBs especially. AE-emitting radionuclides are most efficient when incorporated into DNA. When shuttled into the vicinity of the cell nucleus where they cause direct

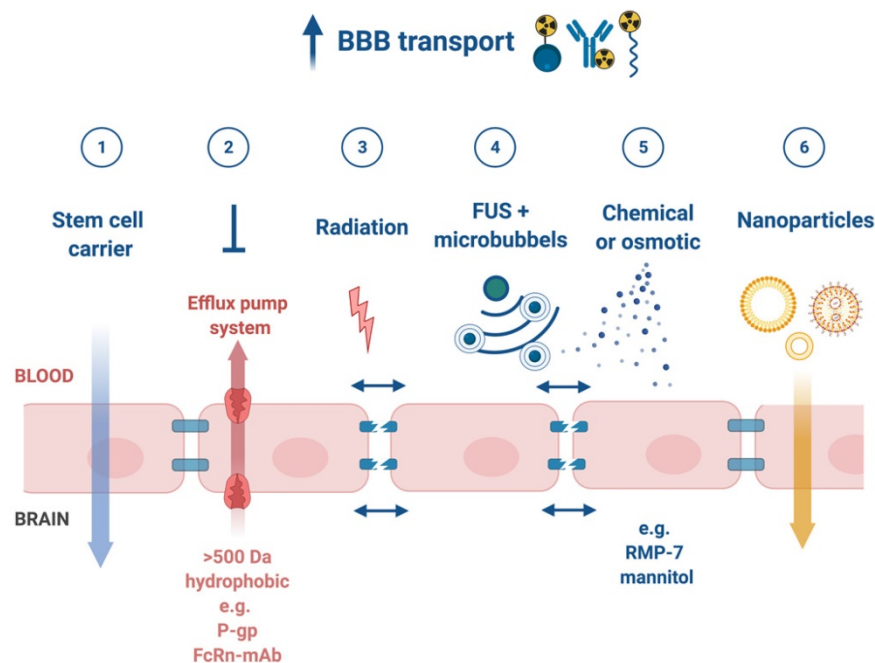


**Figure 5. Strategies to enhance blood-brain barrier (BBB) penetration.** (1) harnessing the homing ability of certain stem cells, (2) low affinity to efflux pumps or co-administration with inhibitors of efflux pumps, (3) targeted irradiation, (4) a combination of low-intensity focused ultrasound (FUS) pulses and circulating microbubbles, (5) infusion of hypertonic solutions, such as mannitol or vasodilator and bradykinin analog RMP-7 and (6) nanoparticle-mediated delivery systems [118].

DNA double strand breaks (DSB). Hence internalisation into the GB cells and into the nucleus is a key design aspect when considering the properties of the radionuclide combination with suitable pharmaceuticals [155]. Tumour-targeted macromolecules including antibodies that bind to internalising receptors have been investigated: a locoregional administration of these favours GB cell incorporation [161,162]. For example, binding of the radiopharmaceutical [<sup>125</sup>I]iodo-mAb-425 to the extracellular domain of the EGFR results in internalisation of the antibody-receptor complex. The specific nuclear binding of the complex then transfers iodine-125 into the cell nucleus and enables its use as a radiation source [163]. Another important criterion of AE emitters is a high MA. It has a direct effect on the amount of energy delivered

to a single tumour cell per receptor-recognition event and may cause a lack of essential crossfire effects [155]. Although preclinical studies have shown substantial therapeutic efficacy of AE-emitters, the small number of human investigations have generally not reported clinical efficacy with the exception of some positive results with [<sup>125</sup>I]iodo-deoxyuridine ([<sup>125</sup>I]iodo-UdR) [164,165] and [<sup>111</sup>In]<sup>in</sup>-DTPA-octreotide [160,167]. Treating GB patients with a [<sup>125</sup>I]iodo mAb 425/TMZ combination resulted in improvements of survival with minimal normal tissue toxicity, which subsequently led to the registration of a Phase III clinical trial (NCT01317888) [166,167].

### 4.2 Optimal radionuclide half-life for therapeutic application

The physical half-life of the therapeutic

radionuclide should match the biological half-life of the targeted compound in order to obtain an optimal effective half-life for therapy. However, the administration route is important. When injected into the GB tumour, matching the physical and biological half-life that may be less crucial but the locoregional distribution time of the compound taken to reach the GB cells is particularly relevant. The residence-time of a radiopharmaceutical *in vivo* can be typically several days (especially with intact mAbs) or merely a few minutes for small molecules. In case of IV administration, a fast (or moderate) blood clearance capability might be more suitable as this allows for the use of radionuclides with shorter physical half-lives and minimal hematologic toxicities [111,122]. However, a very short physical half-life places limits in terms of radiopharmaceutical preparation time and supply chain between preparation and injection.

Both the target location and the mechanism of tumoural cell uptake should match the selected radionuclide for therapy. If the target is expressed on the cell membrane, a β-emitter and a half-life of 45 min could suffice, with the prerequisite that the compound reaches the target in an appropriate time frame (to avoid multiple treatment cycles). Short-lived radionuclides might influence the uptake by infiltrating GB cells negatively, which plays a major role in GB progression and recurrence (Figure 7) [168]. Given a compound is internalised post-binding without leakage from the target site, an AE- or α-particle emitter, providing a longer half-life e.g. up to 10 days should be considered. Negligible toxicity can only be expected if it is proven that the radionuclide is fully entrapped within intracellular macromolecular structures. In a situation where permeation out of the tumor cell can not be excluded, a high-energy, short-lived radionuclide (e.g. bismuth-213) may be recommended. In the case of AE-emitters, a longer half-life is required to provide the necessary time for its internalisation into the nucleus.

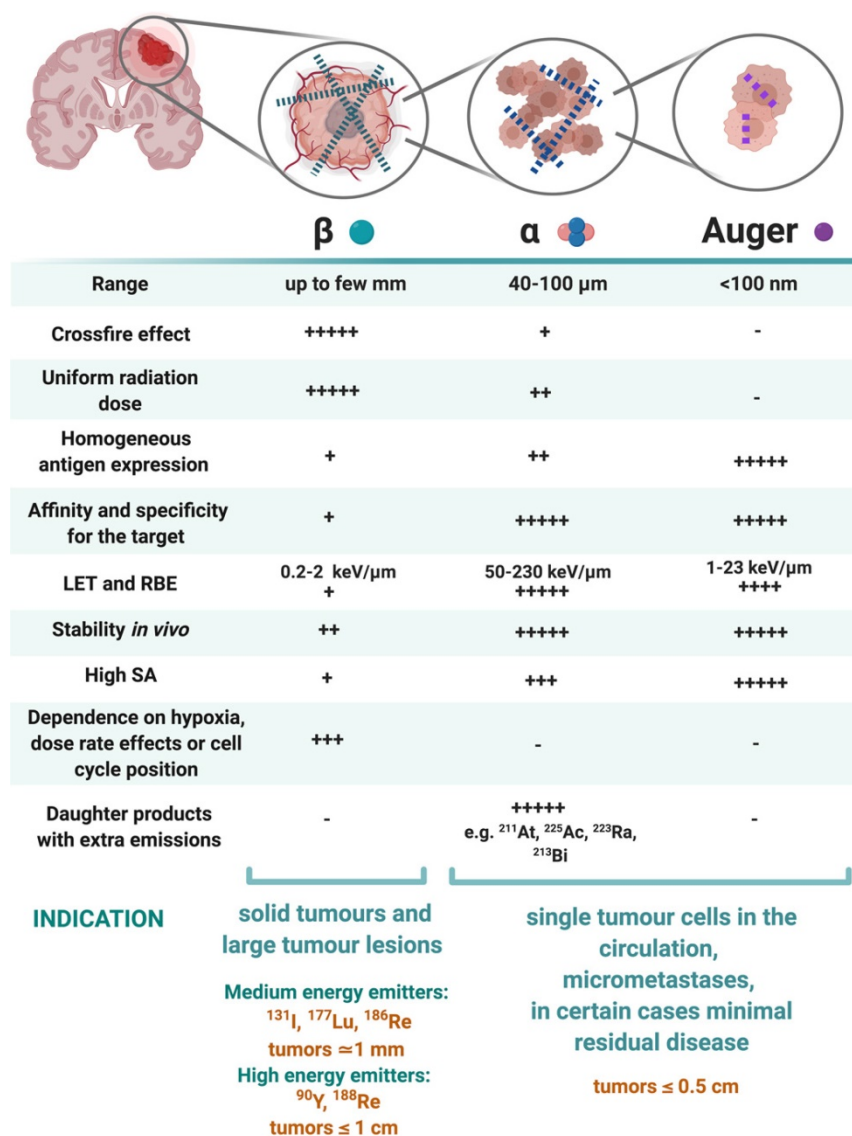
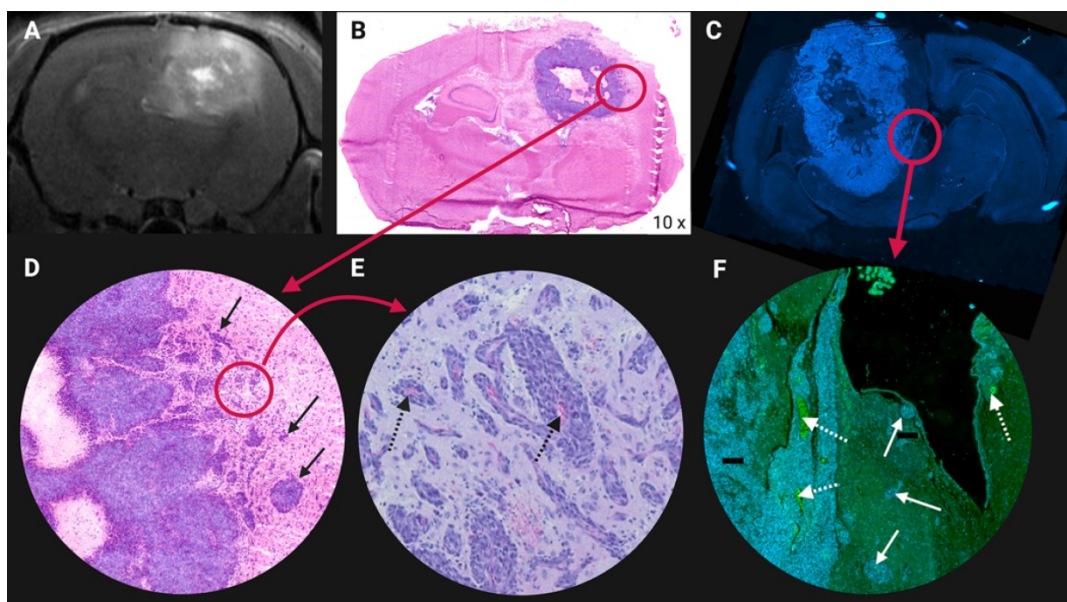


Figure 6. Characteristics of β-emitting radionuclides versus α particle- and Auger electron-emitting radionuclides. Abbreviations: Linear energy transfer (LET), relative biological effectiveness (RBE), specific activity (SA) [130,147,155,156].



**Figure 7. Illustration of glioblastoma (GB) cell invasion at the tumor lesion rim in an orthotopic F98 GB rat model.** (A) Contrast enhanced T1-weighted magnetic resonance image. Higher contrast leakage in the tumour rim and in the centre of the tumour corresponds to central tumour necrosis. (B) Hematoxylin & Eosin staining. (C) 4',6-diamidino-2-phenylindole (DAPI) nuclear staining of another F98 GB rat brain section. (D-E-F) Tumour cells infiltrating the surrounding normal brain tissue, see arrows. (E-F) Abundant blood vessels in the perinecrotic tumour, see dashed arrows. Adapted with permission from [507], copyright 2014 Journal of Neuro-Oncology.

As an example, the 7.2 h half-life of astatine-211 is long enough for multistep mAb labelling procedures and is a reasonable match with the PK of intact mAbs and fragments administered in non-intravenous settings [125]. Based on the information provided in this and the previous section there is no universal fit. Radionuclides for TRT with a physical half-life ranging from *six hours to seven days* to enable optimal distribution of the radiopharmaceutical in commonly large infiltrative GB tumours and to allow feasible production logistics, may be recommended [154,169].

#### 4.3 Selection of a combined treatment strategy

Generally, a combined treatment strategy is suggested to advance GB treatment efficacy aim to address the following challenges: i) the infiltrative character of the tumour beyond a safety margin makes it impossible to surgically resect all GB cells, ii) systemic chemotherapy reaches the cerebral compartment only to a limited extent and iii) hypoxia and an acidotic milieu of the intratumoral and peritumoral microenvironment reduce the efficacy of EBRT and chemotherapy. Additionally, tumour heterogeneity and the multiple pathways involved could lead to signalling redundancy [93]. Currently, TRT can be considered as a potent, additive treatment after the standard treatment for primary GB or as an auxiliary treatment when the tumour tissue seems to be radio- and/or chemoresistant. In case of recurrent GB, TRT could now be considered as a primary option or as salvage therapy if re-EBRT or re-chemotherapy

becomes ineffective. Intracavitary RIT, in combination with EBRT, has recently been reviewed as a therapeutic strategy of high potential [106]. As is the case for EBRT, TRT causes DNA damage and is therefore likely to be enhanced by combination with chemotherapeutic radiosensitisers.

Since radiopharmaceuticals (mainly peptides and mAbs) have relatively reduced drug-drug interactions, combinations of radiopharmaceuticals with chemotherapeutics may reduce interactions compared to a combination of different chemotherapeutics [135,137]. Advantageously, if locally administered, no systemic side effects are caused which may increase the systemic toxicity of chemotherapy [105]. Hence, TRT is now applied in combined-modality regimen [170]. Basu *et al.* suggested that combining standard treatments with peptide receptor radionuclide therapy (PRRT) is attractive for patients with relatively aggressive and metastatic tumours. Monotherapy will probably be unsuccessful as inter-tumour or inter-patient heterogeneity can play a key role in many cancers, particularly in GB. Hence, therapies aiming to interfere with the protective tumour microenvironment (TME) may also use a combined strategy, pairing TRT with emerging cytotoxic agents instead of conventional chemotherapy [10,171]. Other strategies might combine two synergistic TRT agents. Next to different ionizing radiation (featuring efficacy against different tumour sizes), molecular carriers with different biological properties (antibodies, peptides, organic molecules) and binding affinities to multiple tumour-associated targets are the tools to

cause the desired antitumoral effects [110,170,172,173]. Pre-clinically, the combination of both [ $^{64}\text{Cu}$ ]Cu-cyclam-RAFT-c(RGDfK) $_4$  and [ $^{64}\text{Cu}$ ]Cu-ATSM achieved a desired anti-GB effect compared to either radiopharmaceutical because of the more uniform intratumoural distribution of radioactivity [55].

## 5. Toxicity of TRT

### 5.1 Treatment related cerebral toxicity

In current clinical practice, the treatment of GB tumours with standard EBRT is still compromised by the dose-limiting early and late toxicity to the normal brain tissue [125]. Worsening cerebral edema and focal deficit are considered as early EBRT induced toxicity, while delayed toxicity symptoms may include leukoencephalopathy and cognitive decline, parkinsonism and radiation necrosis (RN). The major variables influencing the development of RN in EBRT are the radiation dose, fraction size and irradiation volume [16,174,175]. Due to the localisation in a closed cavity, the risk of symptomatic increase of the intracranial pressure is high [105]. Toxicity also increases with greater utilization of stereotactic radiosurgery and combined modality therapy for brain tumours [16,154,176]. **Figure 8** illustrates these therapy related side effects and how they sometimes mimic a recurrent tumour on contrast-enhanced MRI [16,176,177]. TRT induces toxicity during and after the treatment of GB. Its severity depends on a variety of factors covered in the following section.

#### 5.1.1 Toxicity influenced by the targeting efficiency

Toxicity to the brain is heavily dependent on the threshold of expression on a relevant target in the normal brain tissue as compared to the tumor (see 3.1., for crucial considerations on target selection). Ideally, the therapeutic index should be infinitely high to acquire high efficiency with minimal health

risks, but in practice, this is impossible to achieve [108]. However, compared to systemic chemotherapy, TRT already offers a marked improvement by allowing a tumour specific treatment. Substantial off-target distribution of the radiopharmaceutical often leads to tissue toxicity which may be widespread, with radiosensitivity the limiting factor. For example, this has been reported for the bone marrow (typically >1.5 Gy) or for lung and kidneys (1.5–2.0 Gy) [108,178]. Particularly for RIT, determining parameters for an appropriate pretargeting strategy will have a great effect on the toxicity profile which would otherwise be prohibitive. However, the longevity of this therapy efficiency remains to be determined [148,149]. With regard to normal tissue protection, in certain cases blocking agents can be used. For example, as both astatine and iodine belong to the halogen elements, a pre-treatment with potassium perchlorate can effectively prevent uptake of free astatine-211 and iodine-131 in cells expressing the sodium iodine symporter, e.g. in the thyroid [130].

#### 5.1.2 Toxicity influenced by radionuclide stability and the nuclear recoil effect

The stability of the radiolabelling, minimal dissociation from the targeting vector or dissociation after binding the target, are of utmost importance to prevent free radionuclides dispersing to off-target organs. This may be caused by formation of unstable complexes between the radiometal and a possibly unsuitable chelating agent. This potentially causes chemical instability, metabolism of the radiopharmaceutical or a higher affinity of the chelator for other metals resulting in transchelation and transmetallation processes [179]. A crucial mechanism unique to  $\alpha$ -emitting isotopes is the *nuclear recoil effect* causing the release of radioactive daughter nuclei (often  $\alpha$ -emitters themselves) from the original radiopharmaceutical. This mechanism

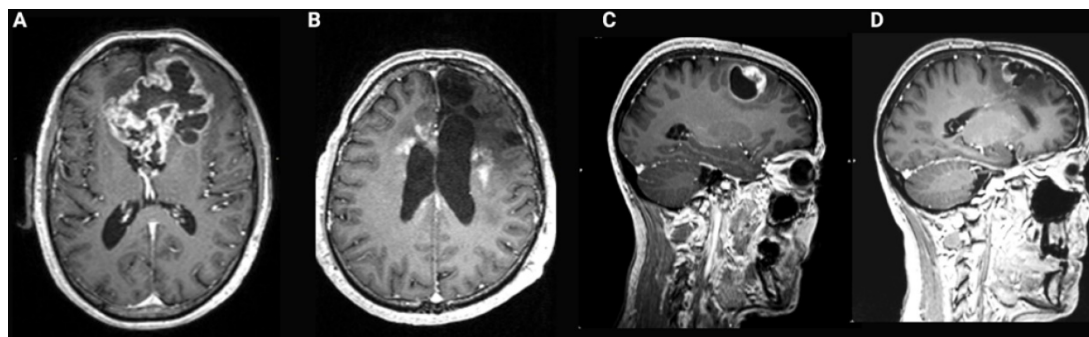


**Figure 8.** Contrast-enhanced T1-weighted brain magnetic resonance imaging (MRI) of glioblastoma (GB). (A) Common presentation of bulky bifrontal GB with irregular (nodular) contrast enhancement surrounding central tumor necrosis. (B) Illustration of radiation necrosis appearing as multiple foci of pathological contrast enhancement, periventricular in the left and right frontal lobe as well as anteriorly and posteriorly in the corpus callosum. (C) Nodular contrast-enhancement in a GB tumor on T1-weighted brain MRI pre-resection. (D) New irregular contrast-enhancement at the resection cavity at 1 year after a complete surgical resection reflecting tumor recurrence or treatment-related changes which have a similar appearance on MRI [31].

and the resulting toxicity has been reviewed in great depth in current literature [180,181]. For application in GB, toxicity may be circumvented by local administration preventing the (daughter) alpha emitters to reach systemic circulation, as demonstrated for TAT using [<sup>225</sup>Ac]Ac-DOTAGA-SP TAT [105]. Toxicity can also be prevented by internalisation of the radiopharmaceutical following binding and entrapment within GB cells [168]. Although there are no nuclear recoil effects associated with astatine-211, the properties of this isotope cause unique challenges and pitfalls regarding stability as previously reviewed [182,183]. Copper-64, an ideal example, circumvents toxicity associated with free radionuclide (due to instability or other sources) because free copper-64 also targets tumor tissue *in vivo* [184]. Further reports investigating the recoil effect and suitable strategies to avoid its pathophysiology are anticipated.

### 5.1.3 Toxicity influenced by physical properties of the radionuclides

When comparing TRT with EBRT, some distinct similarities exist, however, the two treatment modalities have profound differences. Like EBRT, the therapeutic index and the total absorbed dose delivered to the tumour determine the therapeutic success of TRT. Both irradiation types induce DNA damage, which leads to cell cycle arrest, DNA damage repair, cell proliferation, senescence or apoptosis. However, in GB, irradiation induced neovascularization, preferential activation of the DNA damage checkpoint and enhanced DNA repair capacity (mediated by the presence of glioma stem cells) leads to radioresistance and recurrence [185-187]. Evidence is also suggesting that radiotherapy has lasting effects on the structure and composition of the GB microenvironment, facilitating tumor aggressiveness upon recurrence [188]. Interestingly, combining EBRT or TRT with radiosensitizing agents could sensitize GB tumors to irradiation effects, while minimizing deleterious side effects towards surrounding normal tissues [189].

Although normally well tolerated, TRT sometimes imposes unnecessary radiation burden onto normal tissue in the vicinity of the tumour. This may occur due to the inadequate selection of radionuclide ( $\beta^-$ -emitters with the highest crossfire effect) with a larger particle path length than the tumour outline would suggest [190]. An important difference between EBRT and TRT is the rate at which the total dose is delivered, which impacts the biological outcome. A dose of 30 Gy delivered to a tumour over a period of many weeks at a dose rate that is exponentially decreasing, as is typically the

treatment regimen with TRT, will have a very different effect from that of the same amount delivered at the much higher dose rate used in EBRT [127]. It is plausible that apoptosis might be one of the mechanisms that is responsible for the higher levels of cell death at low dose rates in TRT, while others hypothesise that synchronisation in sensitive phases of cell cycle or defects in the detection of low levels of DNA damage might lie at the origin [178,191-202]. In addition, radiation-induced bystander effects (RIBE) may play a significant role at low dose rates [155,178,199,202-206]. It is also increasingly apparent that the paradigm of direct cell killing by the induction of DNA DSB is insufficient, since cell killing has been observed when only the cell cytoplasm was irradiated (known as non-DNA-centered effects) and in non-irradiated areas due to RIBE. In glioma cells RIBE has been shown to be mediated by nitric oxide, p53 and phosphoinositide 3-kinase. Importantly, similar signaling pathways are induced in bystander cells that are not traversed directly by  $\alpha$ -particles [207,208]. Off-target effects (e.g., bystander and abscopal effects) must be considered both at low and high doses, although it is still not known whether epidemiologically, these effects will be translated statistically to an increase or decrease of the risk for healthy tissues [209]. Interestingly, radiation may serve as a mechanism to improve the effectiveness of immunotherapy (e.g. anti-PD-L1) and change immunologically 'cold' GB tumors to 'hot' tumors by recruiting immune cells, resulting in a radiation-induced abscopal response [210]. Abscopal effects of both EBRT and TRT attenuating growth of metastatic lesions elsewhere in the body is less relevant as GB is typically restricted to a single lesion (95%) within the central nervous system, with a low frequency of metastasis (0.5%) [105,211,212]. Further studies are needed to validate the inverse dose-rate effect and to improve understanding of the radiobiological mechanisms involved.

### 5.1.4 Toxicity influenced by dosimetry

The European Association of Nuclear Medicine Dosimetry Committee listed the steps required for an adequate TRT dosimetric assessment [134,213]. Accurate individualised patient dosimetry with diagnostic functional imaging (SPECT/CT or preferably higher resolution PET/CT) or similar techniques are necessary to obtain an accurate risk-benefit analysis regarding normal tissue toxicity [178,214]. Ideally, isotopes of the same element should be used for diagnostic imaging and therapy to improve detection of therapeutic radiopharmaceutical biodistribution (e.g. yttrium-86 for yttrium-90). TRT related dosimetric calculations must be performed for

both target organs and organs-at-risk. The commonly used approach is based on the medical internal radiation dose (MIRD) formalism [215,216]. More technical details on three-dimensional image-based dosimetry in TRT is described elsewhere [162,202,217-218]. As individual parameters, the dimension of the cavity, the degree of radiopharmaceutical binding to the cells and the percolation into the brain-adjacent tissue were combined [222]. Dosimetry using Monte-Carlo simulations also showed valuable insights for TRT of early brain metastases and concluded a preference for  $\alpha$ -emitters [223]. For very short range TRT agents such as AE emitters, it might be necessary to determine the absorbed dose at a cellular level, instead of only at the organ level [108,134,155]. However, current imaging techniques do not possess the resolution required to resolve activity distributions at the microscopic or even nanoscopic scale. Hence, pre-clinical studies on cellular dosimetry and organ dosimetry using tumour xenograft models are essential [155,162]. In addition, in the field of TAT, developments in microdosimetry are expanding [216,224,225].

### 5.1.5 Toxicity influenced by immunogenicity

A specific toxicity concern in RIT is the induction of antibody immunogenicity post-administration. This elicits a human anti-mouse or human anti-chimeric antibody response, which can result in anaphylaxis or symptoms of serum sickness [135,156,226]. This was noted in a phase II trial in 192 GB patients of adjuvant RIT with [ $^{125}\text{I}$ ]iodo-mAb 425. Four patients developed human anti-mouse antibodies preventing further administration. The development of humanized and fully human mAbs could prevent this immunogenic response [155,227]. The avidin-biotin pretargeting system in GB has also shown to induce high immunogenicity of streptavidin in almost all patients (90%) [147,148]. Small peptides (<4 kDa) are generally believed to be poor immunogens, despite some exceptions being observed [135]. To limit immunogenicity (preferable a  $\text{LD}_{50} > 1.5$  g per kg of body weight), small molecules and peptides are preferable to mAbs. The design of these radiopharmaceuticals should involve strategies to reduce immunogenicity such as avoiding the inclusion of antigenic amino acid sequences and employing structural modifications, such as glycosylation or PEGylation, which tend to shield antigenic determinants from detection by the immune system [135,154].

### 5.1.6 Toxicity specifically associated with the CED tumour administration route

In CED, the therapeutic agent is delivered

directly into the tumor which imposes a significant concentration differential across the tumour boundary dependant on leakage into the surrounding tissue, thereby minimising systemic toxicity and neurotoxicity. Local injection also minimizes renal risk from potential tubular re-uptake of the radiopharmaceutical [105,228]. Inflammation adjacent to the catheter tract and at the catheter tip is shown to be limited to within a 50 mm radius and CED does not produce cerebral edema or any measurable increase in intracranial pressure [128,129]. However, increased interstitial fluid pressure within the brain tumour can drive the infusate into relatively low-pressure areas in surrounding normal tissues. Furthermore, catheter-induced tissue damage can occur and backflow may be significant in cortical infusions, leading to subsequent widespread distribution of the agent within the subarachnoid space. The latter can also be induced by leakage from the postsurgical cavity to cerebrospinal fluid spaces, in the event of a connection, which is a major contraindication for TRT. It can lead to an inflammatory reaction of the brain, a diminished concentration of the radiopharmaceutical within the tumour and an increased risk for widespread neurotoxicity [105,128]. An adequate stereotactic positioning of catheters and a careful application of the compound is of utmost importance. Co-injection of the imaging counterpart together with the therapeutic dose allows short time imaging of the tumor and study of the whole body distribution, and is recommended for monitoring adequate distribution [93].

## 5.2 Clinical toxicity resulting from TRT of GB

In general, current clinical results show that newly diagnosed and recurrent brain tumor patients who have been treated with TRT often show only limited adverse effects. It should be noted that not all clinical trials contain plausible evidence on clinical toxicity. The most relevant examples for each radioisotope are described in the following paragraphs.

### 5.2.1 Iodine-131

In phase I/II trials including diverse malignant gliomas different iodine-131-labelled tenascin-mAbs were injected directly into the tumor or the resection cavity, resulting in minimal toxicity [96,126,229-233]. Systemic and neurological toxicity were negligible in 10 recurrent GB patients receiving doses ranging from 111-1147 MBq per cycle [ $^{131}\text{I}$ ]iodo-BC-2 stereotactically [231]. Similarly, in 30 recurrent GB patients, a higher intratumoral dose of 1100 MBq [ $^{131}\text{I}$ ]iodo-BC-4 did not result in adverse systemic effects [236]. This approach was confirmed in a large phase I/II clinical trial

including 111 patients who suffered diverse malignant gliomas. For the phase II component, patients received a mean dose of 1.29–2.78 GBq with minimal toxicity [233]. In another phase II trial, 43 patients with recurrent malignant glioma (GB: n=33), 3.7 GBq of [<sup>131</sup>I]iodo-m81C6 was injected directly into the surgically created resection cavity (SCRC) followed by chemotherapy with acceptable tolerability and toxicity. Acute, primarily reversible, hematologic toxicity was the most common significant adverse event (23%). In 12% of the population acute neurotoxicity developed but this resolved spontaneously or after short-term corticosteroid administration in all except one patient [96]. The maximum-tolerated dose of [<sup>131</sup>I]iodo-m81C6 into the SCRC was 4.44 GBq in a phase I trial which involved 42 malignant glioma patients with no prior EBRT or chemotherapy [232]. A dosimetric study did not detect neurological toxicity while minimal hematologic toxicity occurred with the maximum tolerated administration of 3.7 GBq [<sup>131</sup>I]iodo-m81C6 [95]. Akabani *et al.* in 2005 suggested an optimal absorbed dose of 44 Gy to the 2 cm cavity margins to reduce the incidence of neurologic toxicity [234].

In 2008, a targeted 44 Gy boost of [<sup>131</sup>I]iodo-m81C6 was delivered to the SCRC followed by EBRT and chemotherapy in 21 newly diagnosed malignant glioma patients (GB, n=16), which was well tolerated and had an encouraging survival outcome [235]. The dosing regimen of an [<sup>131</sup>I]iodo-chTNT-1/B mAb targeting DNA histone H1 complex (Cotara®) was determined to be 37.0 to 55.5 MBq/cm<sup>3</sup> without toxicity [236–238]. In a cohort of 51 patients with histologically confirmed malignant glioma (GB n=45) which received Cotara via CED and the treatment-emergent, drug-related CNS adverse events included brain edema (16%), hemiparesis (14%), and headache (14%). These events were mostly reversed with corticosteroid co-treatment. Systemic adverse events were predominantly mild [238]. Intracavitary-administered [<sup>131</sup>I]iodo-TM-601, a recombinant version of chlorotoxin, was well tolerated, without dose-limiting toxicities or clinically significant acute adverse events during infusion of [<sup>131</sup>I]iodo-TM-601 at any dosage being observed during the 22-day observation period. Grade 3 or 4 toxicities related to the study drug or method of administration were not observed in the immediate or long-term follow-up periods [239]. In a human trial of systemic endo radio-therapy with [<sup>131</sup>I]iodo-IPA (up to 6.6 GBq), patients did not present with acute or late radiotoxicity, neurotoxicity, and haematological or renal adverse events were not observed. This first-in-human investigation was performed in two patients with progressive gliomas, which were

initially diagnosed as low-grade astrocytoma (WHO II) and oligodendroglioma (WHO II), respectively [240].

### 5.2.2 Yttrium-90

Adverse events remained well controllable with the fractionated dosage regimen of [<sup>131</sup>I]iodo- or [<sup>90</sup>Y]Y-anti-tenascin mAb applied in 55 malignant glioma patients (GB n=40) [229]. In 73 recurrent GB patients treated with the “3 step” [<sup>90</sup>Y]Y-biotin based loco-regional RIT, safety and efficacy was also shown [149]. [<sup>90</sup>Y]Y-DOTAGA-SP was locally administered into the tumours of 14 pilot study patients except for critically located tumours which were injected with [<sup>177</sup>Lu]Lu-DOTAGA-SP and [<sup>213</sup>Bi]Bi-DOTAGA-SP instead. Drug-related toxicity did not present but disease stabilisation or improved neurologic status was observed in 13 of the 20 patients while neurological function improved in 5 out of 14 GB patients within 2 weeks [241]. In a prospective phase I study involving 17 GB patients, [<sup>90</sup>Y]Y-DOTAGA-SP treatment was well tolerated by all patients without acute toxicity or other side effects [247]. Of 43 GB patients treated with 0.4 to 3.7 GBq of [<sup>90</sup>Y]Y-DOTA-lanreotide using a fractionated 1- 6 therapy cycle, disease regression and a subjective improvement in quality of life measures was reported in 5 patients while 14 patients presented with stabilised disease [62]. When [<sup>90</sup>Y]Y-DOTA-TOC was administered to 3 GB cases in three or four fractions at intervals of 3 to 4 months (1.7 to 2.2 GBq), the only observed adverse effects were a reoccurrence of an epileptic seizure for one patient and a mild transient headache for another. In general all patients reported an improved quality of life [59]. In an extended pilot study by Schumacher *et al.*, 10 low-grade and anaplastic glioma patients received local administration of varying fractions of [<sup>90</sup>Y]Y-DOTA-TOC, either into the tumour or the resection cavity without associated intermediate- to long-term toxicity [60].

### 5.2.3 Rhenium-188

The radiolabelled anti-EGFR ligand [<sup>188</sup>Re]Re-nimotuzumab was administered intracavitary to 3 patients with anaplastic astrocytoma and 8 GB patients in an open, uncontrolled, dose-escalation phase I clinical trial. In patients treated with 370 MBq (n=6) transitory worsening of pre-existing neurological symptoms was observed. Two patients treated with 555 MBq (n=4) developed early severe neurological symptoms and one patient also developed late severe toxicity involving RN. Single doses of [<sup>188</sup>Re]Re-nimotuzumab were also locoregionally administered to 9 recurrent GB

patients with a maximum tolerated dose of 370 MBq [243].

#### 5.2.4 Lutetium-177

A progressive pontine GB case, pretreated with EBRT and TMZ, [<sup>177</sup>Lu]Lu-DOTAGA-SP (1.13 GBq) was injected via a transcerebellar catheter without side effects. Clinical and radiologic improvement lasted for 5 months. It is of note that two more cases within the same study (but presenting with oligoastrocytoma and astrocytoma, WHO grade III) received higher doses of [<sup>177</sup>Lu]Lu-DOTAGA-SP (2.25 and 6.38 GBq). Impaired neurologic function markedly improved significantly in both within 2 weeks after injection. However, intermediate or long-term toxicity could not be evaluated in a patient who died following tumor progression [241].

#### 5.2.5 Astatine-211

Anti-tenascin 81C6 mAb was also labelled with astatine-211 (71–347 MBq) and injected in the surgically created resection cavity of 18 recurrent malignant brain tumors (GB, n=14). While dose-limiting toxicity did not occur, 6 patients experienced reversible grade 2 neurotoxicity, and the median survival time for GB patients was 52 weeks. This compares favourably to 23–31 weeks for patients receiving conventional therapies [244].

#### 5.2.6 Bismuth-213

In a pilot study 5 patients with critically located gliomas (WHO grades II-IV) were locally injected with [<sup>213</sup>Bi]Bi-DOTA-SP. Treatment was tolerated without additional neurological deficit or local or systemic toxicity [242]. In a case presenting with progressive GB, intracavitary injection of 375 MBq of [<sup>213</sup>Bi]Bi-DOTAGA-SP was tolerated well [241]. Nine recurrent GB patients received 1 - 6 intracavitary doses of [<sup>213</sup>Bi]Bi-DOTA-SP in 2-month intervals (median 5.8 GBq), which was well tolerated with mild transient adverse reactions (mainly headaches caused by transient perifocal edema) [114]. In a more recent trial treatment with activity up to 11.2 GBq [<sup>213</sup>Bi]Bi-DOTA-SP was well tolerated in 20 patients with recurrent GB with mild and transient adverse reactions (edema, epileptic seizures, aphasia) [93,105]. During [<sup>213</sup>Bi]Bi-DOTA-SP infusion, facial erythema was observed in a few patients: a systemic effect caused by a small amount of [<sup>213</sup>Bi]Bi-DOTA-SP absorbed into the blood [105].

#### 5.2.7 Actinium-225

Local administration of [<sup>225</sup>Ac]Ac-DOTAGA-SP was well tolerated, with mild, transient observations of edema, aphasia or epileptic seizures [93,105]. In one patient with the tumour located in the left temporal

lobe, injection of the [<sup>225</sup>Ac]Ac-DOTAGA-SP induced hemiparesis and hemianopia 3 days later, lasting several months [105].

#### 5.2.8 Iodine-125

In a phase II clinical trial [<sup>125</sup>I]iodo-mAb 425 was administered intravenously or intra-arterially as an adjuvant therapy in 118 GB patients (mean dose of 5.2 GBq). Acute and chronic toxicity presented as an exception in 1 of the 118 patients as hypothyroidism [166]. In a second phase II clinical trial of 192 GB patients subjected to surgery and EBRT followed by 3 weekly intravenous injections of 1.8 GBq, grade 3/4 toxicological events did not occur [227].

## 6. Validating new radiopharmaceuticals

The transition of radiopharmaceutical therapeutics to a clinical setting have been extensively reviewed, including therapeutic radionuclide production, preclinical evaluations and Good Manufacturing Practice (GMP) perspectives; however, these mostly lack information that would address GB specifically [245,246]. Current regulatory status and broad guidelines regarding the clinical translation of radiopharmaceuticals, with particular emphasis to the European context, has also been reviewed [247–249]. Further guidance is anticipated specifically regarding radiopharmaceuticals targeting GB, necessary because of the complex radiobiological considerations they entail. Thus, the need for monographs for therapeutic products is urgent and standardisation of quality control and assurance procedures are of utmost importance. A major limitation of radiopharmaceutical commercialisation is meeting product demand and special requirements of the market in nuclear medicine adequately. An excellent example of the translation to the clinical setting is the report on Lutathera® ([<sup>177</sup>Lu]Lu-DOTA-TATE), describing its product characteristics, quality control procedures with an application guide [57]. In this section the relevant knowledge, technicalities and major factors influencing the validation of radiopharmaceuticals, especially for prospective GB imaging and therapy will be discussed.

### 6.1 Target-based selection of compound candidates

Since the physiology and pathology of GB tumours is so unique, it is important to use complimentary techniques to increase the probability of accurate characterisation. After identifying a promising GB target (Section 3.1), exploration of target specific compound candidates involves stringent *in vitro* investigations. Carager *et al.*

discusses most recent systems for *in vitro* brain cancer research but those selected are defined by the targeted GB pathophysiology [250]. Importantly, the advent of *in vitro* three-dimensional GB colloid models include a better representation of *in vivo* cell environments (eg. hypoxic cell status) which could result in more accurate predictions of efficacy and sensitivity before any *in vivo* investigations are launched [251–253]. Central necrosis may occupy as much as 80% of the total GB tumor mass and includes “dormant” hypoxic tumor cells that may be very radioresistant [189,254]. In addition, the use of an *in silico* molecular modelling step addressing the design of radiopharmaceuticals for GB is strongly recommended. For the selection process of the optimal complexation strategy for radiometal-complexing bioconjugates, it should be noted that available published data, often published concerning the non-medicinal isotopes of a certain radiometal (available from radioassays for *in vitro* investigations), are not applicable as input for further compound candidate selection. Designing radiopharmaceuticals by adaptation of naturally-occurring bioactive molecules, conventional drug candidates, or established molecular imaging probes remains a sound approach. That being said, however, the timelines and success rates may potentially be improved by incorporating proteomics, genomics and computational methods in the design process of new candidates [255,256]. Elegant study examples are the *in silico* modelling of antibody immunogenicity potential and the calculation of radiobiological mechanisms applied to cancer cells for translation to bulky tumours [81,257]. Interestingly, Rockne *et al.* suggest the creation of a virtual *in silico* tumour with the same growth kinetics as that in a particular patient to predict efficacy based on *in vitro* responses. Although this study looked at the response to RT, translating this concept to radiopharmaceutical design is plausible [258]. *In silico* modelling offers the means of combining both *in vitro* data and computational power to create intricate pharmacokinetic-pharmacodynamic modelling to facilitate the design process and potential to improve therapeutic outcome. Therefore it should be incorporated into the theranostic protocol [259].

## 6.2 Radiosynthesis requirements

A variety of strategies and optimised protocols for efficient labelling of peptides, mAbs and other targeting vectors have been published but specific details to develop GB-specific radiopharmaceuticals are scarce [259–262]. The vast application of radiometal isotopes emphasises the intricate nature of complexation chemistry in GB therapy. When considering metal therapeutic radionuclides, the

choice of chelators to be incorporated in the radiopharmaceutical to yield the most stable complex is crucial for recommending a metal-radioisotope as appropriate (Table 2) [263–266]. If certain *in vitro* applications to characterize a radiopharmaceutical are preferred, it is important to meet the stipulated criteria qualifying their use, when performing these tests on cells or tissue. For example, the radioligand association constants obtained from any chelator-ligand pair (without any radioisotope) can already differ markedly from its radioisotope-chelator-ligand complex derived from radiosynthesis (also relevant to its formulation). In addition, free radionuclides *in vivo*, either from lack of complexation integrity or poor labelling, can lead to unfavourable organ toxicity. If radiopharmaceutical instability (*in vivo* or benchtop) is an issue, multiple strategies for stabilization thereof have been reviewed [267]. For instance, it is considered good practice to add diethylenetriamine pentaacetate (DTPA) after radiolabelling some metallic based therapeutic radiopharmaceuticals to chelate any uncomplexed radionuclides.

The chemical considerations of astatine-211 and iodine-131 as therapeutic halogens are unique with different constraints [182,268–270]. Production and isolation of astatine-211 is well described and feasible but complete radiopharmaceutical production infrastructure is less widely spread. Lindegeren *et al.* describes the inherent intricacies involved and provides insights into how the chemistry infrastructure could be developed [269]. One of the most important factors to consider is the MA of the final radiopharmaceutical. If the production methods introduce carrier molecules into the formulation (e.g. carrier-added lutetium-177) then the targeting vectors labelled with non-radioactive nuclides (such as lutetium-176) may compete with target binding reducing uptake of the radiopharmaceutical. An example of a sophisticated system is to use uncomplexed copper-64 dichloride produced with high specific activity for GB without additional influences on MA. Optimal internalisation can take place at the target through the copper transporter in GB [184].

## 6.3 Quality control validation

Since therapeutic radiopharmaceuticals have unique characteristics including different types of emissions and half-lives, quality control can be challenging. The methods used are often sparingly applied to therapeutic radiopharmaceuticals in comparison to diagnostic radiopharmaceuticals. The longer half-lives of some therapeutic radionuclides complicates the common procedures used for quality

control, i.e. sterility testing and testing for pyrogens. Therefore, this requires additional infrastructure investment for “in-house” quality control. The emission characteristics of  $\alpha$ -emitters and pure  $\beta$ -emitters complicates high performance liquid chromatography (HPLC) analysis, but it is strongly recommended that the quality control is not only performed by unvalidated instant thin-layer chromatography (ITLC) methods. Subtle changes in stability of the vectors and effects of radiolysis would not necessarily manifest clearly using ITLC analysis. Regarding therapeutic peptides, it is important to not only focus on radiochemical stability but also take into account subtle changes in peptide structure (causing chemical instability) that could be brought about by radiolysis. Importantly, certain  $\alpha$ -particle emitting radionuclides may necessitate special QC requirements. For example, since actinium-225 does not emit  $\gamma$ -rays, a delay of 60 min is necessary after ITLC to obtain radiochemical equilibrium between actinium-225 and its daughter nuclide francium-221 [271,272]. Once the radiosynthesis parameters and quality control techniques are established, automation of radiopharmaceutical production can be of considerable support achieving robust, GMP compliant products for clinical trials and providing proven validated radiation protection for operators [273-275].

#### 6.4 *In vivo* validation using GB models

Rodent GB tumour models which have been the main research tools of preclinical investigations for over 30 years may be subdivided into three categories: ethyl-nitrosourea (ENU) -induced gliomas, genetically engineered models (GEMMs) and patient-derived xenograft or glioma cell models (PDX or PDGC); as summarised in **Table 3** [276-278]. *In vivo* validation of novel theranostic compounds should include *in vivo* studies on biodistribution, tumour uptake, therapy monitoring and toxicity [279]. Particularly important for GB is determination of the optimal administration method by comparing intravenous administration (BBB passage testing) with CED or intra-tumoral injection. The distribution and the residence time of the targeting compound throughout the GB tumour and in healthy brain tissue should be analysed comparatively. In cognisance of this, efficient retention via CED in GB models has been reported [165,280,281]. The efflux effect of the selected radiopharmaceutical at the BBB can be studied in biodistribution experiments or PET imaging while co-injecting a P-gp blocker (eg. tariquidar or loperamide) [47]. In addition, PET biomarkers have been designed to image (and quantify) these undesired efflux transporters present

on the BBB [282]. Overall survival analysis and therapy follow-up using PET/SPECT/MRI imaging should be performed to test the efficacy of single and fractionated doses, including an estimation of the delivered therapeutic dose. Multidrug approaches, including the currently used first-line chemotherapeutic agent TMZ should be included. Auxiliary tests to study dose-limiting and off target effects would require blood/urine/faeces sample collection and post-mortem histology.

As highlighted by Lenting *et al.*, valid brain tumour models should fulfill critical needs to yield relevant data for the prospective success of radiopharmaceuticals in Nuclear Medicine [276,283]. For therapy studies, the tumours should be either non- or weakly immunogenic in syngeneic hosts. Subcutaneously (heterotopic) GB tumour models are technically simple and enable rapid determination of treatment efficacy. However, these result in encapsulated, non-invasive tumours and caution is advised when therapeutic activity focuses on disturbing the interaction with the TME [276,279,284,285]. Orthotopic GB models include a CNS micro-environment and would be more appropriate to test the BBB passage of a new TRT compound [284]. In case of a RIT agent, preclinical testing with the currently available glioma tumour models remains outstanding. As the immune-compromised status of the recipient mice renders PDXs inadequate for this purpose, humanised mice are required. In addition, the use of PDX models is often hampered by donor availability and limited propagation [277]. ENU-induced gliomas recapitulate human gliomas most faithfully with respect to genetic heterogeneity and immunocompetence, but often lack reproducibility [276]. As expected, each of the listed animal models has its advantages and limitations. An emerging alternative is represented by the organoids generated from human samples and so-called organoid-derived GB xenografts, including the generated live biobank established by Jacob *et al.* [10,286-288]. Hence, the TRT efficacy should be tested in a combination of suitable models to compile sufficient information for optimal design of the clinical protocol.

#### 6.5 Data required for clinical translation

Before a new radiopharmaceutical may be introduced in the clinic, a range of assessments (**Figure 9**) are required [245,247,289]. An investigational medicinal product dossier (IMPD) is required for regulatory boards. Information regarding the IMPD requirements in the USA and Europe pertinent to radiopharmaceuticals is available, but it is important to take into account regional requirements

and to work with local governing bodies [249,290,291]. If the theranostic partnership contains two separate radiopharmaceuticals (e.g. [ $^{68}\text{Ga}$ ]Ga-DOTA-TATE and [ $^{177}\text{Lu}$ ]Lu-DOTA-TATE), two separate radiopharmaceutical production validations must be performed. A significant amount of information concerning the release criteria, analytical procedures and their validation must be provided [247]. Most importantly, validation ensures a robust method (taking into account operator variability) and focuses on reproducibility of manufacture and quality of the environment. Following product validation, nonclinical (*in vitro* and *in vivo*) safety data (**Figure 9**) is imperative. It is of significance that FDA guidelines require that, for diagnostic procedures, risks are low and the associated translation requires much less *in vivo* valuation [292,293]. However, caution is advised as assumptions regarding radiopharmaceutical safety based on experience of diagnostic radiopharmaceuticals may be inaccurate if applied to therapeutic equivalents. These therapeutic radiopharmaceuticals may demonstrate inherent additional toxicity (often connected to off target effects). Their *in vivo* stability can be more critical; they are also often injected in repeat doses in shorter time frames than required for diagnostics. Consequently, additional tests (selectivity, pharmacokinetics, sensitivity and safety) beyond those usually required for diagnostic radiopharmaceuticals are included by the validation

process. In particular for GB, the *in silico* calculations of radiation dosimetry and the toxicity profiling may become more complex and must be performed stringently.

## 7. Future perspective

Prospective strategies for a multi-targeted approach may include the use of heterobivalent or hetero-multivalent ligands which may bind simultaneously or monovalently to their different molecular targets. This is supported by the observation of Reubi *et al.* that non-endocrine tumors (including GB) concomitantly express several peptide receptors at a high density [294]. Considering that strategies successfully reversing GB hypoxia are likely to improve the response to radiation significantly, a prospective treatment strategy is proposed. This entails the administration of a tumour tissue penetrating *hypoxia-promoting* TRT agent to treat the centrally located tumour region in parallel with the administration of an anti-proliferating TRT agent to target the viable tumour boundaries adequately. As a higher LET radiation is less dependent on the oxygen enhancement ratio,  $\alpha$ -particle and AE emitters might be more effective in targeting hypoxic regions. In addition, targeting with high LET irradiation initially may be the best option to tackle the most radio-refractory cells from the very beginning of treatment because of the characteristic rapid progression of GB.

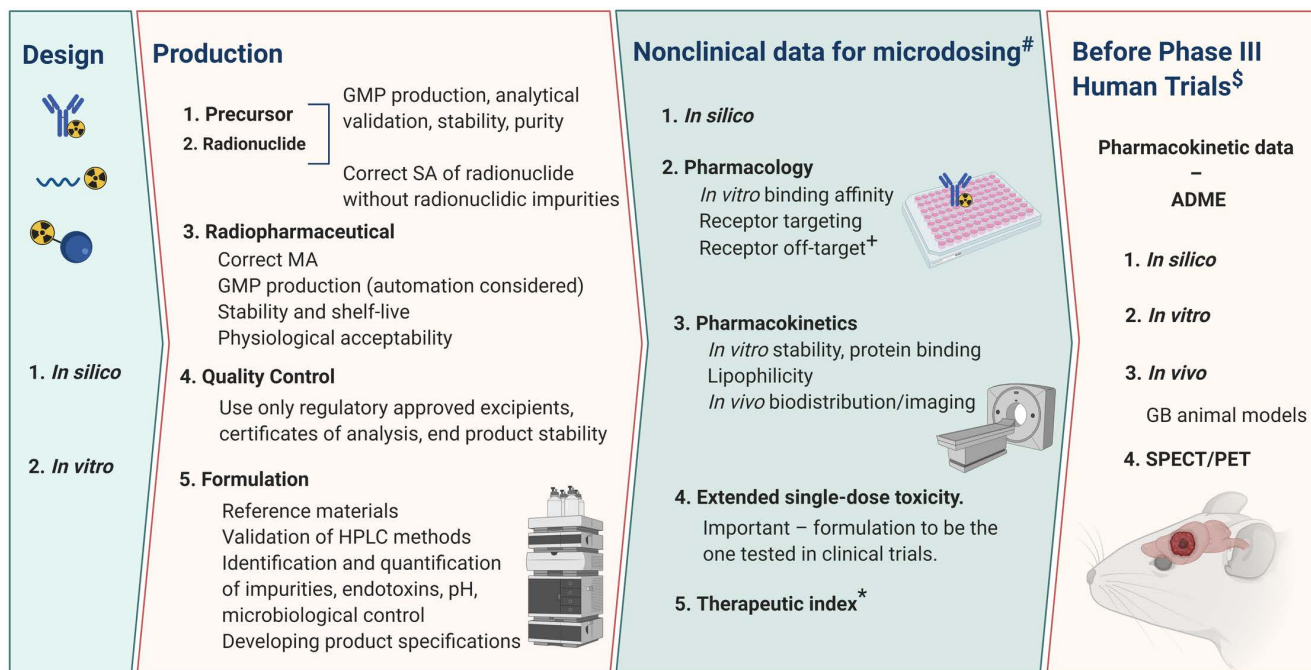


**Figure 9.** Quality data required for translation of a radiopharmaceutical. The sequential approach to an adequate validation of radiopharmaceuticals is illustrated; certain tests and validation steps may not depend on each other and are therefore often performed in parallel. Abbreviated and footnoted content: Absorption Distribution Metabolism Excretion (ADME), good manufacturing practice (GMP), molar activity (MA), specific activity (SA), glioblastoma (GB), positron emission tomography (PET), single-photon emission computed tomography (SPECT). (<sup>\$</sup>) i.e.: target validation, (<sup>\*</sup>) a requirement only for the validation of therapeutic radiopharmaceuticals, (<sup>#</sup>) not required for microdosing e.g. radiopharmaceuticals (<100  $\mu\text{g}$ ); e.g. genotoxicity, safety pharmacology, repeat dose toxicity. (+) radiolabelling may alter the pharmacological characterisation of the targeting molecule; pharmacological effects should be ruled out at the anticipated clinical dose [247].

**Table 3.** Overview and characteristics of different rodent tumor models for glioblastoma imaging

Model	Methodology	Pro	Con	Cell lines/models	References
ENU-induced	<ul style="list-style-type: none"> <li>Exposure <i>in utero</i> to ENU (DNA damage induces brain tumors embryos);</li> <li>Dissection and culturing of these tumors <i>in vitro</i> to create animal GB models.</li> </ul>	<ul style="list-style-type: none"> <li>Immunotherapeutic research tool.</li> <li>Commercially available.</li> <li>Extensively studied.</li> <li>Provides genetic brain heterogeneity, micro-environment</li> <li>Intact immune system and BBB.</li> </ul>	<ul style="list-style-type: none"> <li>Often ENU tumor characteristic differs from human GB;</li> <li>GB tumor formation poorly reproducible.</li> </ul>	C6, 9L, T9, RG2, F98, BT4C, and RT-2	[278,283, 498-504]
GEMM	<ul style="list-style-type: none"> <li>Gene mutations result in spontaneous tumor formation;</li> <li>Transgenic mouse lines are commonly derived by direct pronuclear microinjection of transgenes into fertilized oocytes, followed by implantation into pseudo-pregnant females;</li> <li>Gene targeting of embryonic stem cells by electroporation;</li> <li>Viral-mediated methods;</li> <li>Cre recombinase transgenics</li> </ul>	<ul style="list-style-type: none"> <li>Close genetic resemblance to human GB tumors: suitable to investigate behavior of genetically defined gliomas.</li> <li>Identify the molecular events responsible for tumor initiation and progression.</li> <li>Analyze the role of the microenvironment</li> <li>Studies on drug distribution to glioma cells in the brain.</li> </ul>	<ul style="list-style-type: none"> <li>Does not completely reflect the intratumoral genomic and phenotypic heterogeneity;</li> <li>Tumor initiation cannot be controlled.</li> </ul>	EGFR amplification/Ras-gene activation (classical GB); NF1 depletion (mesenchymal GB); PDGF amplification (proneural GB)	[276,278,279, 284,504-506]
PDX	<ul style="list-style-type: none"> <li>Surgically obtained human glioma specimens. After preparing cell/tissue cultures these can also be implanted heterotopically or orthotopically in immunocompromised rodents;</li> </ul>	<ul style="list-style-type: none"> <li>Recapitulate genetic and phenotypic features of the original tumor</li> </ul>	<ul style="list-style-type: none"> <li>Relatively low engraftment and variable growth rate hamper standardization and experimental planning.</li> <li>Requires immunodeficient animals.</li> </ul>	IDH1 <sup>R132H</sup> -E478	[276,285,504]
PDGC	<ul style="list-style-type: none"> <li>Immediate implantation of surgically obtained material into the brain of the animal</li> </ul>	<ul style="list-style-type: none"> <li>High engraftment and growth rates;</li> <li>Good reproducibility;</li> <li>Reliable disease growth and progression</li> </ul>	<ul style="list-style-type: none"> <li>Does not recapitulate genetic and phenotypic features of original tumor.</li> <li>Requires immunodeficient animals</li> </ul>	U87, and U251	

Footnotes and abbreviated content: Ethyl-nitrosourea (ENU)-induced gliomas, genetically engineered models (GEMM) and patient-derived xenograft or glioma cell models (PDX or PDGC), platelet-derived growth factor (PDGF), blood brain barrier (BBB), glioblastoma (GB), neurofibromatosis type 1 gene (NF1), epidermal growth factor receptor (EGFR), deoxyribonucleic acid (DNA).

Strategic combined administration of an <sup>211</sup>At-labelled compound in tandem with an <sup>131</sup>I-labelled compound to maximise dose deposition in residual tumour margins, is expected to be successful [125]. A <sup>131</sup>I-labelled chimeric mAb ([<sup>131</sup>I]iodo-chTNT-1/B; Cotara®) is a valid first TRT option for patients presenting with largely hypoxic GB, as its target (histone H1 complexed to DNA) is abundantly present within the necrotic core of GB tumours [111,237,238]. Possibly more relevant in future, a different radionuclide cocktail for GB treatment is RGD-based integrin antagonists radiolabeled with either lutetium-177 or yttrium-90. Hypoxia may trigger the recruitment of  $\alpha\beta3$  integrins to the cellular membrane of such conditioned GB cells. Blocking  $\alpha\beta3$  integrins with RGD reduces the intracellular levels of the hypoxia-inducible factor 1 $\alpha$  [300]. Besides targeting hypoxia, TRT compounds that directly bind to targets expressed in necrotic or apoptotic cells as part of the GB core may be recommended. However, the available data is limited despite the development of imaging biomarkers, such as [<sup>18</sup>F]F-pyrophosphate, [<sup>18</sup>F]F-glucuric acid, [<sup>99m</sup>Tc]Tc-Annexin-V and [<sup>18</sup>F]F-2-(5-fluoropentyl)-2-methyl malonic acid [301-303]. Radiation- and chemoresistance are major obstacles in GB treatment and add another concept to be explored: *radiosensitizer radiopharmaceuticals (RR)*. Low-LET radiation may be potentiated by inhibitors of DNA damage repair or

disruptors of cell cycle control. Radionuclides with high-LET might be optimally combined with radiosensitizers that do not depend on the generation of reactive oxygen species [170]. Hence, RR targeting DNA repair pathways, cell cycle progression or growth factors could be administered first to enhance the cytotoxicity of subsequently administered ionizing radiation. Different types of radiosensitizers, including small molecules, macromolecules and nanomaterials, were recently reviewed [299]. An elegant example is the administration of a <sup>131</sup>I-labelled PARP inhibitor, which was recently tested in a GB animal model *in vivo*, but its therapeutic efficacy still needs to be confirmed [280,299]. **Figure 10** suggests a few recommendations for possible future TRT (combined) treatment strategies for GB.

Alongside the promising future perspectives of TRT, other radiation-based treatment options are likely to bring additional new developments for future GB therapy. Radiosurgery, brachytherapy (BT), a new method of BT, termed diffusing  $\alpha$ -emitters RT (DaRT), and boron neutron capture therapy (BNCT) have been explored for GB management with varying outcomes [301-305]. A new avenue that diminishes normal tissue toxicity whilst maintaining an equivalent tumour response is the development of ultra-high dose rate (FLASH) RT. In FLASH RT, the dose is delivered at  $\geq 40$  Gy/sec compared to dose rates of approximately 1-4 Gy/min in conventional

EBRT [306]. This technique provided encouraging results in an *in vivo* study using a murine GB model but is currently still limited to superficial tumors using electron beams [307].

### 8. Summary and Outlook

TRT can be considered as an adjuvant treatment to the standard treatment for primary or recurrent GB or as a secondary treatment when the tumor tissue is radio- and/or chemo-refractory. For recurrent GB all current treatment interventions are only given with a palliative intent. In these cases, TRT and biomarkers/imaging (MRI/PET/SPECT) might offer new possibilities for individualised treatment based on a combination of clinical findings, the genetic and molecular profile of the patient in relation to his/ her GB pathology. Such advanced molecular imaging enables, for example, the calculation of optimal dosage to achieve maximal treatment response with minimal toxicity and to prevent over-treatment [308].

Given the fact that recurrence of GB is probably inevitable, TRT could be more effective if given immediately after standard therapy or immediately after diagnosis of recurrence, depending on the clinical state of the patient [105]. Clinical reports

supporting the outcome of the latter principles are expected to emerge shortly. The major types of TRT that are being explored for GB therapy include PRRT, ligand based radionuclide therapy and RIT. Main considerations for the development of new radiopharmaceuticals for brain tumours are summarised in **Figure 11**, utilizing the three most radiolabelled vectors.

Isotope availability, the parameters of radiosynthesis and off-target toxicity are significant limitations to achieving improved process standardization. Two major requisites for successful TRT of GB are evident: i) a well differentiated tumour that expresses the desired target in ample quantities without normal physiological target functions and ii) highly specific ligands with high molar activity that are able to overcome biological barriers. BBB crossing (often disrupted by GB), tumour diffusion, internalisation and intracellular accumulation are significantly affected by the vector design irrespective of the selected optimal radionuclide. Additionally, strategies to enhance BBB crossing or CED administrations need to be considered to increase TRT effects.

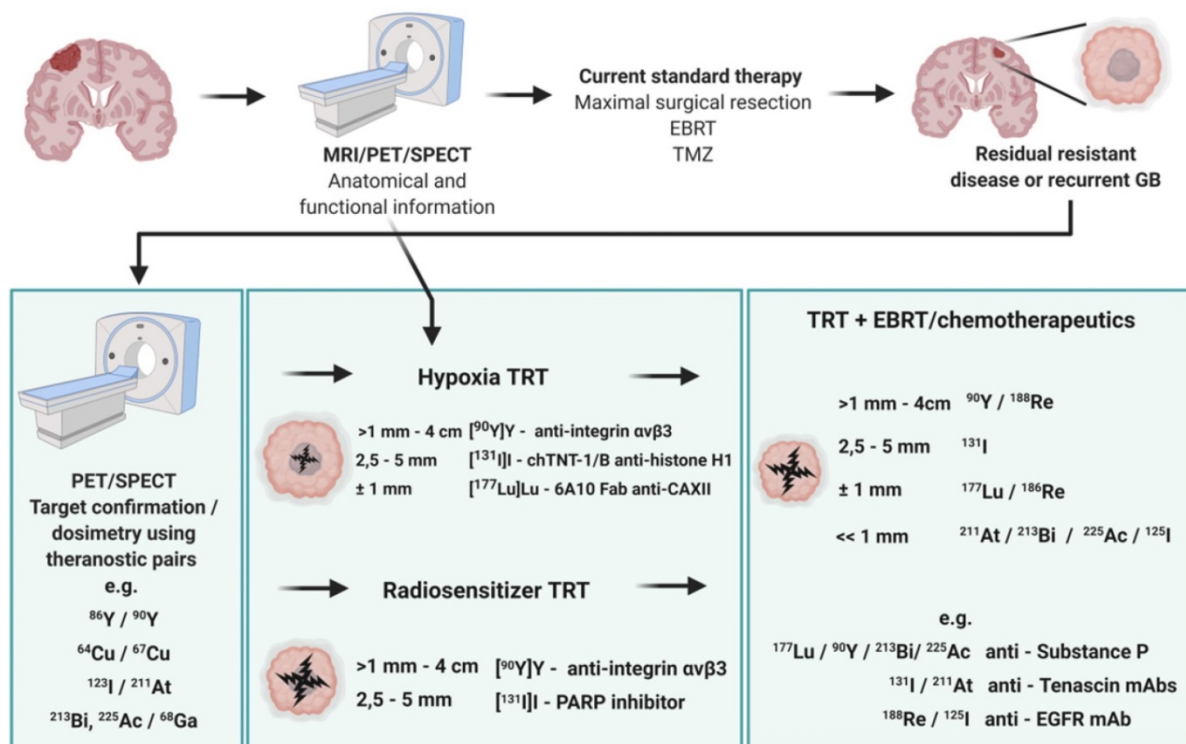


**Figure 10. Future scenario: combined targeted radionuclide therapy of glioblastoma tumours.** The prospective glioblastoma management will include practicing of various combinations of therapeutic tools. Abbreviated content: glioblastoma (GB), targeted radionuclide therapy (TRT), temozolomide (TMZ), external beam radiotherapy (EBRT), magnetic resonance imaging (MRI), positron emission tomography (PET), single-photon emission computed tomography (SPECT).

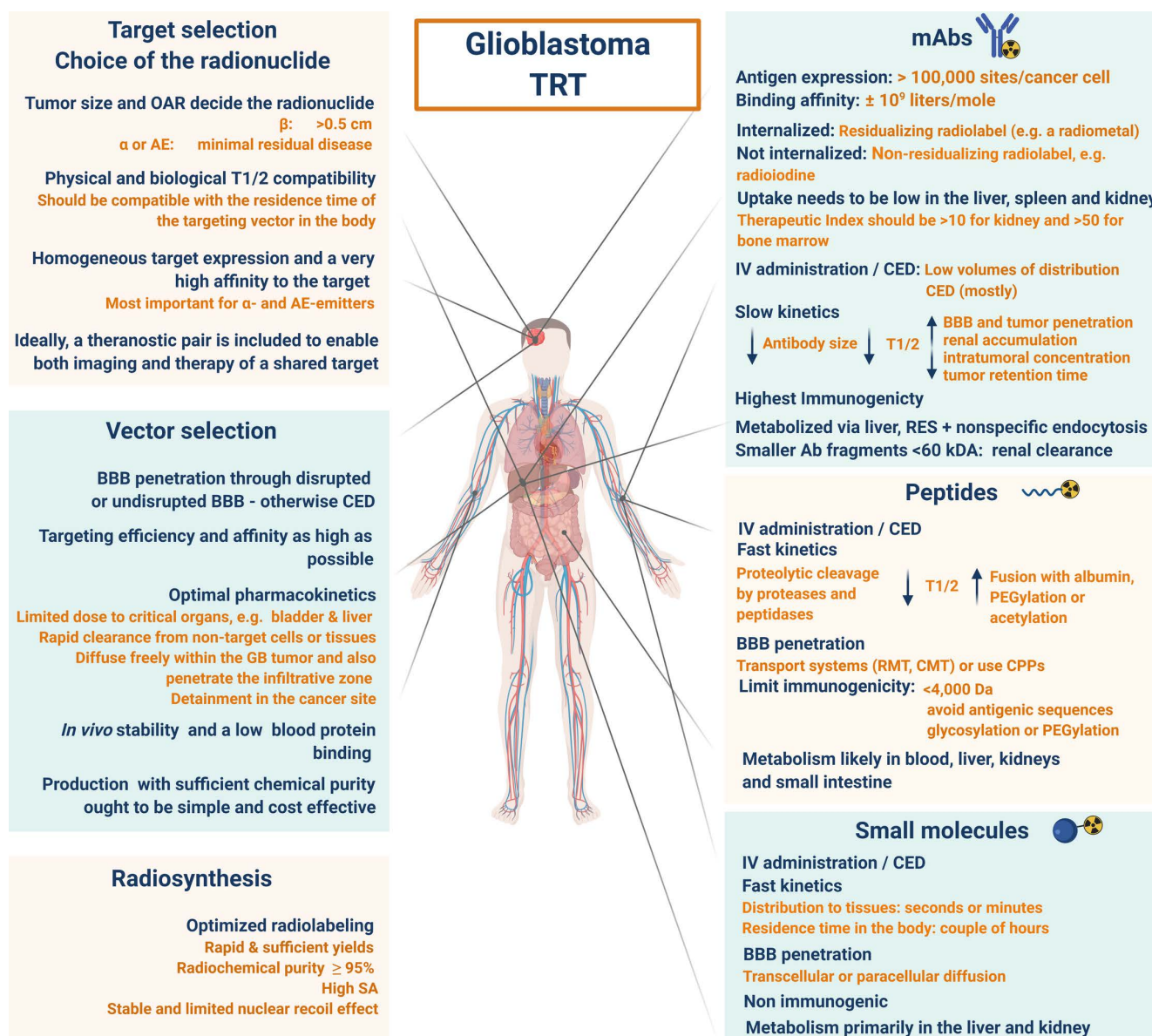


**Figure 11. Summary of targeted radionuclide therapy of glioblastoma.** Main consideration for the development of new radiopharmaceuticals for brain tumours, comparing three different radiolabelled vectors (small molecules, peptides and monoclonal antibodies (mAbs)). Abbreviations and footnoted contents: Auger electron (AE), blood-brain barrier (BBB), convection-enhanced delivery (CED), cell-penetrating peptides (CPP), intravenous (IV), organs at risk (OAR), reticulo-endothelial system (RES), receptor-mediated transport (RMT), specific activity (SA), targeted radionuclide therapy (TRT), carrier-mediated transport (CMT), half-life (T1/2).

It is imperative that proper consideration may be given to large-scale production of radionuclides for TRT, with its organisation in an economic and GMP-compliant manner. Scarcely available radionuclides or those with an expensive production infrastructure, despite having attractive characteristics, are unlikely to be used routinely [154].

A limited number of clinical studies using AE emitters as cancer therapy tools have been performed [155]. In GB patients, anti-EGFR [ $^{125}$ I]-Iodo-mAb 425 did show promising results [227]. Available  $\alpha$ -particle emitters, with their short range and high LET and RBE seem appropriate for GB therapy as they may minimize harm to surrounding healthy brain tissue thereby triggering high cell kill-rates, with minimal

dependency on cell cycle and oxygenation status [168]. In contrast, the longer range and cross-fire effect of  $\beta$ -emitters engender them to a more heterogeneous target distribution [10]. Further research on inverse dose rate effects that may affect the absorbed dose-effect relationship in TRT should be the focus of future preclinical studies in radiobiology. Besides performing accurate dosimetry, the most relevant biological endpoints must also be identified. Current clinical results show that brain tumor patients who have been treated with all three types of therapeutic radionuclides generally show limited adverse effects. A combined treatment strategy may produce more effective outcomes by targeting multiple pathways critical for cancer progression. Optimally

(randomised, multi-centered) controlled trials are urgently needed to establish the ideal management strategy for GB, in particular concerning AE emitters, combining radiopharmaceuticals and demonstrating its alliance with other systemic therapies, such as immunotherapy [178].

## Abbreviations

AE: Auger electrons; AMT: adsorptive-mediated transcytosis; BBB: blood-brain barrier; CED: convection enhanced delivery; CMT: carrier-mediated transport; CNS: central nervous system; CPP: cell-penetrating peptides; CXCR4: Chemokine receptor 4; DSB: double strand breaks; DTPA: diethylenetriamine pentaacetate; EGFR: epidermal growth factor receptor; EBRT: external beam radiotherapy; ENU: ethyl-nitrosourea; EPHR: Ephrin receptors; FAPI: fibroblast activation protein; FDA: Food and Drug Administration; GB: glioblastoma; GEMMs: genetically engineered models; GMP: Good Manufacturing Practice; IDH: isocitrate dehydrogenase; IMPD: investigational medicinal product dossier; ITLC: instant thin layer chromatography; LET: linear energy transfer; MA: molar activity; mTOR: mammalian target of rapamycin; MIRd: medical internal radiation dose; MMP: Matrix-metalloproteinases; MRI: magnetic resonance imaging; PARP: poly (ADP-ribose) polymerase; PDX/PDGC: patient-derived xenograft or glioma cell models; PET: positron emission tomography; PRRT: peptide receptor radionuclide therapy; PSMA: prostate-specific membrane antigen; PTEN: phosphatase and tensin homolog; RBE: relative biological effectiveness; RGD: Arginine-glycine-aspartate; RIBE: radiation-induced bystander effects; RIT: radio-immunotherapy; RMT: receptor-mediated transport; RN: radiation necrosis; RT: radiation therapy; SA: specific activity; SCRC: surgically created resection cavity; SP: substance-P; SPECT: single photon emission tomography; SSR2: somatostatin receptor 2; TERT: telomerase reverse transcriptase; TME: tumour micro-environment; TMZ: temozolomide; TRT: targeted radionuclide therapy; TSPO: translocator protein; VEGFR: vascular endothelial growth factor receptor; WHO: world health organization.

## Acknowledgements

Figures are created with BioRender.com. For nomenclature rules followed in this article, refer to [314,315].

## Competing Interests

The authors have declared that no competing interest exists.

## References

- Omuro A, DeAngelis LM. Glioblastoma and other malignant gliomas: A clinical review. *J Am Med Assoc.* 2013; 310: 1842–50.
- Maier EA, Bachoo RM. Glioblastoma. Rosenberg's molecular and genetic basis of neurological and psychiatric disease. Fifth Edition. Elsevier Inc; 2014.
- Weller M, Weber RG, Willscher E, Vera Riehrer V, Hentschel B, Kreuz M, et al. Molecular classification of diffuse cerebral WHO grade II/III gliomas using genome- and transcriptome-wide profiling improves stratification of prognostically distinct patient groups. *Acta Neuropathol.* 2015; 129: 679–93.
- Louis DN, Perry A, Reifenberger G, von Deimling A, Figarella-Branger D, Cavenee WK, et al. The 2016 World Health Organization classification of tumors of the central nervous system: a summary. *Acta Neuropathol.* 2016; 131: 803–20.
- Mendes M, Stupp R, Pais A, Vitorino C. Targeted theranostic nanoparticles for brain tumor treatment. *Pharmaceutics.* 2018; 10: 1–45.
- Siu A, Wind JJ, Iorgulescu JB, Chan TA, Yamada Y, Sherman JH. Radiation necrosis following treatment of high grade glioma—a review of the literature and current understanding. *Acta Neurochir.* 2012; 154: 191–201.
- Touat M, Idbaih A, Sanson M, Ligon KL. Glioblastoma targeted therapy: updated approaches from recent biological insights. *Ann Oncol.* 2017; 28: 1457–72.
- Ahmed R, Oborski MJ, Hwang M, Lieberman FS, Mountz JM. Malignant gliomas: Current perspectives in diagnosis, treatment, and early response assessment using advanced quantitative imaging methods. *Cancer Manag Res.* 2014; 6: 149–70.
- Stupp R, Mason WP, van den Bent MJ, Michael Weller M, Fisher B, Taphoorn MJB, et al. Radiotherapy plus concomitant and adjuvant temozolomide for glioblastoma. *N Engl J Med.* 2005; 352: 987–96.
- Valtorta S, Salvatore D, Rainone P, Belloli S, Bertoli G, Moresco RM. Molecular and cellular complexity of glioma. Focus on tumour microenvironment and the use of molecular and imaging biomarkers to overcome treatment resistance. *Int J Mol Sci.* 2020; 21: 1–44.
- Da Ros M, De Gregorio V, Iorio AL, Giunti L, Guidi M, de Martino M, et al. Glioblastoma chemoresistance: The double play by microenvironment and blood-brain barrier. *Int J Mol Sci.* 2018; 19: 2879.
- Pearson JRD, Regad T. Targeting cellular pathways in glioblastoma multiforme. *Signal Transduct Target Ther.* 2017; 2: 1–11.
- Wang H, Xu T, Jiang Y, Xu H, Yan Y, Fu D, et al. The challenges and the promise of molecular targeted therapy in malignant gliomas. *neoplasia.* 2015; 17: 239–55.
- Bailey C, Vidal A, Bonnemaire C, Kraeber-Bodéré F, Chérel M, Pallardy A, et al. Potential for nuclear medicine therapy for glioblastoma treatment. *Front Pharmacol.* 2019; 10: 1–9.
- Jain KK. A critical overview of targeted therapies for glioblastoma. *Front Oncol.* 2018; 8: 1–19.
- Jain R, Narang J, Sundgren PM, Hearshen D, Saksena S, Rock JP, et al. Treatment induced necrosis versus recurrent/progressing brain tumor: Going beyond the boundaries of conventional morphologic imaging. *J Neurooncol.* 2010; 100: 17–29.
- Wen PY, Macdonald DR, Reardon DA, Cloughesy TF, Sorensen AG, Galanis E, et al. Updated response assessment criteria for high-grade gliomas: Response assessment in neuro-oncology working group. *J Clin Oncol.* 2010; 28: 1963–72.
- Bolcaen J, Acou M, Descamps B, Kersemans K, Deblaere K, Vanhove C, et al. PET for therapy response assessment in glioblastoma. In: De Vleeschouwer S, Glioblastoma. Brisbane: Codon Publications. 2017.
- Albert NL, Weller M, Suchorska B, Galldiks N, Soffietti R, Kim MM, et al. Response assessment in neuro-oncology working group and European Association for Neuro-Oncology recommendations for the clinical use of PET imaging in gliomas. *Neuro Oncol.* 2016; 18: 1199–208.
- La Fougère C, Suchorska B, Bartenstein P, Kreth FW, Tonn JC. Molecular imaging of gliomas with PET: Opportunities and limitations. *Neuro Oncol.* 2011; 13: 806–19.
- Galldiks N, Lohmann P, Albert NL, Tonn JC, Langen K-J. Current status of PET imaging in neuro-oncology. *Neuro-Oncology Adv.* 2019; 1: 1–11.
- Langbein T, Weber WA, Eiber M. Future of theranostics: An outlook on precision oncology in nuclear medicine. *J Nucl Med.* 2019; 60: 135–195.
- Yordanova A, Eppard E, Kürpig S, Bundschuh RA, Schönberger S, Gonzalez-Carmona M, et al. Theranostics in nuclear medicine practice. *Oncol Targets Ther.* 2017; 10: 4821–8.
- Lee DY, Li KCP. Molecular theranostics: a primer for the imaging professional. *Am J Roentgenol.* 2011; 197: 318–24.
- Ballinger JR. Theranostics and precision medicine special feature: Review article theranostic radiopharmaceuticals: established agents in current use. *Br J Radiol.* 2018; 91: 20170969.
- Kulkarni HR, Baum RP. Patient selection for personalized peptide receptor radionuclide therapy using Ga-68 somatostatin receptor PET/CT. *PET Clin.* 2014; 9: 83–90.
- Mansoor NM, Thust S, Militano V. PET imaging in glioma techniques and current evidence. *Nucl Med Commun.* 2018; 39: 1064–80.
- Schwarzenberg J, Czernin J, Cloughesy TF, Ellingson BM, Pope WB, Geist C, et al. 3'-deoxy-3'-18F-fluorothymidine PET and MRI for early survival predictions in patients with recurrent malignant glioma treated with bevacizumab. *J Nucl Med.* 2012; 53: 29–36.

29. Fueger BJ, Czernin J, Cloughesy T, Silverman DH, Geist CL, Walter MA, et al. Correlation of 6-18F-fluoro-L-dopa PET uptake with proliferation and tumor grade in newly diagnosed and recurrent gliomas. *J Nucl Med.* 2010; 51: 1532-8.
30. Calabria FF, Barbarisi M, Gangemi V, Grillea G, Cascini GL. Molecular imaging of brain tumors with radiolabeled choline PET. *Neurosurg Rev.* 2018; 41: 67-76.
31. Bolcaen J, Acou M, Boterberg T, Vanhove C, De Vos F, Van den Broecke C, et al. 18F-FCho PET and MRI for the prediction of response in glioblastoma patients according to the RANO criteria. *Nucl Med Commun.* 2017; 38: 242-9.
32. Kwee SA, Ko JP, Jiang CS, Watters MR, Coel MN. Solitary brain lesions enhancing at MR imaging: evaluation with fluorine 18 fluorocholine PET. *Radiology.* 2007; 244: 557-65.
33. Alongi P, Quartuccio N, Arnone A, Kokomani A, Allocca M, Nappi AG, et al. Brain PET/CT using prostate cancer radiopharmaceutical agents in the evaluation of gliomas. *Clin Transl Imaging.* 2020; 8: 433-48.
34. Vetrano IG, Laudicella R, Alongi P. Choline PET/CT and intraoperative management of primary brain tumors. New insights for contemporary neurosurgery. *Clin Transl Imaging.* 2020; 8: 401-4.
35. Villena Martín M, Pena Pardo FJ, Jiménez Aragón F, Borrás Moreno JM, García Vicente AM. Metabolic targeting can improve the efficiency of brain tumor biopsies. *Semin Oncol.* 2020; 47: 148-54.
36. Drake LR, Hillmer AT, Cai Z. Approaches to PET imaging of glioblastoma. *Molecules.* 2020; 25(3): 568.
37. Su Z, Roncaroli F, Durrenberger PF, Coope DJ, Karabatsou K, Hinz R, et al. The 18-kDa mitochondrial translocator protein in human gliomas: An11C-(R)PK11195 PET imaging and neuropathology study. *J Nucl Med.* 2015; 56: 512-7.
38. Unterrainer M, Fleischmann DF, Lindner S, Brendel M, Rupprecht R, Tonn JC, et al. Detection of cerebrospinal fluid dissemination of recurrent glioblastoma using TSPO-PET with 18F-GE-180. *Clin Nucl Med.* 2018; 43: 518-9.
39. Carney B, Carlucci G, Salinas B, Di Gialleonardo V, Kossatz S, Vansteene A, et al. Non-invasive PET imaging of PARP1 expression in glioblastoma models. *Mol Imaging Biol.* 2016; 18: 386-92.
40. Huang M, Xiong C, Lu W, Zhou M, Huang Q, Weinberg J, et al. Dual-modality micro-positron emission tomography/computed tomography and near-infrared fluorescence imaging of EphB4 in orthotopic glioblastoma xenograft models. *Mol Imaging Biol.* 2014; 16: 74-84.
41. Michel LS, Dyroff S, Brooks FJ, Spayd KJ, Lim S, Engle JT, et al. PET of poly (ADP-ribose) polymerase activity in cancer: Preclinical assessment and first in-human studies. *Radiology.* 2017; 282: 453-63.
42. Zmuda F, Blair A, Liuzzi MC, Malviya G, Chalmers AJ, Lewis D, et al. An 18 F-labeled Poly(ADP-ribose) polymerase positron emission tomography imaging agent. *J Med Chem.* 2018; 61: 4103-14.
43. Salinas B, Irwin CP, Kossatz S, Alexander Bolaender A, Chiosis G, Pillarsetty N, et al. Radioiodinated PARP1 tracers for glioblastoma imaging. *Eur J Nucl Med Mol Imaging Res.* 2015; 5: 1-14.
44. Truillet C, Cunningham JT, Parker MFL, Huynh LT, Conn CS, Ruggero D, et al. Noninvasive measurement of mTORC1 signaling with 89Zr-Transferrin. *Clin Cancer Res.* 2017; 23: 3045-52.
45. Benezra M, Hambarzumyan D, Penate-Medina O, Darren R Veach DR, Pillarsetty N, Smith-Jones P, et al. Fluorine-labeled dasatinib nanoformulations as targeted molecular imaging probes in a PDGFB-driven murine glioblastoma model. *Neoplasia.* 2012; 14: 1132-43.
46. Bernard-Gauthier V, Bailey JJ, Berke S, Schirmacher R, Leahy JW. Recent advances in the development and application of radiolabeled kinase inhibitors for PET imaging. *Molecules.* 2015; 20: 22000-27.
47. Slobbe P, Poot AJ, Windhorst AD, Van Dongen GAMS. PET imaging with small-molecule tyrosine kinase inhibitors: TKI-PET. *Drug Discov Today.* 2012; 17: 1175-87.
48. Sun J, Cai L, Zhang K, Pu PY, Yang WD, Gao S. A pilot study on EGFR-targeted molecular imaging of PET/CT. *Clin Nucl Med.* 2014; 39: e20-6.
49. Albano D, Tomasini D, Bonù M, Giubbini R, Bertagna F. 18F-Fluciclovine (18F-FACBC) PET/CT or PET/MRI in gliomas/glioblastomas. *Ann Nucl Med.* 2020; 34: 81-6.
50. Kondo A, Ishii H, Aoki S, Suzuki M, Nagasawa H, Kubota K, et al. Phase IIa clinical study of [18F]fluciclovine: efficacy and safety of a new PET tracer for brain tumors. *Ann Nucl Med.* 2016; 30: 608-18.
51. Michaud L, Beattie BJ, Akhurst T, Dunphy M, Zanzonico P, Finn R, et al. F-Fluciclovine (18 F-FACBC) PET imaging of recurrent brain tumors. *Eur J Nucl Med Mol Imaging.* 2020; 47(6):1353-1367.
52. Antonios JP, Soto H, Everson RG, Moughon DL, Wang AC, Orpilla J, et al. Detection of immune responses after immunotherapy in glioblastoma using PET and MRI. *Proc Natl Acad Sci U S A.* 2017; 114: 10220-5.
53. Zhang H, Liu N, Gao S, Hu X, Zhao W, Tao R, et al. Can an 18F-ALF-NOTA-PRGD2 PET/CT scan predict treatment sensitivity to concurrent chemoradiotherapy in patients with newly diagnosed glioblastoma? *J Nucl Med.* 2016; 57: 524-9.
54. Jin ZH, Furukawa T, Degardin M, Sugyo A, Tsuji AB, Yamasaki T, et al.  $\alpha$ V $\beta$ 3 integrin-targeted radionuclide therapy with 64Cu-cyclam-RAFT-c-(RGDfK)-4. *Mol Cancer Ther.* 2016; 15: 2076-85.
55. Jin ZH, Tsuji AB, Degardin M, Sugyo A, Yoshii Y, Nagatsu K, et al. Uniform intratumoral distribution of radioactivity produced using two different radioagents, (64Cu)-cyclam-RAFT-c-(RGDfK)-4 and (64Cu)-ATSM, improves therapeutic efficacy in a small animal tumor model. *EJNMMI Res.* 2018; 8: 54.
56. Jin ZH, Furukawa T, Ohya T, Degardin M, Sugyo A, Tsuji AB, et al. 67Cu-radiolabeling of a multimeric RGD peptide for  $\alpha$ V $\beta$ 3 integrin-targeted radionuclide therapy: stability, therapeutic efficacy, and safety studies in mice. *Nucl Med Commun.* 2017; 38: 347-55.
57. Hennrich U, Benešová M. [68Ga]Ga-DOTA-TOC: The first FDA-approved 68Ga- radiopharmaceutical for PET imaging. *Pharmaceuticals.* 2020; 13: 1-12.
58. Lapa C, Linsenmann T, Lückert K, Samnick S, Herrmann K, Stoffer C, et al. Tumor-associated macrophages in glioblastoma multiforme-a suitable target for somatostatin receptor-based imaging and therapy? *PLoS One.* 2015; 10: e0122269.
59. Heute D, Kostron H, Von Guggenberg E, Ingorokva S, Gabriel M, Dobrozemsky G, et al. Response of recurrent high-grade glioma to treatment with 90Y-DOTATOC. *J Nucl Med.* 2010; 51: 397-400.
60. Schumacher T, Hofer S, Eichhorn K, Wasner M, Zimmerer S, Freitag P, et al. Local injection of the 90Y-labelled peptidic vector DOTATOC to control gliomas of WHO grades II and III: An extended pilot study. *Eur J Nucl Med.* 2002; 29: 486-93.
61. Merlo A, Hausmann O, Wasner M, Steiner P, Otte A, Jermann E, Freitag P, et al. Locoregional regulatory peptide receptor targeting with the diffusible somatostatin analogue 90Y-labeled DOTA0-D-Phe1-Tyr3-octreotide (DOTATOC): a pilot study in human gliomas. *Clin Cancer Res.* 1999; 5: 1025-33.
62. Virgolini I, Britton K, Buscombe J, Moncayo R, Paganelli G, Riva P. 111In- and 90Y-DOTA-lanreotide: Results and implications of the Mauritius trial. *Semin Nucl Med.* 2002; 32: 148-55.
63. Lindner T, Loktev A, Giesel F, Kratochwil C, Altmann A, Haberkorn U. Targeting of activated fibroblasts for imaging and therapy. *EJNMMI Radiopharm Chem.* 2019; 4: 1-15.
64. Röhrich M, Loktev A, Wefers AK, Altmann A, Paech D, Adeberg S, et al. IDH-wildtype glioblastomas and grade III/IV IDH-mutant gliomas show elevated tracer uptake in fibroblast activation protein-specific PET/CT. *Eur J Nucl Med Mol Imaging.* 2019; 46: 2569-80.
65. Windisch P, Röhrich M, Regnery S, Tonndorf-Martini E, Held T, Lang K, et al. Fibroblast activation protein (FAP) specific PET for advanced target volume delineation in glioblastoma. *Radiother Oncol.* 2020; 150: 159-63.
66. Panicelli P, Villano C, Cistaro A, Bruno A, Barbatto F, Piccardo A, et al. Imaging of brain tumors with Copper-64 chloride: Early experience and results. *Cancer Biother Radiopharm.* 2016; 31: 159-67.
67. Hino-Shishikura A, Tateishi U, Shibata H, Yoneyama T, Nishii T, Torii I, et al. Tumor hypoxia and microscopic diffusion capacity in brain tumors: A comparison of 62Cu-diacetyl-bis (N4-methylthiosemicarbazone) PET/CT and diffusion-weighted MR imaging. *Eur J Nucl Med Mol Imaging.* 2014; 41: 1419-27.
68. Tateishi K, Tateishi U, Nakanowatari S, Ohtake, Minamimoto R, Suenaga J, et al. 62Cu-diacetyl-bis (N4-methylthiosemicarbazone) PET in human gliomas: Comparative study with [18F]fluorodeoxyglucose and L-methyl-[11C]methionine PET. *Am J Neuroradiol.* 2014; 35: 278-84.
69. Gangemi V, Mignogna C, Guzzi G, Lavano A, Bongarzone S, Cascini GL, et al. Impact of [64Cu][Cu(ATSM)] PET/CT in the evaluation of hypoxia in a patient with glioblastoma: A case report. *BMC Cancer.* 2019; 19: 8-11.
70. Cai W, Chen K, He L, Cao Q, Koong A, Chen X. Quantitative PET of EGFR expression in xenograft-bearing mice using 64Cu-labeled cetuximab, a chimeric anti-EGFR monoclonal antibody. *Eur J Nucl Med Mol Imaging.* 2007; 34: 850-8.
71. Mitran B, Güler R, Roche FP, Lindström E, Selvaraju RK, Fleetwood F, et al. Radionuclide imaging of VEGFR2 in glioma vasculature using biparatopic antibody conjugate: Proof-of-principle in a murine model. *Theranostics.* 2018; 8: 4462-76.
72. Chen K, Cai W, Li ZB, Wang H, Chen X. Quantitative PET imaging of VEGF receptor expression. *Mol Imaging Biol.* 2009; 11: 15-22.
73. Hu K, Shang J, Xie L, Hanyu M, Zhang Y, Yang Z, et al. PET imaging of VEGFR with a novel 64Cu-labeled peptide. *ACS Omega.* 2020; 5: 8508-14.
74. Cai W, Chen K, Mohamedali KA, Cao Q, Gambhir SS, Rosenblum MG, et al. PET of vascular endothelial growth factor receptor expression. *J Nucl Med.* 2006; 47: 2048-56.
75. Pérès EA, Toutain J, Paty L-P, et al. (64)Cu-ATSM/(64)Cu-Cl(2) and their relationship to hypoxia in glioblastoma: a preclinical study. *Eur J Nucl Med Mol Imaging Res.* 2019; 9: 114.
76. Sai KKS, Sattiraju A, Almaguel FG, et al. Peptide-based PET imaging of the tumor restricted IL13RA2 biomarker. *Oncotarget.* 2017; 8: 50997-1007.
77. Offenhäuser C, Al-Ejeh F, Puttick S, Ensby KS, Bruce ZC Jamieson PR, et al. EphA3 pay-loaded antibody therapeutics for the treatment of glioblastoma. *Cancers.* 2018; 10: 519.
78. Bertagna F, Albano D, Cerudelli E, Gazzilli M, Giubbini R, Treglia G. Potential of radiolabeled PSMA PET/CT or PET/MRI diagnostic procedures in gliomas/glioblastomas. *Curr Radiopharm.* 2019; 13: 94-8.
79. Mahzouni P, Shavakhi M. Prostate-specific membrane antigen expression in neovasculature of glioblastoma multiforme. *Adv Biomed Res.* 2019; 8: 18.
80. Wernicke AG, Edgar MA, Lavi E, Liu H, Salerno P, Bander NH, et al. Prostate-specific membrane antigen as a potential novel vascular target for treatment of glioblastoma multiforme. *Arch Pathol Lab Med.* 2011; 135: 1486-9.
81. Nomura N, Pastorino S, Jiang P, et al. Prostate specific membrane antigen (PSMA) expression in primary gliomas and breast cancer brain metastases. *Cancer Cell Int.* 2014; 14(1): 16.

82. Sasikumar A, Joy A, Pillai MRA, Nanabala R, Anees KM, Jayaprakash PG, et al. Diagnostic value of <sup>68</sup>Ga PSMA-11 PET/CT imaging of brain tumors - preliminary analysis. *Clin Nucl Med.* 2017; 42: e41-8.
83. Verma P, Malhotra G, Goel A, Rakshit S, Chandak A, Chedda R, et al. Differential uptake of <sup>68</sup>Ga-PSMA-HBED-CC (PSMA-11) in low-grade versus high-grade gliomas in treatment-naive patients. *Clin Nucl Med.* 2019; 44: e318-22.
84. Kunikowska J, Charzyńska I, Kuliński R, Pawlak D, Maurin M, Królicki L. Tumor uptake in glioblastoma multiforme after iv injection of [<sup>177</sup>Lu]Lu-PSMA-617. *Eur J Nucl Med Mol Imaging.* 2020; 47: 1605-6.
85. Albert NL, Unterrainer M, Fleischmann DF, Lindner S, Vettermann F, Brunegraf A, et al. TSPO PET for glioma imaging using the novel ligand 18F-GE-180: First results in patients with glioblastoma. *Eur J Nucl Med Mol Imaging.* 2017; 44: 2230-8.
86. Kumar A, Ballal S, Yadav MP, et al. <sup>177</sup>Lu-/<sup>68</sup>Ga-PSMA theranostics in recurrent glioblastoma multiforme: Proof of concept. *Clin Nucl Med.* 2020; 45: e512-3.
87. Salas Fragomeni RA, Pienta KJ, Pomper MG, Gorin MA, Rowe SP. Uptake of prostate-specific membrane antigen-targeted 18F-DCFPyL in Cerebral radionecrosis: Implications for diagnostic imaging of high-grade gliomas. *Clin Nucl Med.* 2018; 43: e419-21.
88. Matsuda M, Ishikawa E, Yamamoto T, Hatano K, Joraku A, Iizumi Y, et al. Potential use of prostate specific membrane antigen (PSMA) for detecting the tumor neovasculature of brain tumors by PET imaging with 89Zr-Df-IAB2M anti-PSMA minibody. *J Neurooncol.* 2018; 138: 581-9.
89. Salas Fragomeni RA, Menke JR, Holdhoff M, Ferrigno C, Laterra JJ, Solnes LB, et al. Prostate-specific membrane antigen-targeted imaging with [<sup>18</sup>F]DCFPyL in high-grade gliomas. *Clin Nucl Med.* 2017; 42: e433-5.
90. Marafi F, Sasikumar A, Fathallah W, Esmail A. <sup>18</sup>F-PSMA 1007 brain PET/CT imaging in glioma recurrence. *Clin Nucl Med.* 2020; 45: E61-2.
91. Oliveira D, Stegmayr C, Heinzl A, Ermet J, Neumaier B, Shah NJ, et al. High uptake of <sup>68</sup>Ga-PSMA-HBED-CC and 18F-DCFPyL in the peritumoral area of rat gliomas due to activated astrocytes. *EJNMMI Res.* 2020; 10(1): 55.
92. Drude N, Tienken L, Mottaghy FM. Theranostic and nanotheranostic probes in nuclear medicine. *Methods.* 2017; 130: 14-22.
93. Królicki L, Bruchertseifer F, Kunikowska J, Koziara H, Królicki B, Jakuciński M, et al. Safety and efficacy of targeted alpha therapy with <sup>213</sup>Bi-DOTA-substance P in recurrent glioblastoma. *Eur J Nucl Med Mol Imaging.* 2019; 46: 614-22.
94. Lapa C, Lücknerath K, Kleinlein I, Monoranu CM, Linsenmann T, Kessler AF, et al. <sup>68</sup>Ga-pentixafor-PET/CT for imaging of chemokine receptor 4 expression in glioblastoma. *Theranostics.* 2016; 6: 428-34.
95. Akabani G, Reist CJ, Cokgor I, Friedman AH, Friedman HS, Coleman RE et al. Dosimetry of <sup>131</sup>I-labeled 81C6 monoclonal antibody administered intravenously to surgically created resection cavities in patients with malignant brain tumors. *J Nucl Med.* 1999; 40: 631-8.
96. Reardon DA, Akabani G, Coleman RE, Friedman AH, Friedman HS, Herndon 2nd JE, et al. Salvage radioimmunotherapy with murine iodine-131-labeled antitenascin monoclonal antibody 81C6 for patients with recurrent primary and metastatic malignant brain tumors: Phase II study results. *J Clin Oncol.* 2006; 24: 115-22.
97. Le Rhun E, Preusser M, Roth P, Reardon DA, van den Bent M, Wen P, et al. Molecular targeted therapy of glioblastoma. *Cancer Treat Rev.* 2019; 80: 101896.
98. Lee ST, Burvenich I, Scott AM. Novel target selection for nuclear medicine studies. *Semin Nucl Med.* 2019; 49: 357-68.
99. Shergalis A, Bankhead A, Luesakul U, Muangsin N, Neamati N. Current challenges and opportunities in treating glioblastomas. *Pharmacol Rev.* 2018; 70: 412-45.
100. Chuang DF, Lin X. Targeted Therapies for the Treatment of Glioblastoma in Adults. *Curr Oncol Rep.* 2019; 21(7):61.
101. Autelitano F, Loyaux D, Roudières S, Déon C, Guette F, Fabre P, et al. Identification of novel tumor-associated cell surface sialoglycoproteins in human glioblastoma tumors using quantitative proteomics. *PLoS One.* 2014; 9: e110316.
102. He J, Liu Y, Xie X, Zhu T, Soules M, DiMeco F, et al. Identification of cell surface glycoprotein markers for glioblastoma-derived stem-like cells using a lectin microarray and LC-MS/MS approach. *J Proteome Res.* 2010; 9: 2565-72.
103. Baeza-Kallee N, Bergès R, Soubéran A, Colin C, Denicolai E, Appay R, et al. Glycolipids recognized by A2B5 antibody promote proliferation, migration, and clonogenicity in glioblastoma cells. *Cancers.* 2019; 11 (9): 1267.
104. Reardon DA, Turner S, Peters KB, Desjardins A, Carolina N. A review of VEGF / VEGFR-targeted therapeutics for recurrent glioblastoma. *J Natl Compr Canc Netw.* 2011; 9: 414-27.
105. Królicki L, Kunikowska J, Bruchertseifer F, Koziara H, Królicki B, Jakuciński M, et al. <sup>225</sup>Ac- and <sup>213</sup>Bi-substance P analogues for glioma therapy. *Semin Nucl Med.* 2020; 50: 141-51.
106. Reulen HJ, Suero Molina E, Zeidler R, Gildehaus FJ, Böning G, Gosewisch A, et al. Intracavitary radioimmunotherapy of high-grade gliomas: present status and future developments. *Acta Neurochir.* 2019; 161: 1109-24.
107. Spencer D, Auffinger B, Murphy J, Muroski ME, Qiao J, Gorind Y, et al. Hitting a moving target: Glioma stem cells demand new approaches in glioblastoma therapy. *Curr Cancer Drug Targets.* 2017; 17: 236-54.
108. Larson S, Carrasquillo JA, Cheung N-KV, Press OW. Radioimmunotherapy of human tumours. *Nat Rev Cancer.* 2015; 15: 347-60.
109. Montay-Gruel P, Meziani L, Yakkala C, Vozenin MC. Expanding the therapeutic index of radiation therapy by normal tissue protection. *Br J Radiol.* 2019; 92(1093): 20180008.
110. National Research Council (US) and Institute of Medicine (US) Committee on State of the Science of Nuclear Medicine. *Advancing Nuclear Medicine Through Innovation.* In: Targeted Radionuclide Therapy. Washington (DC): National Academies Press (US); 2007.
111. Puttermans J, Lahoutte T, D'huyvetter M, Devoogdt N. Beyond the barrier: Targeted radionuclide therapy in brain tumors and metastases. *Pharmaceutics.* 2019; 11(8): 376.
112. Pruis JJ, van Dongen GAMS, Veldhuijzen van Zanten SEM. The added value of diagnostic and theranostic PET imaging for the treatment of CNS tumors. *Int J Mol Sci.* 2020; 21: 1-24.
113. Maza S, Kiewe P, Munz DL, Korfel A, Hamm B, Jahnke K, et al. First report on a prospective trial with yttrium-90-labeled ibritumomab tiuxetan (Zevalin) in primary CNS lymphoma. *Neuro Oncol.* 2009; 11: 423-9.
114. Królicki L, Bruchertseifer F, Kunikowska J, Koziara H, Królicki B, Jakuciński M, et al. Prolonged survival in secondary glioblastoma following local injection of targeted alpha therapy with <sup>213</sup>Bi-substance P analogue. *Eur J Nucl Med Mol Imaging.* 2018; 45: 1636-44.
115. Taylor OG, Brzozowski JS, Skelding KA. Glioblastoma multiforme: An overview of emerging therapeutic targets. *Front Oncol.* 2019; 9: 1-11.
116. Chaturvedi S, Mishra AK. Small molecule radiopharmaceuticals - A review of current approaches. *Front Med.* 2016; 3: 1-18.
117. Huse JT, Holland EC. Targeting brain cancer: Advances in the molecular pathology of malignant glioma and medulloblastoma. *Nat Rev Cancer.* 2010; 10: 319-31.
118. Arvanitis CD, Ferraro GB, Jain RK. The blood-brain barrier and blood-tumour barrier in brain tumours and metastases. *Nat Rev Cancer.* 2020; 20: 26-41.
119. Cavaco M, Gaspar D, Castanho MARB, Neves V. Antibodies for the treatment of brain metastases, a dream or a reality? *Pharmaceutics.* 2020; 12(1): 62.
120. Ahmad AM. Potential pharmacokinetic interactions between antiretrovirals and medicinal plants used as complementary and African traditional medicines. *Biopharm Drug Dispos.* 2007; 28: 135-43.
121. Veldhuijzen van Zanten SEM, De Witt Hamer PC, van Dongen GAMS. Brain access of monoclonal antibodies as imaged and quantified by <sup>89</sup>Zr-antibody PET: Perspectives for treatment of brain diseases. *J Nucl Med.* 2019; 60: 615-6.
122. van Dongen GAMS, Poot AJ, Vugts DJ. PET imaging with radiolabeled antibodies and tyrosine kinase inhibitors: immuno-PET and TKI-PET. *Tumour Biol.* 2012; 33: 607-15.
123. Luurtsema G, de Lange ECM, Lammertsma AA, Franssen EJF. Transport across the blood-brain barrier: Stereoselectivity and PET-tracers. *Mol Imaging Biol.* 2004; 6: 306-18.
124. Trippier PC. Selecting good 'drug-like' properties to optimize small molecule blood-brain barrier penetration. *Curr Med Chem.* 2016; 23: 1392-407.
125. Zalutsky MR, Reardon DA, Pozzi OR, Vaidyanathan G, Bigner DD. Targeted  $\alpha$ -particle radiotherapy with <sup>211</sup>At-labeled monoclonal antibodies. *Nucl Med Biol.* 2007; 34: 779-85.
126. Riva P, Arista A, Franceschi G, Frattarelli M, Sturiale C, Riva N, et al. Local treatment of malignant gliomas by direct infusion of specific monoclonal antibodies labeled with <sup>131</sup>I: Comparison of the results obtained in recurrent and newly diagnosed tumors. *Cancer Res.* 1995; 55(23S): 5952s-6s.
127. Sgouros G, Bodei L, McDevitt MR, Nedrow JR. Radiopharmaceutical therapy in cancer: clinical advances and challenges. *Nat Rev Drug Discov.* 2020; 19(9): 589-608.
128. Vogelbaum MA, Iannotti CA. Convection-enhanced delivery of therapeutic agents into the brain. 1st edition. *Handbook of Clinical Neurology.* Elsevier B.V.; 2012: (104)355-62.
129. Lopez KA, Waziri AE, Canoll PD, Bruce JN. Convection-enhanced delivery in the treatment of malignant glioma. *Neur Res.* 2006; 28: 542-8.
130. Elgqvist J, Frost S, Pouget JP, Albertsson P. The potential and hurdles of targeted alpha therapy - clinical trials and beyond. *Front Oncol.* 2014; 4: 1-10.
131. Ung TH, Malone H, Canoll P, Bruce JN. Convection-enhanced delivery for glioblastoma: targeted delivery of antitumor therapeutics. *CNS Oncol.* 2015; 4: 225-34.
132. Jahangiri A, Chin AT, Flanagan PM, Chen R, Bankiewicz K, Aghi MK. Convection-enhanced delivery in glioblastoma: A review of preclinical and clinical studies. *J Neurosurg.* 2017; 126: 191-200.
133. Chacko AM, Li C, Pryma DA, Brem S, Coukos G, Muzlykantov V. Targeted delivery of antibody-based therapeutic and imaging agents to CNS tumors: Crossing the blood-brain barrier divide. *Expert Opin Drug Deliv.* 2013; 10: 907-26.
134. Malcolm J, Falzone N, Lee BQ, Vallis KA. Targeted radionuclide therapy: New advances for improvement of patient management and response. *Cancers.* 2019; 11(2): 268.
135. Diao L, Meibohm B. Pharmacokinetics and pharmacokinetic-pharmacodynamic correlations of therapeutic peptides. *Clin Pharmacokinet.* 2013; 52: 855-68.
136. Pardridge WM. Targeting neurotherapeutic agents through the blood-brain barrier. *Arch Neurol.* 2002; 59: 35-40.
137. Keizer RJ, Huitema ADR, Schellens JHM, Beijnen JH. Clinical pharmacokinetics of therapeutic monoclonal antibodies. *Clin Pharmacokinet.* 2010; 49: 493-507.
138. Park EJ, Zhang YZ, Vykhodtseva N, McDannold N. Ultrasound-mediated blood-brain/blood-tumor barrier disruption improves outcomes with

- trastuzumab in a breast cancer brain metastasis model. *J Control Release*. 2012; 163: 277–84.
139. Sehlin D, Syvänen S. Engineered antibodies : new possibilities for brain PET? *Eur J Nucl Med Mol Imaging*. 2019; 11: 2848–58.
  140. Razpotnik R, Novak N, Curin Šerbec V, Rajčević U. Targeting malignant brain tumors with antibodies. *Front Immunol*. 2017; 8: 1–14.
  141. Pourgholi F, Hajivalili M, Farhad JN, Kafil HS, Yousefi M. Nanoparticles: Novel vehicles in treatment of glioblastoma. *Biomed Pharmacother*. 2016; 77: 98–107.
  142. Karim R, Palazzo C, Evrard B, Piel G. Nanocarriers for the treatment of glioblastoma multiforme: Current state of the art. *J Control Release*. 2016; 227: 23–37.
  143. Sun C, Ding Y, Zhou L, Shi D, Sun L, Webster TJ, et al. Noninvasive nanoparticle strategies for brain tumor targeting. *Nanomedicine*. 2017; 13: 2605–21.
  144. Aparicio-Blanco J, Torres-Suárez AI. Towards tailored management of malignant brain tumors with nanotheranostics. *Acta Biomater*. 2018; 73: 52–63.
  145. Saraiva C, Praça C, Ferreira R, Santos T, Ferreira L, Bernardino L. Nanoparticle-mediated brain drug delivery: Overcoming blood-brain barrier to treat neurodegenerative diseases. *J Control Release*. 2016; 235: 34–47.
  146. Cheng Y, Morshed RA, Auffinger B, Tobias AL, Lesniak MS. Multifunctional nanoparticles for brain tumor imaging and therapy. *Adv Drug Deliv Rev*. 2014; 66: 42–57.
  147. Grana CM, Chinol M, de Cicco C, Bartolomei M, Cremonesi M, Bodei L, et al. Eleven-year experience with the avidin-biotin pretargeting system in glioblastoma: Toxicity, efficacy and survival. *Open Nucl Med J*. 2012; 4: 14–20.
  148. Verhoeven M, Seimille Y, Dalm SU. Therapeutic applications of pretargeting. *Pharmaceutics*. 2019; 11(9): 434.
  149. Bartolomei M, Mazzetta C, Handkiewicz-Junak D, Bodei L, Rocca P, Grana C, et al. Combined treatment of glioblastoma patients with locoregional pre-targeted 90Y-biotin radioimmunotherapy and temozolomide. *Q J Nucl Med Mol Imaging*. 2004; 48: 220–8.
  150. Séhédic D, Chourpa I, Tétaud C, Griveau A, Loussouarn C, Avril S, et al. Locoregional confinement and major clinical benefit of (188)Re-loaded CXCR4-targeted nanocarriers in an orthotopic human to mouse model of glioblastoma. *Theranostics*. 2017; 7: 4517–36.
  151. de Kruijff RM, van der Meer AJGM, Windmeijer CAA, Kouwenberg JJM, Morgenstern A, Bruchertseifer F, et al. The therapeutic potential of polymersomes loaded with 225Ac evaluated in 2D and 3D *in vitro* glioma models. *Eur J Pharm Biopharm*. 2018; 127: 85–91.
  152. Ananda S, Nowak AK, Cher L, Dowling A, Brown C, Simes J, et al. Phase 2 trial of temozolomide and pegylated liposomal doxorubicin in the treatment of patients with glioblastoma multiforme following concurrent radiotherapy and chemotherapy. *J Clin Neurosci*. 2011; 18: 1444–8.
  153. Ersahin D, Doddamani I, Cheng D. Targeted radionuclide therapy. *Cancers*. 2011; 3: 3838–55.
  154. Gudkov SV, Shilyagina NY, Vodenev VA, Zvyagin AV. Targeted radionuclide therapy of human tumors. *Int J Mol Sci*. 2015; 17: 1–19.
  155. Ku A, Facca VJ, Cai Z, Reilly RM. Auger electrons for cancer therapy – a review. *EJNMMI Radiopharm Chem*. 2019; 4(1): 27.
  156. Karagiannis T. Comparison of different classes of radionuclides for potential use in radioimmunotherapy. *Hell J Nucl Med*. 2007; 10: 82–8.
  157. Soyland C, Hassfjell SP. Survival of human lung epithelial cells following *in vitro* alpha-particle irradiation with absolute determination of the number of alpha-particle traversals of individual cells. *Int J Radiat Biol*. 2000; 76: 1315–22.
  158. Colwell N, Larion M, Giles AJ, Seldomridge AN, Sizzdahkhani S, Gilbert MR, et al. Hypoxia in the glioblastoma microenvironment: Shaping the phenotype of cancer stem-like cells. *Neuro Oncol*. 2017; 19: 887–96.
  159. Staudacher AH, Liapis V, Brown MP. Therapeutic targeting of tumor hypoxia and necrosis with antibody  $\alpha$ -radioconjugates. *Antib Ther*. 2018; 1: 75–83.
  160. Graf F, Fahrner J, Maus S, Morgenstern A, Bruchertseifer F, Venkatachalam S, et al. DNA double strand breaks as predictor of efficacy of the alpha-particle emitter Ac-225 and the electron emitter Lu-177 for somatostatin receptor targeted radiotherapy. *PLoS One*. 2014; 9: e88239.
  161. Cornelissen B, A Vallis K. Targeting the nucleus: An overview of auger-electron radionuclide therapy. *Curr Drug Discov Technol*. 2010; 7: 263–79.
  162. Sgouros G, Bodei L, McDevitt MR, Nedrow JR. Radiopharmaceutical therapy in cancer: Clinical advances and challenges. *Nat Rev Drug Discov*. 2020; 19: 589–608.
  163. Wygoda Z, Kula D, Bierzyńska-Macyszyn G, Larysz D, Jarzab M, Wlasczyk P, et al. Use of monoclonal anti-EGFR antibody in the radioimmunotherapy of malignant gliomas in the context of EGFR expression in grade III and IV tumors. *Hybridoma*. 2006; 25: 125–32.
  164. Rebischung C, Hoffmann D, Stéfani L, Desruet MD, Wang K, Adelstein SJ, et al. First human treatment of resistant neoplastic meningitis by intrathecal administration of MTX Plus 125IuDR. *Int J Radiat Biol*. 2008; 84: 1123–9.
  165. Thisgaard H, Halle B, Aaberg-Jessen C, Olsen BB, Nautrup Therkelsen AS, Dam JH, et al. Highly effective auger-electron therapy in an orthotopic glioblastoma xenograft model using convection-enhanced delivery. *Theranostics*. 2016; 6: 2278–91.
  166. Emrich JG, Brady LW, Quang TS, Class R, Miyamoto C, Black P, et al. Radioiodinated (I-125) monoclonal antibody 425 in the treatment of high grade glioma patients: Ten-year synopsis of a novel treatment. *Am J Clin Oncol*. 2002; 25: 541–6.
  167. Quang TS, Brady LW. Radioimmunotherapy as a novel treatment regimen: 125I-labeled monoclonal antibody 425 in the treatment of high-grade brain gliomas. *Int J Radiat Oncol Biol Phys*. 2004; 58: 972–5.
  168. Morgenstern A, Apostolidis C, Kratochwil C, Sathekge M, Krolicki L, Bruchertseifer F. An overview of targeted alpha therapy with 225 actinium and 213 bismuth. *Curr Radiopharm*. 2018; 11: 200–8.
  169. Yeong CH, Cheng M, Ng KH. Therapeutic radionuclides in nuclear medicine: Current and future prospects. *J Zhejiang Univ Sci B*. 2014; 15: 845–63.
  170. Gill MR, Falzone N, Du Y, Vallis KA. Targeted radionuclide therapy in combined-modality regimens. *Lancet Oncol*. 2017; 18: e414–23.
  171. De Vleeschouwer BG. Glioblastoma: To target the tumor cell or the microenvironment? In: De Vleeschouwer S, Glioblastoma. Brisbane: Codon Publications; 2017.
  172. Seregni E, Maccauro M, Chiesa C, Mariani L, Pascali C, Mazzaferro V, et al. Treatment with tandem [90Y]DOTA-TATE and [177Lu]DOTA-TATE of neuroendocrine tumours refractory to conventional therapy. *Eur J Nucl Med Mol Imaging*. 2014; 41: 223–30.
  173. de Jong M. Combination radionuclide therapy using 177Lu-and 90Y-labeled somatostatin analogs. *J Nucl Med*. 2005; 46: 13–7.
  174. Lawrence YR, Li XA, el Naqa I, Hahn CA, Marks LB, Merchant TE, et al. Radiation dose-volume effects in the brain. *Int J Radiat Oncol Biol Phys*. 2010; 76 Suppl: S20–7.
  175. Ruben JD, Dally M, Bailey M, Smith R, McLean CA, Fedele P. Cerebral radiation necrosis: incidence, outcomes, and risk factors with emphasis on radiation parameters and chemotherapy. *Int J Radiat Oncol Biol Phys*. 2006; 65: 499–508.
  176. Chao ST, Suh JH, Raja S, Lee SY, Barnett G. The sensitivity and specificity of FDG PET in distinguishing recurrent brain tumor from radionecrosis in patients treated with stereotactic radiosurgery. *Int J Cancer*. 2001; 96: 191–7.
  177. Bolcaen J, Lybaert K, Moerman L, Descamps B, Deblaere K, Boterberg T, et al. Kinetic modeling and graphical analysis of 18F-fluoromethylcholine (FCho), 18F-fluoroethyltyrosine (FET) and 18F-fluorodeoxyglucose (FDG) PET for the discrimination between high-grade glioma and radiation necrosis in rats. *PLoS One*. 2016; 11: 1–16.
  178. Pouget JP, Lozza C, Deshayes E, Boudousq V, Navarro-Teulon I. Introduction to radiobiology of targeted radionuclide therapy. *Front Med*. 2015; 2: 12.
  179. Lubberink M, Wilking H, Öst A, Ilan E, Sandström M, Andersson C, et al. *In vivo* instability of (177)Lu-dotatate during peptide receptor radionuclide therapy. *J Nucl Med*. 2020; 61: 1337–40.
  180. Miederer M, Scheinberg DA, McDevitt MR. Realizing the potential of the actinium-225 radionuclide generator in targeted alpha-particle therapy applications. *Adv Drug Deliv Rev*. 2008; 60: 1371–82.
  181. Schwartz J, Jaggi JS, O'Donoghue JA, Ruan S, McDevitt M, Larson SM, et al. Renal uptake of bismuth-213 and its contribution to kidney radiation dose following administration of actinium-225-labeled antibody. *Phys Med Biol*. 2011; 56: 721–33.
  182. Guérard F, Gestin JF, Brechbiel MW. Production of [211At]-astatinated radiopharmaceuticals and applications in targeted  $\alpha$ -particle therapy. *Cancer Biother Radiopharm*. 2013; 28: 1–20.
  183. Poty S, Francesconi LC, McDevitt MR, Morris MJ, Lewis JS.  $\alpha$ -emitters for radiotherapy: From basic radiochemistry to clinical studies—part 1. *J Nucl Med*. 2018; 59: 878–84.
  184. Ferrari C, Niccoli Asabella A, Villano C, Giacobbi B, Coccetti D, Panichelli P, et al. Copper-64 dichloride as theranostic agent for glioblastoma multiforme: A preclinical study. 2015; 2015: 129764.
  185. Bao S, Wu Q, McLendon RE, Hao Y, Shi Q, Hjelmeland AB, et al. Glioma stem cells promote radioresistance by preferential activation of the DNA damage response. *Nature*. 2006; 444: 756–60.
  186. Otomo T, Hishii M, Arai H, Sato K, Sasai K. Microarray analysis of temporal gene responses to ionizing radiation in two glioblastoma cell lines: up-regulation of DNA repair genes. *J Radiat Res*. 2004; 45: 53–60.
  187. Deshors P, Toulas C, Arnauduc F, Malric L, Siegfried A, Nicaise Y, et al. Ionizing radiation induces endothelial transdifferentiation of glioblastoma stem-like cells through the Tie2 signaling pathway. *Cell Death Dis*. 2019; 10: 816.
  188. Gupta K, Burns TC. Radiation-induced alterations in the recurrent glioblastoma microenvironment: Therapeutic implications. *Front Oncol*. 2018; 8: 503.
  189. Kareliotis G, Tremi I, Kaitatzi M, Drakaki E, Serafetinides AA, Makropoulou M, et al. Combined radiation strategies for novel and enhanced cancer treatment. *Int J Radiat Biol*. 2020; 96: 1087–103.
  190. Dekempeneer Y, Keyaerts M, Krasniqi A, Puttemans J, Muyldermans S. Targeted alpha therapy using short-lived alpha-particles and the promise of nanobodies as targeting vehicle. *Expert Opin Biol Ther*. 2016; 16: 1035–47.
  191. Friesen C, Lubatschowski A, Kotzerke J, Buchmann I, Reske SN, Debatin KM. Erratum: Beta-irradiation used for systemic radioimmunotherapy induces apoptosis and activates apoptosis pathways in leukaemia cells. *Eur J Nucl Med Mol Imaging*. 2003; 30: 1262.
  192. Knox SJ, Levy R, Miller RA, Uhland W, Schiele J, Ruehl W, et al. Determinants of the antitumor effect of radiolabeled monoclonal antibodies. *Cancer Res*. 1990; 50: 4935–40.
  193. Knox SJ. Overview of studies on experimental radioimmunotherapy. *Cancer Res*. 1995; 55(23S): 5832s–6s.

194. Gridley DS, Rizvi A, Luo-Owen X, Makinde AY, Pecaut MJ. Low dose, low dose rate photon radiation modifies leukocyte distribution and gene expression in CD4+ T cells. *J Radiat Res.* 2009; 50: 139–50.
195. Williams JA, Williams JR, Yuan X, Dillehay LE. Protracted exposure radiosensitization of experimental human malignant glioma. *Radiat Oncol Investig.* 1998; 6: 255–63.
196. Joiner MC, Marples B, Lambin P, Short SC, Turesson I. Low-dose hypersensitivity: Current status and possible mechanisms. *Int J Radiat Oncol Biol Phys.* 2001; 49: 379–89.
197. Mirzaie-Joniani H, Eriksson D, Sheikholvaezin A, Johansson A, Löfroth P-O, Johansson L, et al. Apoptosis induced by low-dose and low-dose-rate radiation. *Cancer.* 2002; 94: 1210–4.
198. Piron B, Paillas S, Boudousq V, Pelegrin A, Bascoul-Mollevi C, Chouin N, et al. DNA damage-centered signaling pathways are effectively activated during low dose-rate auger radioimmunotherapy. *Nucl Med Biol.* 2014; 41 Suppl: e75–83.
199. Murray D, McEwan AJ. Radiobiology of systemic radiation therapy. *Cancer Biother Radiopharm.* 2007; 22: 1–23.
200. DeNardo GL, Schlom J, Buchsbaum DJ, Meredith RF, O'Donoghue JA, Sgouros G, et al. Rationales, evidence, and design considerations for fractionated radioimmunotherapy. *Cancer.* 2002; 94: 1332–48.
201. Meyn, RE. Apoptosis and response to radiation: Implications for radiation therapy. *Oncology.* 1997; 11: 349–65.
202. Sgouros G, Frey E, Wahl R, He B, Prideaux A, Hobbs R. Three-Dimensional Imaging-Based Radiobiological Dosimetry. *Semin Nucl Med.* 2008; 38: 321–34.
203. Boyd M, Ross SC, Dorrens J, Fullerton NE, Tan KW, Zalutsky MR, et al. Radiation-induced biologic bystander effect elicited *in vitro* by targeted radiopharmaceuticals labeled with  $\alpha$ -,  $\beta$ -, and auger electron-emitting radionuclides. *J Nucl Med.* 2006; 47: 1007–15.
204. Kishikawa H, Wang K, Adelstein SJ, Kassis AI. Inhibitory and stimulatory bystander effects are differentially induced by iodine-125 and iodine-123. *Radiat Res.* 2006; 165: 688–94.
205. Howell RW, Bishayee A. Bystander effects caused by nonuniform distributions of DNA-incorporated 125I. *Micron.* 2002; 33: 127–32.
206. Xue LY, Butler NJ, Makrigiorgos GM, Adelstein SJ, Kassis AI. Bystander effect produced by radiolabeled tumor cells *in vivo*. *Proc Natl Acad Sci U S A.* 2002; 99: 13765–70.
207. Sokolov M, Neumann R. Changes in gene expression as one of the key mechanisms involved in radiation-induced bystander effect. *Biomed reports.* 2018; 9: 99–111.
208. Wang R, Zhou T, Liu W, Zuo L. Molecular mechanism of bystander effects and related abscopal/cohort effects in cancer therapy. *Oncotarget.* 2018; 9: 18637–47.
209. Pouget JP, Georgakilas AG, Ravanat JL. Targeted and off-target (bystander and abscopal) effects of radiation therapy: Redox mechanisms and risk/benefit analysis. *Antioxidants Redox Signal.* 2018; 29: 1447–87.
210. Ene CI, Kreuser SA, Jung M, Zhang H, Arora S, Moyes KW, et al. Anti-PD-L1 antibody direct activation of macrophages contributes to a radiation-induced abscopal response in glioblastoma. *Neuro Oncol.* 2020; 22: 639–51.
211. Lah TT, Novak M, Breznik B. Brain malignancies: Glioblastoma and brain metastases. *Semin Cancer Biol.* 2020; 60: 262–73.
212. Rajani KR, Carlstrom LP, Parney IF, Johnson AJ, Warrington AE, Burns TC. Harnessing Radiation Biology to Augment Immunotherapy for Glioblastoma. *Front Oncol.* 2018; 8: 656.
213. Lassmann M, Chiesa C, Flux G, Bardies M. EANM Dosimetry Committee guidance document: Good practice of clinical dosimetry reporting. *Eur J Nucl Med Mol Imaging.* 2011; 38: 192–200.
214. Flux G, Bardies M, Monsieurs M, Savolainen S, Strand SE, Lassmann M, et al. The impact of PET and SPECT on dosimetry for targeted radionuclide therapy. *Z Med Phys.* 2006; 16: 47–59.
215. Bolch WE, Eckerman KF, Sgouros G, Thomas SR. MIRD pamphlet No. 21: A generalized schema for radiopharmaceutical dosimetry-standardization of nomenclature. *J Nucl Med.* 2009; 50: 477–84.
216. Sgouros G, Roeske JC, McDevitt MR, Palm S, Allen BJ, Fisher DR, et al. MIRD pamphlet No. 22: Radiobiology and dosimetry of  $\alpha$ -particle emitters for targeted radionuclide therapy. *J Nucl Med.* 2010; 51: 311–28.
217. Dewaraja YK, Frey EC, Sgouros G, Brill AB, Roberson P, Zanzonico PB, et al. MIRD pamphlet no. 23: Quantitative SPECT for patient-specific 3-dimensional dosimetry in internal radionuclide therapy. *J Nucl Med.* 2012; 53: 1310–25.
218. Ljungberg M, Sjogreen Gleisner K. 3-D image-based dosimetry in radionuclide therapy. *IEEE Trans Radiat Plasma Med Sci.* 2018; 2: 527–40.
219. Furlhang EE, Chui CS, Kolbert KS, Larson SM, Sgouros G. Implementation of a monte carlo dosimetry method for patient-specific internal emitter therapy. *Med Phys.* 1997; 24: 1163–72.
220. Kolbert KS, Sgouros G, Scott AM, Bronstein JE, Malane RA, Zhang J, et al. Implementation and evaluation of patient-specific three-dimensional internal dosimetry. *J Nucl Med.* 1997; 38: 301–8.
221. Prideaux AR, Song H, Hobbs RF, He B, Frey EC, Ladenson PW, et al. Three-dimensional radiobiologic dosimetry: Application of radiobiologic modeling to patient-specific 3-dimensional imaging-based internal dosimetry. *J Nucl Med.* 2007; 48: 1008–16.
222. Ferrari M, Cremonesi M, Bartolomei M, Bodei L, Chinol M, Fiorenza M, et al. Dosimetric model for locoregional treatments of brain tumors with 90Y-conjugates: clinical application with 90Y-DOTATOC. *J Nucl Med.* 2006; 47: 105–12.
223. Falzone N, Ackerman NL, de la Fuente Rosales L, Bernal MA, Liu X, Peeters SG, et al. Dosimetric evaluation of radionuclides for VCAM-1- targeted radionuclide therapy of early brain metastases. *Theranostics.* 2018; 8: 292–303.
224. Huang C, Guatelli S, Oborn BM, Allen BJ. Microdosimetry for targeted alpha therapy of cancer. *Comput Math Methods Med.* 2012; 2012: 153212.
225. Hofmann W, Li WB, Friedland W, Miller BW, Madas B, Bardies M, et al. Internal microdosimetry of alpha-emitting radionuclides. *Radiat Environ Biophys.* 2020; 59: 29–62.
226. Ryman JT, Meibohm B. Pharmacokinetics of monoclonal antibodies. *CPT Pharmacometrics Syst Pharmacol.* 2017; 6: 576–88.
227. Li L, Quang TS, Gracely EJ, Kim JH, Enrich JG, Yaeger TE, et al. A phase II study of anti-epidermal growth factor receptor radioimmunotherapy in the treatment of glioblastoma multiforme. *J Neurosurg.* 2010; 113: 192–8.
228. Moll S, Nিকেleit V, Mueller-Brand J, Brunner FP, Maecke HR, Mihatsch MJ. A new cause of renal thrombotic microangiopathy: Yttrium 90-DOTATOC internal radiotherapy. *Am J Kidney Dis.* 2001; 37: 847–51.
229. Reulen HJ, Poepperl G, Goetz C, Gildehaus FJ, Schmidt M, Tatsch K, et al. Long-term outcome of patients with WHO Grade III and IV gliomas treated by fractionated intracavitary radioimmunotherapy. *J Neurosurg.* 2015; 123: 760–70.
230. Riva P, Arista A, Sturiale C, Moscatelli G, Tison V, Mariani M, et al. Treatment of intracranial human glioblastoma by direct intratumoral administration of 131I-labelled anti-tenascin monoclonal antibody BC-2. *Int J Cancer.* 1992; 51: 7–13.
231. Riva P, Arista A, Tison V, Sturiale C, Franceschi G, Spinelli A, et al. Intralésional radioimmunotherapy of malignant gliomas. An effective treatment in recurrent tumors. *Cancer.* 1994; 73: 1076–82.
232. Cokgor I, Akabani G, Kuan CT, Friedman HS, Friedman AH, Coleman RE, et al. Phase I trial results of iodine-131-labeled antitenascin monoclonal antibody 81C6 treatment of patients with newly diagnosed malignant gliomas. *J Clin Oncol.* 2000; 18: 3862–72.
233. Riva P, Franceschi G, Frattarelli M, Riva N, Guiducci G, Cremonini AM, et al. 131I radiocoupled antibodies for the locoregional radioimmunotherapy of high-grade malignant glioma—phase I and II study. *Acta Oncol.* 1999; 38: 351–9.
234. Akabani G, Reardon DA, Coleman RE, Wong TZ, Metzler SD, Bowsher JE, et al. Dosimetry and radiographic analysis of 131I-labeled anti-tenascin 81C6 murine monoclonal antibody in newly diagnosed patients with malignant gliomas: A phase II study. *J Nucl Med.* 2005; 46: 1042–51.
235. Reardon DA, Zalutsky MR, Akabani G, Coleman RE, Friedman AH, Herndon 2nd JE, et al. A pilot study: 131I-Antitenascin monoclonal antibody 81c6 to deliver a 44-Gy resection cavity boost. *Neuro Oncol.* 2008; 10: 182–9.
236. Hdeib A, Sloan A. Targeted radioimmunotherapy: the role of 131I-chTNT-1/B mAb (Cotara®) for treatment of high-grade gliomas. *Future Oncol.* 2012; 659–69.
237. Shapiro WR, Carpenter SP, Roberts K, Shan JS. 131I-chTNT-1/B mAb: Tumour necrosis therapy for malignant astrocytic glioma. *Expert Opin Biol Ther.* 2006; 6: 539–45.
238. Patel SJ, Shapiro WR, Laske DW, Jensen RL, Asher AL, Wessels BW, et al. Safety and feasibility of convection-enhanced delivery of Cotara for the treatment of malignant glioma: Initial experience in 51 patients. *Neurosurgery.* 2005; 56: 1243–52.
239. Mamelak AN, Rosenfeld S, Bucholz R, Raubitschek A, Nabors LB, Fiveash JB, et al. Phase I single-dose study of intracavitary-administered iodine-131-TM-601 in adults with recurrent high-grade glioma. *J Clin Oncol.* 2006; 24: 3644–50.
240. Baum RP, Kluge A, Gildehaus FJ, Bronzel M, Schmidt K, Schuchardt C, et al. Systemic endoradiotherapy with carrier-added 4-[131I]iodo-L-phenylalanine: Clinical proof-of-principle in refractory glioma. *Nucl Med Mol Imaging.* 2011; 45: 299–307.
241. Kneifel S, Cordier D, Good S, Ionescu MCS, Ghaffari A, Hofer S, et al. Local targeting of malignant gliomas by the diffusible peptidic vector 1,4,7,10-tetraazacyclododecane-1-glutaric acid-4,7,10-triacetic acid-substance P. *Clin Cancer Res.* 2006; 12: 3843–50.
242. Cordier D, Forrer F, Bruchertseifer F, Morgenstern A, Apostolidis C, Good S, et al. Targeted alpha-radionuclide therapy of functionally critically located gliomas with 213Bi-DOTA-[Thi8, Met(02)11]- substance P: A pilot trial. *Eur J Nucl Med Mol Imaging.* 2010; 37: 1335–44.
243. Torres LA, Coca MA, Batista JF, Hernández A, Crombet T, Ramos M, et al. Biodistribution and internal dosimetry of the Re-labelled humanized monoclonal antibody anti-epidermal growth factor receptor, nimotuzumab, in the locoregional treatment of malignant gliomas. *Nucl Med Commun.* 2008; 29: 66–75.
244. Zalutsky MR, Reardon DA, Akabani G, Coleman RE, Friedman AH, Friedman HS, et al. Clinical experience with  $\alpha$ -particle-emitting 211 At: Treatment of recurrent brain tumor patients with 211 At-labeled chimeric antitenascin monoclonal antibody 81C6. *J Nucl Med.* 2008; 49: 30–8.
245. Talip Z, Favaretto C, Geistlich S, Van Der Meulen NP. A step-by-step guide for the novel radiometal production for medical applications: Case studies with 68Ga, 44Sc, 177Lu and 161Tb. *Molecules.* 2020; 25: 966.
246. Kuznetsov RA, Bobrovskaya KS, Svetukhin VV, Fomin AN, Zhukov AV. Production of Lutetium-177: Process aspects. *Radiochemistry.* 2019; 61: 381–95.
247. Peitl KP, Rangger C, Garnuszek P, Mikolajczak R, Hubalewska-Dydejczyk A, Maina T, et al. Clinical translation of theranostic radiopharmaceuticals:

- Current regulatory status and recent examples. *J Labelled Comp Radiopharm.* 2019; 62: 673-83.
248. P Peñuelas I, Elsinga PH. The Clinical Translation Process in Europe. In: Lewis JS, Windhorst AD, Zeglis BM, Ed. *Radiopharmaceutical chemistry*, 1<sup>st</sup> ed. Switzerland: Springer; 2019: 607-18.
  249. Sequeira S, Lyashchenko SK. The clinical translation process in the United States. In: Lewis JS, Windhorst AD, Zeglis BM, Ed. *Radiopharmaceutical chemistry*, 1<sup>st</sup> ed. Switzerland: Springer; 2019: 619-25.
  250. Caragher S, Chalmers AJ, Gomez-Roman N. Glioblastoma's next top model: Novel culture systems for brain cancer radiotherapy research. *Cancers.* 2019; 11: 44.
  251. Plummer S, Wallace S, Ball G, Lloyd R, Schiapparelli P, et al. A human iPSC-derived 3D platform using primary brain cancer cells to study drug development and personalized medicine. *Sci Rep.* 2019; 9: 1407.
  252. Ozturk MS, Lee VK, Zou H, Friedel RH, Intes X, Dai G. High-resolution tomographic analysis of *in vitro* 3D glioblastoma tumor model under long-term drug treatment. *Sci Adv.* 2020; 6: eaay7513.
  253. Musah-Eroje A, Watson S. A novel 3D *in vitro* model of glioblastoma reveals resistance to temozolomide which was potentiated by hypoxia. *J Neurooncol.* 2019; 142: 231-40.
  254. Drevelegas A. *Imaging of brain tumors with histological correlations*, 2nd ed. Berlin Heidelberg: Springer-Verlag; 2011.
  255. Veliky I. Prospective of 68Ga-radiopharmaceutical development. *Theranostics.* 2014; 4: 47-80.
  256. Demir ES, Ozgenç E, Ekinci M, Gundogdu EA, İlem Özdemir D, Asikoglu M. Computational study of radiopharmaceuticals. In: Stefanu A, Ed. *Molecular Docking Molecular Dynamics*. London: IntechOpen; 2019: 85140.
  257. Wu Y, Lu Y, Chen W, Fu J, Fan R. *In silico* experimentation of glioma microenvironment development and anti-tumor therapy. *PLoS Comput Biol.* 2012; 8: e1002355.
  258. Rockne R, Rockhill JK, Mrugala M, Spence AM, Kalet I, Hendrickson K, et al. Predicting the efficacy of radiotherapy in individual glioblastoma patients *in vivo*: a mathematical modeling approach. *Phys Med Biol.* 2010; 55: 3271-85.
  259. Sung JH, Esch MB, Shuler ML. Integration of *in silico* and *in vitro* platforms for pharmacokinetic – pharmacodynamic modeling. *Expert Opin Drug Metab Toxicol.* 2010; 6: 1063-81.
  260. Fani M, Maecke HR. Radiopharmaceutical development of radiolabelled peptides. *Eur J Nucl Med Mol Imaging.* 2012; 39: S11-30.
  261. Fu R, Carroll L, Yahsioglu G, Aboagye EO, Miller PW. Antibody fragment and affibody immunopET imaging agents: radiolabelling strategies and applications. *ChemMedChem.* 2018; 13: 2466-78.
  262. Khalid U, Vi C, Henri J, Macdonald J, Eu P, et al. Radiolabelled aptamers for theranostic treatment of cancer. *Pharmaceuticals.* 2019; 12: 2.
  263. Schubiger PA, Alberto R, Smith A. Vehicles, chelators, and radionuclides: choosing the “building blocks” of an effective therapeutic radioimmunoconjugate. *Bioconjug Chem.* 1996; 7: 165-79.
  264. Liu S, Edwards S. Bifunctional chelators for therapeutic lanthanide radiopharmaceuticals. *Bioconjug Chem.* 2001; 12: 5587451.
  265. Tornesello AL, Buonaguro L, Tornesello ML, Buonaguro FM. New insights in the design of bioactive peptides and chelating agents for imaging and therapy in oncology. *Molecules.* 2017; 22: 1-21.
  266. Jackson JA, Hungnes IN, Ma MT, Rivas C. Bioconjugates of chelators with peptides and proteins in nuclear medicine: historical importance, current innovations, and future challenges. *Bioconjug Chem.* 2020; 31: 483-91.
  267. Evans BJ, King AT, Katsifis A, Matesic L, Jamie JF. Methods to enhance the metabolic stability of peptide-based PET radiopharmaceuticals. *Molecules.* 2020; 25: 2314.
  268. Vaidyanathan G, Zalutsky MR. The radiopharmaceutical chemistry of the radioisotopes of iodine. In: Lewis JS, Windhorst AD, Zeglis BM, Ed. *Radiopharmaceutical chemistry*, 1<sup>st</sup> ed. Switzerland: Springer; 2019: 391-408.
  269. Lindegren S, Albertsson P, Bäck T, Jensen H, Palm S, Aneheim E. Realizing clinical trials with Astatine-211: The chemistry infrastructure. *Cancer Biother Radiopharm.* 2020; 35: 425-36.
  270. Bakker WH, Breeman WAP, Van Der Pluijm ME, De Jong M, Visser TJ, Krenning EP. Iodine-131 labelled octreotide: Not an option for somatostatin receptor therapy. *Eur J Nucl Med.* 1996; 23: 775-81.
  271. International Atomic Energy Agency, Quality control in the production of radiopharmaceuticals. Series: IAEA TECDOC series. Vienna, Austria, 2018; ISSN 1011-4289; no 1856, .
  272. Kratochwil C, Bruchertseifer F, Giesel FL, Weis M, Verburg FA, Mottaghy F, et al. 225Ac-PSMA-617 for PSMA-targeted  $\alpha$ -radiation therapy of metastatic castration-resistant prostate cancer. *J Nucl Med.* 2016; 57: 1941-4.
  273. Aerts J, Ballinger JR, Behe M, Decristoforo C, Elsinga PH, Favre-Chauvet A, et al. Guidance on current good radiopharmacy practice for the small-scale preparation of radiopharmaceuticals using automated modules: A European perspective. *J Labelled Comp Rad.* 2014; 57: 615-20.
  274. Li M, Zhang X, Quinn TP, Lee D, Liu D, Kunkel F, et al. Automated cassette-based production of high specific activity [203/212Pb] peptide-based theranostic radiopharmaceuticals for image-guided radionuclide therapy for cancer. *Appl Radiat Isot.* 2017; 127: 52-60.
  275. Todde S, Peitl PK, Elsinga P, Kozirowski J, Ferrari V, Ocak EM, et al. Guidance on validation and qualification of processes and operations involving radiopharmaceuticals. *EJNMMI Radiopharm Chem.* 2017; 2: 8.
  276. Lenting K, Verhaak R, Ter Laan M, Wesseling P, Leenders W. Glioma: experimental models and reality. *Acta Neuropathol.* 2017; 133: 263-82.
  277. da Hora CC, Schweiger MW, Wurdinger T, Tannous BA. Patient-derived glioma models: from patients to dish to animals. *Cells.* 2019; 8: 1177.
  278. Brem S, Kalil A. *Glioblastoma*. 1<sup>st</sup> ed. Elsevier; 2016.
  279. Janbazian L, Karamchandani J, Das S. Mouse models of glioblastoma: lessons learned and questions to be answered. *J Neurooncol.* 2014; 118: 1-8.
  280. Jannetti SA, Carlucci G, Carney B, Kossatz S, Shanker L, Carter LM, et al. PARP-1-targeted radiotherapy in mouse models of glioblastoma. *J Nucl Med.* 2018; 59: 1225-33.
  281. Allard E, Hindre F, Passirani C, Lemaire L, Lepareur N, Noiret N, et al. 188Re-loaded lipid nanocapsules as a promising radiopharmaceutical carrier for internal radiotherapy of malignant gliomas. *Eur J Nucl Med Mol Imaging.* 2008; 35: 1838-46.
  282. Luurtsema G, Elsinga P, Dierckx R, Boellaard R, van Waarde A. PET tracers for imaging of ABC transporters at the blood-brain barrier: principles and strategies. *Curr Pharm Des.* 2016; 22: 5779-85.
  283. Barth RF, Kaur B. Rat brain tumor models in experimental neuro-oncology: The C6, 9L, T9, RG2, F98, BT4C, RT-2 and CNS-1 gliomas. *J Neurooncol.* 2009; 94: 299-312.
  284. de Vries NA, Beijnen JH, van Tellingen O. High-grade glioma mouse models and their applicability for preclinical testing. *Cancer Treat Rev.* 2009; 35: 714-23.
  285. Huszthy PC, Daphu I, Nicloul SP, Stieber D, Nigro JM, Sakariassen P, et al. *In vivo* models of primary brain tumors: pitfalls and perspectives. *Neuro Oncol.* 2012; 14: 979-93.
  286. Hubert CG, Rivera M, Spangler LC, Wu Q, Mack SC, Prager BC, et al. A three-dimensional organoid culture system derived from human glioblastomas recapitulates the hypoxic gradients and cancer stem cell heterogeneity of tumors found *in vivo*. *Cancer Res.* 2016; 76: 2465-77.
  287. Linkous A, Balamatsias D, Snuderl M, Edwards L, Miyaguchi K. Modeling patient-derived glioblastoma with cerebral organoids. *Cell Rep.* 2019; 26: 3203-11.
  288. Jacob F, Salinas RD, Zhang DY, Nguyen PTT, Schnoll JG, Zheng Hao Wong S, et al. A patient-derived glioblastoma organoid model and biobank recapitulates inter- and intra-tumoral heterogeneity. *Cell.* 2020; 180: 188-204.
  289. Knapp FF, Dash A. Translation of radiopharmaceuticals from bench to bedside: regulatory and manufacturing issues. In: Knapp FF, Dash A, Ed. *Radiopharmaceuticals for therapy*. New Delhi: Springer; 2016: 323-43.
  290. Peñuelas I, Elsinga PH. The clinical translation process in Europe. In: Lewis JS, Windhorst AD, Zeglis BM, Ed. *Radiopharmaceutical chemistry*, 1<sup>st</sup> ed. Switzerland: Springer; 2019: 607-18.
  291. Peñuelas I, Vugts DJ, Decristoforo C, Elsinga PH. The new Regulation on clinical trials in relation to radiopharmaceuticals: when and how will it be implemented? *EJNMMI Radiopharm Chem.* 2019; 4: 2.
  292. [Internet] FDA. Developing medical imaging drug and biological products Part 1 Conducting safety assessments. 2004. <https://www.fda.gov/media/72295>.
  293. [Internet] FDA. Microdose radiopharmaceutical diagnostic drugs: nonclinical study recommendations. 2018. <https://www.fda.gov/regulatory-information/search-fda-guidance-documents/microdose-radiopharmaceutical-diagnostic-drugs-nonclinical-study-recommendations>.
  294. Reubi JC, Maecke HR. Approaches to multireceptor targeting: hybrid radioligands, radioligand cocktails, and sequential radioligand applications. *J Nucl Med.* 2017; 58: 10-16S.
  295. Monteiro AR, Hill R, Pilkington GJ, Madureira PA. The role of hypoxia in glioblastoma invasion. *Cells.* 2017; 6: 45.
  296. Houson H, Mdzinarishvili A, Gali H, Sidorov E, Awasthi V. PET Detection of cerebral necrosis using an infarct-avid agent 2-Deoxy-2-[(18)F]Fluoro-D-Glucuric Acid (FGA) in a mouse model of the brain stroke. *Mol Imaging Biol.* 2020; 22: 1353-61.
  297. Perek N, Sabido O, Le Jeune N, Prevot N, Vergnon J, Clotagatide A, et al. Could 99mTc-glucurate be used to evaluate tumour necrosis? *In vitro* and *in vivo* studies in leukaemic tumour cell line U937. *Eur J Nucl Med Mol Imaging.* 2008; 35: 1290-8.
  298. De Saint-Hubert M, Prinsen K, Mortelmans L, Verbruggen A, Mottaghy FM. Molecular imaging of cell death. *Methods.* 2009; 48: 178-87.
  299. Wang H, Mu X, He H, Zhang X. Cancer Radiosensitizers. *Trends Pharmacol Sci.* 2018; 39: 24-48.
  300. Brown JS, O'Carroll B, Jackson SP, Yap TA. Targeting DNA repair in cancer: beyond PARP inhibitors. *Cancer Discov.* 2017; 7: 20-37.
  301. Barbarite E, Sick JT, Berchmans E, Bregy A, Shah AH, Elsayyad, et al. The role of brachytherapy in the treatment of glioblastoma multiforme. *Neurosurg Rev.* 2017; 40: 195-211.
  302. Arazi L, Cooks T, Schmidt M, Keisari Y, Kelson I. Treatment of solid tumors by interstitial release of recoiling short-lived alpha emitters. *Phys Med Biol.* 2007; 52: 5025-42.
  303. Arazi L. Diffusing alpha-emitters radiation therapy: approximate modeling of the macroscopic alpha particle dose of a point source. *Phys Med Biol.* 2020; 65: 015015.
  304. Miyatake SI, Wanibuchi M, Hu N, Ono K. Boron neutron capture therapy for malignant brain tumors. *J Neurooncol.* 2020; 149: 1-11.
  305. Sun T, Zhang Z, Li B, Chen G, Xie X, Wei Y, et al. Boron neutron capture therapy induces cell cycle arrest and cell apoptosis of glioma stem/progenitor cells *in vitro*. *Radiat Oncol.* 2013; 8: 1-8.
  306. Wilson JD, Hammond EM, Higgins GS, Petersson K. Ultra-high dose rate (FLASH) radiotherapy: silver bullet or fool's gold? *Front Oncol.* 2020; 9: 1-12.

307. Bourhis J, Montay-Gruel P, Gonçalves Jorge P, Bailat C, Petit B, Ollivier J, et al. Clinical translation of FLASH radiotherapy: Why and how? *Radiother Oncol*. 2019; 139: 11-7.
308. Zukotynski K, Jadvar H, Capala J, Fahey F. Targeted radionuclide therapy: practical applications and future prospects. *Biomark Cancer*. 2016; 8: 35-8.
309. Coenen HH, Gee AD, Adam M, Antoni G, Cutler CS, Fujibayashi F, et al. Consensus nomenclature rules for radiopharmaceutical chemistry - Setting the record straight. *Nucl Med Biol*. 2017; 55: v-xi.
310. Coenen HH, Gee AD, Adam M, Antoni G, Cutler CS, Fujibayashi Y, et al. Open letter to journal editors on: International consensus radiochemistry nomenclature guidelines. *J Labelled Comp Radiopharm*. 2018; 61: 402-4.
311. Bogsrud TV, Londalen A, Brandal P, Leske H, Panagopoulos I, Borghammer P, et al. 18F-Fluciclovine PET/CT in suspected residual or recurrent high-grade glioma. *Clin Nucl Med*. 2019; 44: 605-11.
312. Karlberg A, Berntsen EM, Johansen H, Skjulsvik AJ, Reinertsen I, Yan Dai H, et al. 18F-FACBC PET/MRI in diagnostic assessment and neurosurgery of gliomas. *Clin Nucl Med*. 2019; 44: 550-9.
313. Parent EE, Benayoun M, Ibeanu I, Olson JJ, Hadjipanayis CG, Brat DJ, et al. [18F]Fluciclovine PET discrimination between high- and low-grade gliomas. *EJNMMI Res*. 2018; 8: 67.
314. Tsuyuguchi N, Terakawa Y, Uda T, Nakajo K, Kanemura Y. Diagnosis of brain tumors using amino acid transport PET imaging with (18)F-fluciclovine: a comparative study with L-methyl-(11)C-methionine PET Imaging. *Asia Ocean J Nucl Med Biol*. 2017; 5: 85-94.
315. Wakabayashi T, Iuchi T, Tsuyuguchi N, Nishikawa R, Arakawa Y, Sasayama T, et al. Diagnostic performance and safety of positron emission tomography using (18)F-Fluciclovine in patients with clinically suspected high- or low-grade gliomas: A multicenter phase IIb trial. *Asia Ocean J Nucl Med Biol*. 2017; 5: 10-21.
316. Kondo A, Ishii H, Aoki S, Suzuki M, Nagasawa H, Kubota K, et al. Phase IIa clinical study of [(18)F]fluciclovine: efficacy and safety of a new PET tracer for brain tumors. *Ann Nucl Med*. 2016; 30: 608-18.
317. Henderson FJ, Brem S, O'Rourke DM, Nasrallah M, Buch VP, Young AJ, et al. (18)F-Fluciclovine PET to distinguish treatment-related effects from disease progression in recurrent glioblastoma: PET fusion with MRI guides neurosurgical sampling. *Neurooncol Pract*. 2020; 7: 152-7.
318. John F, Robinette NL, Amit-Yousif AJ, Bosnyák E, Barger GR, Shah KD, et al. Multimodal imaging of nonenhancing glioblastoma regions. *Mol Imaging*. 2019; 18: 1536012119885222.
319. Bosnyák E, Kamson DO, Robinette NL, Barger GR, Mittal S, Juhász C. Tryptophan PET predicts spatial and temporal patterns of post-treatment glioblastoma progression detected by contrast-enhanced MRI. *J Neurooncol*. 2016; 126: 317-25.
320. Batista CEA, Juhász C, Muzik O, Kupsky WJ, Barger G, Chugani HT, et al. Imaging correlates of differential expression of indoleamine 2,3-dioxygenase in human brain tumors. *Mol Imaging Biol*. 2009; 11: 460-6.
321. Law I, Albert NL, Arbuzo J, Boellaard R, Drzezga A, Galldiks N, et al. Joint EANM/EANO/RANO practice guidelines/SNMMI procedure standards for imaging of gliomas using PET with radiolabelled amino acids and [(18)F]FDG: version 1.0. *Eur J Nucl Med Mol Imaging*. 2019; 46: 540-57.
322. Lukas RV, Juhász C, Wainwright DA, James CD, Kennedy E, Stupp R, et al. Imaging tryptophan uptake with positron emission tomography in glioblastoma patients treated with indoximod. *J Neurooncol*. 2019; 141: 111-20.
323. John F, Bosnyák E, Robinette NL, Amit-Yousif A, Barger GR, Shah KD, et al. Multimodal imaging-defined subregions in newly diagnosed glioblastoma: impact on overall survival. *Neuro Oncol*. 2019; 21: 264-73.
324. Venneti S, Dunphy MP, Zhang H, Pitter KL, Zanzonico P, Campos C, et al. Glutamine-based PET imaging facilitates enhanced metabolic evaluation of gliomas *in vivo*. *Sci Transl Med*. 2015; 7: 274ra17.
325. Mitra ES, Koglin N, Mosci C, Kumar M, Hoehne A, Visithi Keu K, et al. Pilot preclinical and clinical evaluation of (4S)-4-(3-[18F]Fluoropropyl)-L-Glutamate (18F-FSPG) for PET/CT imaging of intracranial malignancies. *PLoS One*. 2016; 11: e0148628.
326. Hellwig D, Romeike BFM, Ketter R, Moringlane JR, Kirsch C-M, Samnick S. Intra-individual comparison of p-[123I]-iodo-L-phenylalanine and L-3-[123I]-iodo-alpha-methyl-tyrosine for SPECT imaging of gliomas. *Eur J Nucl Med Mol Imaging*. 2008; 35: 24-31.
327. Hellwig D, Ketter R, Romeike BFM, Schaefer A, Farmakis G, Grgic A, et al. Prospective study of p-[123I]iodo-L-phenylalanine and SPECT for the evaluation of newly diagnosed cerebral lesions: specific confirmation of glioma. *Eur J Nucl Med Mol Imaging*. 2010; 37: 2344-53.
328. Hellwig D, Ketter R, Romeike BFM, Sell N, Schaefer A, Moringlane JR, et al. Validation of brain tumour imaging with p-[123I]iodo-L-phenylalanine and SPECT. *Eur J Nucl Med Mol Imaging*. 2005; 32: 1041-9.
329. Verhoeven J, Baguet T, Piron S, Pauwelyn G, Bouckaert C, Descamps B, et al. 2-[(18)F]FELP, a novel LAT1-specific PET tracer, for the discrimination between glioblastoma, radiation necrosis and inflammation. *Nucl Med Biol*. 2020; 82-83: 9-16.
330. Verhoeven J, Hulpsia F, Kersemans K, Bolcaen J, De Lombaerde S, Goeman J, et al. New fluoroethyl phenylalanine analogues as potential LAT1-targeting PET tracers for glioblastoma. *Sci Rep*. 2019; 9: 2878.
331. Bouhrel A, Zhou D, Li A, Yuan L, Rich KM, McConathy J. Synthesis, radiolabeling, and biological evaluation of (R)- and (S)-2-Amino-5-[(18)F]fluoro-2-methylpentanoic acid ((R)-, (S)-[(18)F]FAMPE) as potential positron emission tomography tracers for brain tumors. *J Med Chem*. 2015; 58: 3817-29.
332. Bouhrel A, Alyami W, Li A, Yuan L, Rich K, McConathy J. Effect of  $\alpha$ -Methyl versus  $\alpha$ -hydrogen substitution on brain availability and tumor imaging properties of heptanoic [F-18]Fluoroalkyl amino acids for positron emission tomography (PET). *J Med Chem*. 2016; 59: 3515-31.
333. Michelhaugh SK, Muzik O, Guastella AR, Klinger NV, Polin LA, Cai H, et al. Assessment of tryptophan uptake and kinetics using 1-(2-18F-Fluoroethyl)-L-Tryptophan and  $\alpha$ -11C-Methyl-L-Tryptophan PET imaging in mice implanted with patient-derived brain tumor xenografts. *J Nucl Med*. 2017; 58: 208-13.
334. Guastella AR, Michelhaugh SK, Klinger NV, Kupsky WJ, Polin LA, Muzik O, et al. Tryptophan PET imaging of the kynurenine pathway in patient-derived xenograft models of glioblastoma. *Mol Imaging*. 2016; 15: 1536012116644881.
335. Xin Y, Gao X, Liu L, Ge WP, Jain MK, Cai H. Evaluation of L-1-[(18)F]Fluoroethyl-Tryptophan for PET imaging of cancer. *Mol Imaging Biol*. 2019; 21: 1138-46.
336. Lieberman BP, Ploessl K, Wang L, Qu W, Zha Z, Wise DR, et al. PET imaging of glutaminolysis in tumors by 18F-(2S,4R)4-fluoroglutamine. *J Nucl Med*. 2011; 52: 208-15.
337. Miner MW, Liljenbäck H, Virta J, Merisaari J, Oikonen V, Westermark J, et al. (2S,4R)-4-[(18)F]Fluoroglutamine for *in vivo* PET imaging of glioma xenografts in mice: an evaluation of multiple pharmacokinetic models. *Mol Imaging Biol*. 2020; 22: 969-78.
338. Nozaki S, Nakatani Y, Mawatari A, Shibata N, Hume WE, Hayashinaka E, et al. 18F-FIMP: a LAT1-specific PET probe for discrimination between tumor tissue and inflammation. *Sci Rep*. 2019; 9: 1-9.
339. Li D, Zhao X, Zhang L, Li F, Ji N, Gao Z, et al. 68Ga-PRGD2 PET/CT in the evaluation of glioma: A prospective study. *Mol Pharm*. 2014; 11: 3923-9.
340. Li D, Zhang J, Ji N, Zhao X, Zheng K, Qiao Z, et al. Combined 68Ga-NOTA-PRGD2 and 18F-FDG PET/CT can discriminate uncommon meningioma mimicking high-grade glioma. *Clin Nucl Med*. 2018; 43: 648-54.
341. Schnell O, Krebs B, Carlsen J, Miederer I, Goetz C, Goldbrunner RH, Wester H, et al. Imaging of integrin  $\alpha$ (v) $\beta$ (3) expression in patients with malignant glioma by [18F] Galacto-RGD positron emission tomography. *Neuro Oncol*. 2009; 11: 861-70.
342. Iagaru A, Mosci C, Mittra E, Fischbein N, Harsh G, Li G, et al. Glioblastoma multiforme recurrence: an exploratory study of (18)F FPPRGD2 PET/CT. *Radiology*. 2015; 277: 497-506.
343. Oxboel J, Brandt-Larsen M, Schjoeth-Eskesen C, Myschetzky R, El-Ali HH, Madsen J, et al. Comparison of two new angiogenesis PET tracers 68Ga-NODAGA-E[c(RGDyK)]<sub>2</sub> and 64Cu-NODAGA-E[c(RGDyK)]<sub>2</sub>; *in vivo* imaging studies in human xenograft tumors. *Nucl Med Biol*. 2014; 41: 259-67.
344. Chung YH, Hsu PH, Huang CW, Hsieh WC, Huang FT, Chang WC, et al. Evaluation of prognostic integrin  $\alpha$ 2 $\beta$ 1 PET tracer and concurrent targeting delivery using focused ultrasound for brain glioma detection. *Mol Pharm*. 2014; 11: 3904-14.
345. Liu Z, Jia B, Zhao H, Chen X, Wang F. Specific targeting of human integrin  $\alpha$ (v) $\beta$ (3) with (111)In-labeled Abegrin™ in nude mouse models. *Mol Imaging Biol*. 2011; 13: 112-20.
346. Dearling JJJ, Barnes JW, Panigrahy D, Zimmerman RE, Fahey F, Treves ST, et al. Specific uptake of 99mTc-NC100692, an  $\alpha$ v $\beta$ 3-targeted imaging probe, in subcutaneous and orthotopic tumors. *Nucl Med Biol*. 2013; 40: 788-94.
347. Battle MR, Goggi JL, Allen L, Barnett J, Morrison MS. Monitoring tumor response to antiangiogenic sunitinib therapy with 18F-fluciclatide, an 18F-labeled  $\alpha$ v $\beta$ 3-integrin and  $\alpha$ v $\beta$ 5-integrin imaging agent. *J Nucl Med*. 2011; 52: 424-30.
348. Guo N, Zhang F, Zhang X, Guo J, Lang L, Kiesewetter DO, Niu G, et al. Quantitative evaluation of tumor early response to a vascular-disrupting agent with dynamic PET. *Mol Imaging Biol*. 2015; 17: 865-73.
349. Provost C, Prignon A, Rozenblum-Beddok L, Bruyer Q, Dumont S, Merabte F, et al. Comparison and evaluation of two RGD peptides labelled with (68)Ga or (18)F for PET imaging of angiogenesis in animal models of human glioblastoma or lung carcinoma. *Oncotarget*. 2018; 9: 19307-16.
350. Wu Y, Zhang X, Xiong Z, Cheng Z, Fisher DR, Liu S, et al. microPET imaging of glioma integrin  $\alpha$ (v) $\beta$ (3) expression using (64)Cu-labeled tetrameric RGD peptide. *J Nucl Med*. 2005; 46: 1707-18.
351. Shi J, Kim YS, Zhai S, Liu Z, Chen X, Liu S. Improving tumor uptake and pharmacokinetics of (64)Cu-labeled cyclic RGD peptide dimers with Gly(3) and PEG(4) linkers. *Bioconjug Chem*. 2009; 20: 750-9.
352. Bao X, Wang MW, Luo JM, Wang SY, Zhang YP, Zhang YJ. Optimization of early response monitoring and prediction of cancer antiangiogenesis therapy via noninvasive PET molecular imaging strategies of multifactorial bioparameters. *Theranostics*. 2016; 6: 2084-98.
353. Rainer E, Wang H, Traub-Weidinger T, Widhalm G, Fueger B, Chang J, et al. The prognostic value of [(123)I]-vascular endothelial growth factor ([(123)I]-VEGF) in glioma. *Eur J Nucl Med Mol Imaging*. 2018; 45: 2396-403.
354. Mitran B, Güler R, Roche FP, Lindstrom E, Selvaraju RK, Fleetwood F, et al. Radionuclide imaging of VEGFR2 in glioma vasculature using biparatopic antibody conjugate: proof-of-principle in a murine model. *Theranostics*. 2018; 8: 4462-76.
355. Jansen MHA, Lagerweij T, Sewing AC, Vugts DJ, van Vuurden DG, Molthoff CF, et al. Bevacizumab targeting diffuse intrinsic pontine glioma: results of 89Zr-Bevacizumab PET imaging in brain tumor models. *Mol Cancer Ther*. 2016; 15: 2166-74.

356. Hu K, Shang J, Xie L, Hanyu M, Zhang Y, Yang Z, Xu H, et al. PET Imaging of VEGFR with a novel (64)Cu-labeled peptide. *ACS Omega*. 2020; 5: 8508-14.
357. Chan C, Sandhu J, Guha A, Scollard DA, Wang J, Chen P, et al. A human transferrin-vascular endothelial growth factor (hTf-VEGF) fusion protein containing an integrated binding site for (111)In for imaging tumor angiogenesis. *J Nucl Med*. 2005; 46: 1745-52.
358. Sun J, Cai L, Zhang K, Pu PY, Yang WD, Gao S. A pilot study on EGFR-targeted molecular imaging of PET/CT with <sup>111</sup>C-PD153035 in human gliomas. *Clin Nucl Med*. 2014; 39: 20-6.
359. Pal A, Glekas A, Doubrovina M, Balatoni J, Namavari M, Beresten T, et al. Molecular imaging of EGFR kinase activity in tumors with <sup>124</sup>I-labeled small molecular tracer and positron emission tomography. *Mol Imaging Biol*. 2006; 8: 262-77.
360. Abourbeh G, Dissoki S, Jacobson O, Litchi A, Daniel RB, Laki D, et al. Evaluation of radiolabeled ML04, a putative irreversible inhibitor of epidermal growth factor receptor, as a bioprobe for PET imaging of EGFR-overexpressing tumors. *Nucl Med Biol*. 2007; 34: 55-70.
361. Wehrenberg-Klee E, Redjal N, Leece A, Turker NS, Heidari P, Shah K, et al. PET imaging of glioblastoma multiforme EGFR expression for therapeutic decision guidance. *Am J Nucl Med Mol Imaging*. 2015; 5: 379-89.
362. Cai W, Ebrahimnejad A, Chen K, Cao Q, Li ZB, Tice DA, et al. Quantitative radioimmunoPET imaging of EphA2 in tumor-bearing mice. *Eur J Nucl Med Mol Imaging*. 2007; 34: 2024-36.
363. Chopra A. <sup>125</sup>I-Labeled monoclonal antibody (mAb) 806 targeting the epidermal growth factor receptor deletion variant de2-7 (EGFRvIII). In: *Molecular Imaging and Contrast Agent Database (MICAD)*. Bethesda (US): National Center for Biotechnology Information; 2010.
364. Reilly EB, Phillips AC, Buchanan FG, Kingsbury G, Zhang Y, Meulbroek JA, et al. Characterization of ABT-806, a humanized tumor-specific anti-EGFR monoclonal antibody. *Mol Cancer Ther*. 2015; 14: 1141-51.
365. Miao Z, Ren G, Liu H, Qi S, Wu S, Cheng Z. PET of EGFR expression with an <sup>18</sup>F-labeled antibody molecule. *J Nucl Med*. 2012; 53: 1110-8.
366. Tang Y, Hu Y, Liu W, Chen L, Zhao Y, Ma H, et al. A radiopharmaceutical [<sup>89</sup>Zr]Zr-DFO-nimotuzumab for immunoPET with epidermal growth factor receptor expression *in vivo*. *Nucl Med Biol*. 2019; 70: 23-31.
367. Wu X, Liang H, Tan Y, Yuan C, Li S, Li X, et al. Cell-SELEX aptamer for highly specific radionuclide molecular imaging of glioblastoma *in vivo*. *PLoS One*. 2014; 9: e90752.
368. Cheng S, Jacobson O, Zhu G, Chen Z, Liang SH, Tian R, et al. PET imaging of EGFR expression using an (18)F-labeled RNA aptamer. *Eur J Nucl Med Mol Imaging*. 2019; 46: 948-56.
369. Tolmachev V, Orlova A, Wei Q, Bruskin A, Carlsson J, Gedda L. Comparative biodistribution of potential anti-glioblastoma conjugates [<sup>111</sup>In]DTPA-hEGF and [<sup>111</sup>In]Bz-DTPA-hEGF in normal mice. *Cancer Biother Radiopharm*. 2004; 19: 491-501.
370. Hartimath SV, van Waarde A, Dierckx RAJO, de Vries EFJ. Evaluation of N-[(11)C]methyl-AMD3465 as a PET tracer for imaging of CXCR4 receptor expression in a C6 glioma tumor model. *Mol Pharm*. 2014; 11: 3810-7.
371. Gan H, Cher L, Inglis P, Lwin Z, Lau E, Wichmann C, et al. Phase I safety and bioimaging trial of KB004 (ifabotuzumab) in patients with glioblastoma. *J Nucl Med*. 2020; 61: 1562.
372. Watanabe S, Shiga T, Hirata K, Magota K, Okamoto S, Toyonaga T, et al. Biodistribution and radiation dosimetry of the novel hypoxia PET probe [(18)F]DiFA and comparison with [(18)F]FMISO. *Eur J Nucl Med Mol Imaging Res*. 2019; 9: 60.
373. Torihiro A, Ohtake M, Tateishi K, Hino-Shishikura A, Yoneyama T, Kitazume Y, et al. Prognostic implications of (62)Cu-diacetyl-bis (N(4)-methylthiosemicarbazone) PET/CT in patients with glioma. *Ann Nucl Med*. 2018; 32: 264-71.
374. Tateishi K, Tateishi U, Nakanowatari S, Ohtake M, Minamimoto R, Suenaga J, et al. (62)Cu-diacetyl-bis (N(4)-methylthiosemicarbazone) PET in human gliomas: comparative study with [(18)F]fluorodeoxyglucose and L-methyl-[(11)C]methionine PET. *Am J Neuroradiol*. 2014; 35: 278-84.
375. Gangemi V, Mignogna C, Guzzi G, Lavano A, Bongarzone S, Cascini GL, et al. Impact of [(64)Cu][Cu(ATSM)] PET/CT in the evaluation of hypoxia in a patient with Glioblastoma: a case report. *BMC Cancer*. 2019; 19: 1197.
376. Hu M, Zhu Y, Mu D, Fan B, Zhao S, Yang G, et al. Correlation of hypoxia as measured by fluorine-18 fluorocerythronitroimidazole ((18)F-FETNIM) PET/CT and overall survival in glioma patients. *Eur J Nucl Med Mol Imaging*. 2020; 47: 1427-34.
377. Beppu T, Terasaki K, Sasaki T, Fujiwara S, Matsuura H, Ogasawara K, et al. Standardized uptake value in high uptake area on positron emission tomography with <sup>18</sup>F-FRP170 as a hypoxic cell tracer correlates with intratumoral oxygen pressure in glioblastoma. *Mol Imaging Biol*. 2014; 16: 127-35.
378. Wack LJ, Mönnich D, Van Elmpt W, Zegers CM, Troost EG, Zips D, et al. Comparison of [<sup>18</sup>F]-FMISO, [<sup>18</sup>F]-FAZA and [<sup>18</sup>F]-HX4 for PET imaging of hypoxia - A simulation study. *Acta Oncol*. 2015; 54: 1370-7.
379. Yoshii Y, Matsumoto H, Yoshimoto M, Zhang MR, Oe Y, Kurihara H, et al. Multiple Administrations of (64)Cu-ATSM as a novel therapeutic option for glioblastoma: a translational study using mice with xenografts. *Transl Oncol*. 2018; 11: 24-30.
380. Michel LS, Dyrhoff S, Brooks FJ, Spayd KJ, Lim S, Engle JT, et al. PET of Poly (ADP-Ribose) Polymerase Activity in Cancer: Preclinical Assessment and First In-Human Studies. *Radiology*. 2017; 282: 453-63.
381. Zmuda F, Malviya G, Blair A, Boyd M, Chalmers AJ, Sutherland A, et al. Synthesis and evaluation of a radioiodinated tracer with specificity for Poly(ADP-ribose) Polymerase-1 (PARP-1) *in vivo*. *J Med Chem*. 2015; 58: 8683-93.
382. Pirovano G, Jannetti SA, Carter LM, Sadique A, Kossatz S, Guru N, et al. Targeted brain tumor radiotherapy using an auger emitter. *Clin Cancer Res*. 2020; 26: 2871-81.
383. Carlucci G, Carney B, Brand C, Kossatz S, Irwin CP, Carlin SD, et al. Dual-modality optical/PET imaging of PARP1 in glioblastoma. *Mol Imaging Biol*. 2015; 17: 848-55.
384. Matsuda M, Ishikawa E, Yamamoto T, Hatano K, Joraku A, Iizumi Y, et al. Potential use of prostate specific membrane antigen (PSMA) for detecting the tumor neovasculature of brain tumors by PET imaging with (89)Zr-Df-IAB2M anti-PSMA minibody. *J Neurooncol*. 2018; 138: 581-9.
385. Salas Fragomeni RA, Menke JR, Holdhoff M, Ferrigno C, Laterra JJ, Solnes LB, et al. Prostate-specific membrane antigen-targeted imaging with [<sup>18</sup>F]DCFPyL in high-grade gliomas. *Clin Nucl Med*. 2017; 42: e433-5.
386. Wang S, Wang J, Liu D, Yang D. The value of <sup>68</sup>Ga-PSMA-617 PET/CT in differential diagnosis between low-grade and high-grade gliomas. *J Nucl Med*. 2018; 59: 146.
387. Sasikumar A, Kashyap R, Joy A, Charan Patro K, Bhattacharya P, Reddy Pilaka VK, et al. Utility of <sup>68</sup>Ga-PSMA-11 PET/CT in imaging of glioma-A pilot study. *Clin Nucl Med*. 2018; 43: e304-9.
388. Schwenck J, Tabatabai G, Skardelly M, Reischl G, Beschoner R, Pichler B, et al. *In vivo* visualization of prostate-specific membrane antigen in glioblastoma. *Eur J Nucl Med Mol Imaging*. 2015; 42:170-1.
389. Gupta M, Choudhury PS, Premasagar IC, Gairola M, Ahlawat P. Role of <sup>68</sup>Ga-prostate-specific membrane antigen PET/CT in disease assessment in glioblastoma within 48 hours of surgery. *Clin Nucl Med*. 2020; 45: 204-5.
390. Su Z, Roncaroli F, Durrenberger PF, Roncaroli F, Du Plessis D, Jackson A, et al. The 18-kDa mitochondrial translocator protein in human gliomas: an <sup>111</sup>C-PK11195 PET imaging and neuropathology study. *J Nucl Med*. 2015; 56: 512-7.
391. Unterrainer M, Fleischmann DF, Vettermann F, Ruf V, Kaiser L, Nelwan D, et al. TSPO PET, tumour grading and molecular genetics in histologically verified glioma: a correlative (18)F-GE-180 PET study. *Eur J Nucl Med Mol Imaging*. 2020; 47: 1368-80.
392. Jensen P, Feng L, Law I, Svarer C, Knudsen GM, Mikkelsen JD, et al. TSPO Imaging in glioblastoma multiforme: A direct comparison between <sup>123</sup>I-CLINDE SPECT, <sup>18</sup>F-FET PET, and gadolinium-enhanced MR imaging. *J Nucl Med*. 2015; 56: 1386-90.
393. Cheung YY, Nickels ML, Tang D, Buck JR, Manning HC. Facile synthesis of SSR180575 and discovery of 7-chloro-N,N,5-trimethyl-4-oxo-3-(6-[(18)F]fluoropyridin-2-yl)-3,5-dihydro-4H-pyridazino[4,5-b]indole-1-acetamide, a potent pyridazinoindole ligand for PET imaging of TSPO in cancer. *Bioorg Med Chem Lett*. 2014; 24: 4466-71.
394. Tang D, Nickels ML, Tantawy MN, Buck JR, Manning HC. Preclinical imaging evaluation of novel TSPO-PET ligand 2-(5,7-Diethyl-2-(4-(2-[(18)F]fluoroethoxy)phenyl)pyrazolo[1,5-a]pyrimidin-3-yl)-N,N-diethylacetamide ([<sup>18</sup>F]VUII81008) in glioma. *Mol Imaging Biol*. 2014; 16: 813-20.
395. Winkler A, Boisgard R, Awde AR, Dubois A, Thézé B, Zheng J, et al. The translocator protein ligand [<sup>18</sup>F]DPA-714 images glioma and activated microglia *in vivo*. *Eur J Nucl Med Mol Imaging*. 2012; 39: 811-23.
396. Awde AR, Boisgard R, Thézé B, Dubois A, Zheng J, Dollé F, et al. The translocator protein radioligand <sup>18</sup>F-DPA-714 monitors antitumor effect of erufosine in a Rat 9L intracranial glioma model. *J Nucl Med*. 2013; 54: 2125-31.
397. Pigeon H, Pères EA, Truillet C, Jegou B, Boumezbour F, Caillé F, et al. TSPO-PET and diffusion-weighted MRI for imaging a mouse model of infiltrative human glioma. *Neuro Oncol*. 2019; 21: 755-64.
398. Tang D, Hight MR, McKinley ET, Fu A, Buck JR, Smith RA, et al. Quantitative preclinical imaging of TSPO expression in glioma using N,N-diethyl-2-(2-(4-(2-18F-fluoroethoxy)phenyl)-5,7-dimethylpyrazolo[1,5-a]pyrimidin-3-yl)acetamide. *J Nucl Med*. 2012; 53: 287-94.
399. Zinnhardt B, Pigeon H, Thézé B, Viel T, Wachsmuth L, Fricke JB, Schelhaas S, et al. Combined PET Imaging of the inflammatory tumor microenvironment identifies margins of unique radiotracer uptake. *Cancer Res*. 2017; 77: 1831-41.
400. Buck JR, McKinley ET, Fu A, Abel TW, Thompson RC, Chambless L, et al. Preclinical TSPO ligand PET to visualize human glioma xenotransplants: A preliminary study. *PLoS One*. 2015; 10: e0141659.
401. Buck JR, McKinley ET, Hight MR, Fu A, Tang D, Smith RA, et al. Quantitative, preclinical PET of translocator protein expression in glioma using <sup>18</sup>F-N-fluoroacetyl-N-(2,5-dimethoxybenzyl)-2-phenoxyaniline. *J Nucl Med*. 2011; 52: 107-14.
402. Perrone M, Moon BS, Park HS, Laquintana V, Jung JH, Cotrignelli A, et al. A novel PET imaging probe for the detection and monitoring of translocator protein 18 kDa expression in pathological disorders. *Sci Rep*. 2016; 6: 20422.
403. Blair A, Zmuda F, Malviya G, Tavares AAS, Tamagnan GD, Chalmers AJ, et al. A novel (18)F-labelled high affinity agent for PET imaging of the translocator protein. *Chem Sci*. 2015; 6: 4772-7.
404. Hockaday DC, Shen S, Fiveash J, Raubitschek A, Colcher D, Liu A, et al. Imaging glioma extent with <sup>131</sup>I-TM-601. *J Nucl Med*. 2005; 46: 580-6.
405. de Lucas AG, Schuhmacher AJ, Oteo M, et al. Targeting MT1-MMP as an immunoPET-based strategy for imaging gliomas. *PLoS One*. 2016; 11: e0158634.

406. Zhao J, Wang YL, Li XB, Gao SY, Liu SY, Song YK, et al. Radiosynthesis and preliminary biological evaluation of 18F-Fluoropropionyl-Chlorotoxin as a potential PET tracer for glioma imaging. *Contrast Media Mol Imaging*. 2018; 8439162.
407. Wang LJ, Li HS, Wang QS, Wu HB, Han YJ, Zhou WL, et al. Construction and evaluation of the tumor-targeting, cell-penetrating multifunctional molecular probe iCREKA. *Contrast Media Mol Imaging*. 2018; 7929617.
408. Kasten BB, Jiang K, Cole D, Jani A, Udayakumar N, Gillespie GY, et al. Targeting MMP-14 for dual PET and fluorescence imaging of glioma in preclinical models. *Eur J Nucl Med Mol Imaging*. 2020; 47: 1412-26.
409. Röhrich M, Loktev A, Wefers AK, Altmann A, Paech D, Adebegbe S, et al. IDH-wildtype glioblastomas and grade III/IV IDH-mutant gliomas show elevated tracer uptake in fibroblast activation protein-specific PET/CT. *Eur J Nucl Med Mol Imaging*. 2019; 46: 2569-80.
410. Kratochwil C, Flechsig P, Lindner T, Abderrahim L, Altmann A, Mier W, et al. (68)Ga-FAPI PET/CT: Tracer uptake in 28 different kinds of cancer. *J Nucl Med*. 2019; 60: 801-5.
411. Toms J, Kogler J, Maschauer S, Daniel C, Schmidkonz C, Kuwert T, et al. Targeting fibroblast activation protein: radiosynthesis and preclinical evaluation of an (18)F-labeled FAP inhibitor. *J Nucl Med*. 2020; 61(12): 1806-13.
412. Yamamoto Y, Nishiyama Y, Kimura N, Kameyama R, Kawai N, Hatakeyama T, et al. 11C-acetate PET in the evaluation of brain glioma: comparison with 11C-methionine and 18F-FDG-PET. *Mol Imaging Biol*. 2008; 10: 281-7.
413. Mertens K, Slaets D, Lambert B, Acou M, De Vos F, Goethals I. PET with (18)F-labelled choline-based tracers for tumour imaging: a review of the literature. *Eur J Nucl Med Mol Imaging*. 2010; 37: 2188-93.
414. Tsuchida T, Takeuchi H, Okazawa H, Tsujikawa T, Fujibayashi Y. Grading of brain glioma with 1-11C-acetate PET: comparison with 18F-FDG PET. *Nucl Med Biol*. 2008; 35: 171-6.
415. Kim S, Kim D, Kim SH, Park MA, Chang JH, Yun M. The roles of (11)C-acetate PET/CT in predicting tumor differentiation and survival in patients with cerebral glioma. *Eur J Nucl Med Mol Imaging*. 2018; 45: 1012-20.
416. Witney TH, Pisaneschi F, Alam IS, Trousil S, Kaliszczak M, Twyman F, et al. Preclinical evaluation of 3-18F-fluoro-2,2-dimethylpropionic acid as an imaging agent for tumor detection. *J Nucl Med*. 2014; 55: 1506-12.
417. Santimaria M, Moscatelli G, Viale GL, Giovannoni L, Neri G, Viti F, et al. Immunoscintigraphic detection of the ED-B domain of fibronectin, a marker of angiogenesis, in patients with cancer. *Clin Cancer Res*. 2003; 9: 571-9.
418. Zhang Y, Wang L, Yu S, Hu K, Huang S, Li Y, et al. Synthesis and preclinical evaluation of the fibrin-binding cyclic peptide (18)F-iCREKA: Comparison with its contrasted linear peptide. *Contrast Media Mol Imaging*. 2019; 6315954.
419. Oborski MJ, Laymon CM, Lieberman FS, Drappatz J, Hamilton RL, Mountz JM. First use of (18)F-labeled ML-10 PET to assess apoptosis change in a newly diagnosed glioblastoma multiforme patient before and early after therapy. *Brain Behav*. 2014; 4: 312-5.
420. Oborski MJ, Laymon CM, Lieberman FS, Qian Y, Drappatz J, Mountz JM. [(18)F]ML-10 PET: Initial experience in glioblastoma multiforme therapy response assessment. *Tomography*. 2016; 2: 317-24.
421. Kranz M, Bergmann R, Knies T, Belter B, Neuber C, Cai Z, et al. Bridging from brain to tumor imaging: (S)-(-) and (R)-(+)-[(18)F]Fluspidine for investigation of sigma-1 receptors in tumor-bearing mice. *Molecules*. 2018; 23: 702.
422. Kranz M, Sattler B, Wüst N, Deuther-Conrad W, Patt M, Meyer PM, et al. Evaluation of the enantiomer specific biokinetics and radiation doses of [(18)F]Fluspidine-A new tracer in clinical translation for imaging of  $\sigma$ -receptors. *Molecules*. 2016; 21: 1164.
423. Toussaint M, Deuther-Conrad W, Kranz M, Fischer S, Ludwig FA, Juratli TA, et al. Sigma-1 receptor positron emission tomography: A new molecular imaging approach using (S)-(-)-[(18)F]Fluspidine in glioblastoma. *Molecules*. 2020; 25(9): 2170.
424. Maini CL, Sciuto R, Tofani A, Ferraironi A, Carapella CM, Occhipinti E, et al. Somatostatin receptor imaging in CNS tumours using 111In-octreotide. *Nucl Med Commun*. 1995; 16: 756-66.
425. Kiviniemi A, Gardberg M, Frantzen J, Pesola M, Vuorinen V, Parkkola R, et al. Somatostatin receptor subtype 2 in high-grade gliomas: PET/CT with (68)Ga-DOTA-peptides, correlation to prognostic markers, and implications for targeted radiotherapy. *Eur J Nucl Med Mol Imaging Res*. 2015; 5: 25.
426. Collamati F, Pepe A, Bellini F, Bocci V, Chiodi G, Cremonesi M, et al. Toward radioguided surgery with  $\beta^-$  decays: uptake of a somatostatin analogue, DOTATOC, in meningioma and high-grade glioma. *J Nucl Med*. 2015; 56: 3-8.
427. Kim W, Le TM, Wei L, Poddar S, Bazy J, Wang X, et al. [18F]CFA as a clinically translatable probe for PET imaging of deoxycytidine kinase activity. *Proc Natl Acad Sci U S A*. 2016; 113: 4027-32.
428. Hu H, Huang P, Weiss OJ, Yan X, Yue X, Zhang MG, et al. PET and NIR optical imaging using self-illuminating 64Cu-doped chelator-free gold nanoclusters. *Biomaterials*. 2014; 35: 9868-76.
429. Peeters SGJA, Dubois L, Lieuwings NG, Laan D, Mooijer M, Schuit RC, et al. [(18)F]VM4-037 MicroPET imaging and biodistribution of two *in vivo* CAIX-expressing tumor models. *Mol Imaging Biol*. 2015; 17: 615-9.
430. Hicke BJ, Stephens AW, Gould T, Chang YF, Lynott CK, Heil J, et al. Tumor targeting by an aptamer. *J Nucl Med*. 2006; 47: 668-78.
431. Jacobson O, Yan X, Niu G, Weiss ID, Ma Y, Szajek LP, et al. PET imaging of tenascin-C with a radiolabeled single-stranded DNA aptamer. *J Nucl Med*. 2015; 56: 616-21.
432. Laws MT, Bonomi RE, Gelovani DJ, Llaniguez J, Lu X, Mangner T, et al. Noninvasive quantification of SIRT1 expression-activity and pharmacologic inhibition in a rat model of intracerebral glioma using 2-[18F]BzAHA PET/CT/MRI. *Neurooncol Adv*. 2020; 2: 1-11.
433. Laws MT, Bonomi RE, Kamal S, Gelovani DJ, Llaniguez J, Potukutchi S, et al. Molecular imaging HDACs class IIa expression-activity and pharmacologic inhibition in intracerebral glioma models in rats using PET/CT/(MRI) with [(18)F]JFAHA. *Sci Rep*. 2019; 9: 3595.
434. Chitneni SK, Reitman ZJ, Spicheckler R, Gooden DM, Yan H, Zalutsky MR. Synthesis and evaluation of radiolabeled AGI-5198 analogues as candidate radiotracers for imaging mutant IDH1 expression in tumors. *Bioorg Med Chem Lett*. 2018; 28: 694-9.
435. Chitneni SK, Yan H, Zalutsky MR. Synthesis and evaluation of a (18)F-labeled triazinediamine analogue for imaging mutant IDH1 expression in gliomas by PET. *ACS Med Chem Lett*. 2018; 9: 606-11.
436. Chitneni SK, Reitman ZJ, Gooden DM, Yan H, Zalutsky MR. Radiolabeled inhibitors as probes for imaging mutant IDH1 expression in gliomas: Synthesis and preliminary evaluation of labeled butyl-phenyl sulfonamide analogs. *Eur J Med Chem*. 2016; 119: 218-30.
437. Koyasu S, Shimizu Y, Morinibu A, Saga T, Nakamoto Y, Togashi K, et al. Increased (14)C-acetate accumulation in IDH-mutated human glioblastoma: implications for detecting IDH-mutated glioblastoma with (11)C-acetate PET imaging. *J Neurooncol*. 2019; 145: 441-7.
438. Behr SC, Villanueva-Meyer JE, Li Y, Wang YH, Wei J, Moroz A, et al. Targeting iron metabolism in high-grade glioma with 68Ga-citrate PET/MR. *JCI insight*. 2018; 3: e93999.
439. Huang HL, Huang YC, Lee WY, Yeh CN, Lin KJ, Yu CS. 18F-glutathione conjugate as a PET tracer for imaging tumors that overexpress L-PGDS enzyme. *PLoS One*. 2014; 9: e104118.
440. Huang YC, Huang HL, Yeh CN, Lin KJ, Yu CS. Investigation of brain tumors using (18)F-fluorobutyl ethacrynic amide and its metabolite with positron emission tomography. *Oncotargets Ther*. 2015; 8: 1877-85.
441. Jagoda EM, Lang L, Bhadrasetty V, Histed S, Williams M, Kramer-Marek G, et al. Immuno-PET of the hepatocyte growth factor receptor Met using the 1-armed antibody onartuzumab. *J Nucl Med*. 2012; 53: 1592-600.
442. Price EW, Carnazza KE, Carlin SD, Cho A, Edwards KJ, Sevak KK, et al. (89)Zr-DFC-AMG102 immuno-PET to determine local hepatocyte growth factor protein levels in tumors for enhanced patient selection. *J Nucl Med*. 2017; 58: 1386-94.
443. Luo H, Hong H, Slater MR, Graves SA, Shi S, Yang Y, et al. PET of c-Met in Cancer with <sup>64</sup>Cu-Labeled Hepatocyte Growth Factor. *J Nucl Med*. 2015; 56: 758-63.
444. Evans MJ, Holland JP, Rice SL, Doran MG, Cheal SM, Campos C, et al. Imaging tumor burden in the brain with 89Zr-transferrin. *J Nucl Med*. 2013; 54: 90-5.
445. Li F, Jiang S, Zu Y, Lee DY, Li Z. A tyrosine kinase inhibitor-based high-affinity PET radiopharmaceutical targets vascular endothelial growth factor receptor. *J Nucl Med*. 2014; 55: 1525-31.
446. Nigam S, McCarl L, Kumar R, Edinger RS, Kurland BF, Anderson CJ, et al. Preclinical immunoPET imaging of glioblastoma-infiltrating myeloid cells using Zirconium-89 labeled anti-CD11b antibody. *Mol Imaging Biol*. 2020; 22: 685-94.
447. Strand J, Varasteh Z, Eriksson O, Abrahmsen L, Orlova A, Tolmachev V. Gallium-68-labeled affibody molecule for PET imaging of PDGFR $\beta$  expression *in vivo*. *Mol Pharm*. 2014; 11: 3957-64.
448. Peng Z, Maxwell DS, Sun D, Bhanu Prasad BA, Pal A, Wang S, et al. Imatinib analogs as potential agents for PET imaging of Bcr-Abl and c-KIT expression at a kinase level. *Bioorg Med Chem*. 2014; 22: 623-32.
449. Gaedlicke S, Braun F, Prasad S, Machein M, Firat E, Hettich M, et al. Noninvasive positron emission tomography and fluorescence imaging of CD133+ tumor stem cells. *Proc Natl Acad Sci U S A*. 2014; 111: E692-701.
450. Yang Y, Hernandez R, Rao J, Yin L, Qu Y, Wu J, et al. Targeting CD146 with a 64Cu-labeled antibody enables *in vivo* immunoPET imaging of high-grade gliomas. *Proc Natl Acad Sci U S A*. 2015; 112: E6525-34.
451. Hernandez R, Sun H, England CG, Valdovinos HF, Barnhart TE, Yang Y, et al. ImmunoPET imaging of CD146 expression in malignant brain tumors. *Mol Pharm*. 2016; 13: 2563-70.
452. Behling K, Maguire WF, López Puebla JC, Sprinkle SR, Ruggiero A, O'Donoghue J, et al. Vascular targeted radioimmunotherapy for the treatment of glioblastoma. *J Nucl Med*. 2016; 57: 1576-82.
453. Sattiraju A, Xiong X, Pandya DN, Wadas TJ, Xuan A, Sun Y, et al. Alpha particle enhanced blood brain/tumor barrier permeabilization in glioblastomas using Integrin Alpha-v Beta-3-targeted liposomes. *Mol Cancer Ther*. 2017; 16: 2191-200.
454. Sattiraju A, Solingapuram Sai KK, Xuan A, Pandya DN, Almaguel FG, Wadas TJ, et al. IL13RA2 targeted alpha particle therapy against glioblastomas. *Oncotarget*. 2017; 8: 42997-3007.
455. Ayed T, Pilmé J, Tézé D, Bassal F, Barbet J, Chérel M, et al. 211At-labeled agents for alpha-immunotherapy: On the *in vivo* stability of astatine-agent bonds. *Eur J Med Chem*. 2016; 116: 156-64.
456. Reist CJ, Foulon CF, Alston K, Bigner DD, Zalutsky MR. Astatine-211 labeling of internalizing anti-EGFRvIII monoclonal antibody using N-succinimidyl 5-[211At]astato-3-pyridinecarboxylate. *Nucl Med Biol*. 1999; 26: 405-11.
457. Reardon DA, Akabani G, Coleman R, Friedman AH, Friedman HS, Herndon JE, et al. Phase II trial of murine (131)I-labeled antitenascin monoclonal

- antibody 81C6 administered into surgically created resection cavities of patients with newly diagnosed malignant gliomas. *J Clin Oncol.* 2002; 20: 1389-97.
458. Verburg FA, Sweeney R, Hånscheid H, Dießl S, Israel I, Löhr M, et al. Patients with recurrent glioblastoma multiforme. Initial experience with p-[(131I)]iodo-L-phenylalanine and external beam radiation therapy. *Nuklearmedizin.* 2013; 52: 36-42.
459. Spaeth N, Wyss MT, Pahnke J, Biollaz G, Trachsel E, Drandarov K, et al. Radioimmunotherapy targeting the extra domain B of fibronectin in C6 rat gliomas: a preliminary study about the therapeutic efficacy of iodine-131-labeled SIP(L19). *Nucl Med Biol.* 2006; 33: 661-6.
460. Moosmayer D, Berndorff D, Chang C-H, Sharkey RM, Rother A, Borkowski S, et al. Bispecific antibody pretargeting of tumor neovasculature for improved systemic radiotherapy of solid tumors. *Clin Cancer Res.* 2006; 12: 5587-95.
461. Shankar S, Vaidyanathan G, Affleck DJ, Peixoto K, Bigner DD, Zalutsky MR. Evaluation of an internalizing monoclonal antibody labeled using N-succinimidyl 3-[131I]iodo-4-phosphonomethylbenzoate ((131I)SIPMB), a negatively charged substituent bearing acylation agent. *Nucl Med Biol.* 2004; 31: 909-19.
462. Vaidyanathan G, Affleck DJ, Bigner DD, Zalutsky MR. Improved xenograft targeting of tumor-specific anti-epidermal growth factor receptor variant III antibody labeled using N-succinimidyl 4-guanidinomethyl-3-iodobenzoate. *Nucl Med Biol.* 2002; 29: 1-11.
463. Girard N, Courel MN, Véra P, Delpech B. Therapeutic efficacy of intraslesional 131I-labelled hyaluronectin in grafted human glioblastoma. *Acta Oncol.* 2000; 39: 81-7.
464. Samnick S, Romeike BF, Lehmann T, Israel I, Rube C, Mautes A, et al. Efficacy of systemic radionuclide therapy with p-131I-iodo-L-phenylalanine combined with external beam photon irradiation in treating malignant gliomas. *J Nucl Med.* 2009; 50: 2025-32.
465. Israel I, Brandau W, Farmakis G, Samnick S. Improved synthesis of no-carrier-added p-[124I]iodo-L-phenylalanine and p-[131I]iodo-L-phenylalanine for nuclear medicine applications in malignant gliomas. *Appl Radiat Isot.* 2008; 66: 513-22.
466. Romeike BFM, Hellwig D, Heimann A, Kempfs O, Feiden W, Kirsch CM, et al. Action and efficacy of p-[131I]iodo-L-phenylalanine on primary human glioma cell cultures and rats with C6-gliomas. *Anticancer Res.* 2004; 24: 3971-6.
467. Boiardi A, Bartolomei M, Silvani A, Eoli M, Salmaggi A, Lamperti E, et al. Intratumoral delivery of mitoxantrone in association with 90-Y radioimmunotherapy (RIT) in recurrent glioblastoma. *J Neurooncol.* 2005; 72: 125-31.
468. Veeravagu A, Liu Z, Niu G, Chen K, Jia B, Cai W, et al. Integrin alphavbeta3-targeted radioimmunotherapy of glioblastoma multiforme. *Clin Cancer Res.* 2008; 14: 7330-9.
469. Dash A, Pillai MRA, Knapp Jr FF. Production of (177)Lu for targeted radionuclide therapy: available options. *Nucl Med Mol Imaging.* 2015; 49: 85-107.
470. Banerjee S, Pillai MRA, Knapp FFR. Lutetium-177 therapeutic radiopharmaceuticals: linking chemistry, radiochemistry, and practical applications. *Chem Rev.* 2015; 115: 2934-74.
471. Fiedler L, Kellner M, Gosewisch A, Oos R, Böning G, Lindner S, et al. Evaluation of (177)Lu[Lu]-CHX-A"-DTPA-6A10 Fab as a radioimmunotherapy agent targeting carbonic anhydrase XII. *Nucl Med Biol.* 2018; 60: 55-62.
472. Ávila-Sánchez M, Ferro-Flores G, Jiménez-Mancilla N, Ocampo-García B, Bravo-Villegas G, Luna-Gutiérrez M, et al. Synthesis and preclinical evaluation of the 99mTc-/177Lu-CXCR4-L theranostic pair for *in vivo* chemokine-4 receptor-specific targeting. *J Radioanal Nucl Chem.* 2020; 324: 21-32.
473. Tworowska I, Flores II L, Zielinski R, Nowak J, Lecorche P, Malicet C, et al. Radiotheranostic approach for targeting LDLR in glioblastoma. *J Nucl Med.* 2019; 60: 1024.
474. Jiang L, Miao Z, Kimura RH, Liu H, Cochran JR, Culter CS, et al. Preliminary evaluation of (177)Lu-labeled knottin peptides for integrin receptor-targeted radionuclide therapy. *Eur J Nucl Med Mol Imaging.* 2011; 38: 613-22.
475. Hens M, Vaidyanathan G, Welsh P, Zalutsky MR. Labeling internalizing anti-epidermal growth factor receptor variant III monoclonal antibody with 177Lu: *in vitro* comparison of acyclic and macrocyclic ligands. *Nucl Med Biol.* 2009; 36: 117-28.
476. Hens M, Vaidyanathan G, Zhao X-G, Bigner DD, Zalutsky MR. Anti-EGFRvIII monoclonal antibody armed with 177Lu: *in vivo* comparison of macrocyclic and acyclic ligands. *Nucl Med Biol.* 2010; 37: 741-50.
477. Pillai MRA, Dash A, Knapp FFJ. Rhenium-188: availability from the (188)W/(188)Re generator and status of current applications. *Curr Radiopharm.* 2012; 5: 228-43.
478. Casacó A, López G, García I, Rodríguez JA, Fernández R, Figueredo J, et al. Phase I single-dose study of intracavitary-administered Nimotuzumab labeled with 188 Re in adult recurrent high-grade glioma. *Cancer Biol Ther.* 2008; 7: 333-9.
479. Shi S, Fu W, Lin S, Tian T, Li S, Shao X, et al. Targeted and effective glioblastoma therapy via aptamer-modified tetrahedral framework nucleic acid-paclitaxel nanoconjugates that can pass the blood brain barrier. *Nanomedicine.* 2019; 21: 102061.
480. Vanpouille-Box C, Lacoëuille F, Belloche C, Lepareur N, Lemaire L, Lefeune JJ, et al. Tumor eradication in rat glioma and bypass of immunosuppressive barriers using internal radiation with (188)Re-lipid nanocapsules. *Biomaterials.* 2011; 32: 6781-90.
481. Cikankowitz A, Clavreul A, Tétaud C, Lemaire L, Rousseau A, Lepareur N, et al. Characterization of the distribution, retention, and efficacy of internal radiation of (188)Re-lipid nanocapsules in an immunocompromised human glioblastoma model. *J Neurooncol.* 2017; 131: 49-58.
482. Häfeli UO, Pauer GJ, Unnithan J, Prayson RA. Fibrin glue system for adjuvant brachytherapy of brain tumors with 188Re and 186Re-labeled microspheres. *Eur J Pharm Biopharm.* 2007; 65: 282-8.
483. Zhang X, Peng L, Liang Z, Kou Z, Chen Y, Shi G, et al. Effects of aptamer to U87-EGFRvIII cells on the proliferation, radiosensitivity, and radiotherapy of glioblastoma cells. *Mol Ther Nucleic Acids.* 2018; 10: 438-49.
484. Tan Y, Shi Y, Wu XD, Liang HY, Gao YB, Li SJ, et al. DNA aptamers that target human glioblastoma multiforme cells overexpressing epidermal growth factor receptor variant III *in vitro*. *Acta Pharmacol Sin.* 2013; 34: 1491-8.
485. Liu T, Karlson M, Karlberg AM, Redalen KR. Hypoxia imaging and theranostic potential of [(64)Cu][Cu(ATSM)] and ionic Cu(II) salts: a review of current evidence and discussion of the retention mechanisms. *Eur J Nucl Med Mol Imaging Res.* 2020; 10: 33.
486. Gutfilen B, Souza SAL, Valentini G. Copper-64: A real theranostic agent. *Drug Des Devel Ther.* 2018; 12: 3235-45.
487. Zhou Y, Li J, Xu X, Zhao M, Zhang B, Deng S, et al. (64)Cu-based radiopharmaceuticals in molecular imaging. *Technol Cancer Res Treat.* 2019; 18: 1533033819830758.
488. Catalogna G, Talarico C, Dattilo V, Gangemi V, Calabria F, D'Antona L, et al. The SGK1 kinase inhibitor S113 sensitizes theranostic effects of the 64CuCl2 in human glioblastoma multiforme cells. *Cell Physiol Biochem.* 2017; 43: 108-19.
489. Jørgensen JT, Persson M, Madsen J, Kjær A. High tumor uptake of (64)Cu: implications for molecular imaging of tumor characteristics with copper-based PET tracers. *Nucl Med Biol.* 2013; 40: 345-50.
490. Ahmedova A, Todorov B, Burdzhiev N, Goze C. Copper radiopharmaceuticals for theranostic applications. *Eur J Med Chem.* 2018; 157: 1406-25.
491. Smith NA, Bowers DL, Eht DA. The production, separation, and use of 67Cu for radioimmunotherapy: a review. *Appl Radiat Isot.* 2012; 70: 2377-83.
492. Brady LW, Markoe AM, Woo DV, Amendola BE, Karlsson UL, Rackover MA, et al. Iodine-125-labeled anti-epidermal growth factor receptor-425 in the treatment of glioblastoma multiforme. A pilot study. *Front Radiat Ther Oncol.* 1990; 24: 151-5.
493. Miyamoto CT, Brady LW, Rackover MA, Emrich J, Class R, Bender H, et al. The use of epidermal growth factor receptor-425 monoclonal antibodies radiolabeled with iodine-125 in the adjuvant treatment of patients with high grade gliomas of the brain. *Recent Results Cancer Res.* 1996; 141: 183-92.
494. Foulon CF, Reist CJ, Bigner DD, Zalutsky MR. Radioiodination via D-amino acid peptide enhances cellular retention and tumor xenograft targeting of an internalizing anti-epidermal growth factor receptor variant III monoclonal antibody. *Cancer Res.* 2000; 60: 4453-60.
495. Chopra A. [(125)I]-Labeled monoclonal antibody L8A4 against epidermal growth factor receptor variant III (EGFRvIII). In: *Molecular Imaging and Contrast Agent Database (MICAD)*. Bethesda (US): National Center for Biotechnology Information; 2004.
496. Wu B, You C, Liu X, Cai B. Therapeutic effect of 125IUdR on the glioma cell line C6 *in vitro* and *in vivo*. *Sichuan Da Xue Xue Bao Yi Xue Ban.* 2004; 35(5): 671-4.
497. Saga T, Sakahara H, Nakamoto Y, Sato N, Zhao S, Aoki T, et al. Radioimmunotherapy of human glioma xenografts in nude mice by indium-111 labeled internalising monoclonal antibody. *Eur J Cancer.* 1999; 35: 1281-5.
498. Bryant MJ, Chuah TL, Luff J, Lavin MF, Walker DG. A novel rat model for glioblastoma multiforme using a bioluminescent F98 cell line. *J Clin Neurosci.* 2008; 15: 545-51.
499. Benda P, Sameda K, Messer J, Sweet WH. Morphological and immunohistochemical studies of rat glial tumors and clonal strains propagated in culture. *J Neurosurg.* 1971; 34: 310-23.
500. Ponten J. Neoplastic human glia cells in culture. In: *Fogh J, Ed. Human Tumor cells in vitro*. Boston: Springer; 1975: 175-206.
501. Jacobs VL, Valdes PA, Hickey WF, De Leo JA. Current review of *in vivo* GBM rodent models: emphasis on the CNS-1 tumour model. *ASN Neuro.* 2011; 3: e00063.
502. Schmidek HH, Nielsen SL, Schiller AL, Messer J. Morphological studies of rat brain tumors induced by N-nitrosomethylurea. *J Neurosurg.* 1971; 34: 335-40.
503. Ko L, Koestner A, Wechsler W. Morphological characterization of nitrosourea-induced glioma cell lines and clones. *Acta Neuropathol.* 1980; 51: 23-31.
504. Fomchenko EI, Holland EC. Mouse models of brain tumors and their applications in preclinical trials. *Clin Cancer Res.* 2006; 12: 5288-97.
505. Lim SK, Llaguno SRA, McKay RM, Parada LF. Glioblastoma multiforme: a perspective on recent findings in human cancer and mouse models. *BMB Rep.* 2011; 44: 158-64.
506. El Meskini R, Iacovelli AJ, Kulaga A, Gumprecht M, Martin PL, Baran M, et al. A preclinical orthotopic model for glioblastoma recapitulates key features of human tumors and demonstrates sensitivity to a combination of MEK and PI3K pathway inhibitors. *Dis Model Mech.* 2015; 8: 45-56.
507. Bolcaen J, Descamps B, Deblaere K, Boterberg T, Hallaert G, Van den Broecke C, et al. MRI-guided 3D conformal arc micro-irradiation of a F98 glioblastoma

- rat model using the Small Animal Radiation Research Platform (SARRP). *J Neurooncol.* 2014; 120: 257-66.
508. Hdeib A, Sloan AE. Convection-enhanced delivery of <sup>131</sup>I-chTNT-1/B mAB for treatment of high-grade adult gliomas. *Expert Opin Biol Ther.* 2011; 11: 799-806.
509. Pichler J, Wilson R. IPAX-1: Phase I/II study of <sup>131</sup>I-iodo-phenylalanine combined with external radiation therapy as treatment for patients with glioblastoma multiforme. *J Clin Oncol.* 2020; 38: TPS2578.
510. Cordier D, Merlo A. Long-term results of targeted low-grade glioma treatment with <sup>213</sup>Bi-DOTA-[Thi8, Met(02)11]-Substance P. *Cancer Biother Radiopharm.* 2019; 34: 413-6.
511. Cordier D, Forrer F, Kneifel S, Sailer M, Mariani L, Mäcke H, et al. Neoadjuvant targeting of glioblastoma multiforme with radiolabeled DOTAGA-substance P - Results from a phase I study. *J Neurooncol.* 2010; 100: 129-36.
512. Shi J, Fan D, Dong C, Liu H, Jia B, Zhao H, et al. Anti-tumor effect of integrin targeted (177)Lu-3PRGD2 and combined therapy with Endostar. *Theranostics.* 2014; 4: 256-66.
513. Sundberg AL, Orlova A, Bruskin A, Gedda L, Carlsson J, Blomquist E, et al. [(111)In]Bz-DTPA-hEGF: Preparation and *in vitro* characterization of a potential anti-glioblastoma targeting agent. *Cancer Biother Radiopharm.* 2003; 18: 643-54.
514. Chopra A. <sup>124</sup>I-Labeled residulizing ligand IMP-R4 conjugated chimeric monoclonal antibody ch806 targeting the epidermal growth factor receptor deletion variant de2-7 (EGFRvIII). In: *Molecular Imaging and Contrast Agent Database (MICAD)*. Bethesda (US): National Center for Biotechnology Information; 2010.
515. Yang W, Barth RF, Wu G, Kawabata S, Sferra TJ, Bandyopadhyaya AK, et al. Molecular targeting and treatment of EGFRvIII-positive gliomas using boronated monoclonal antibody L8A4. *Clin Cancer Res.* 2006; 12: 3792-802.